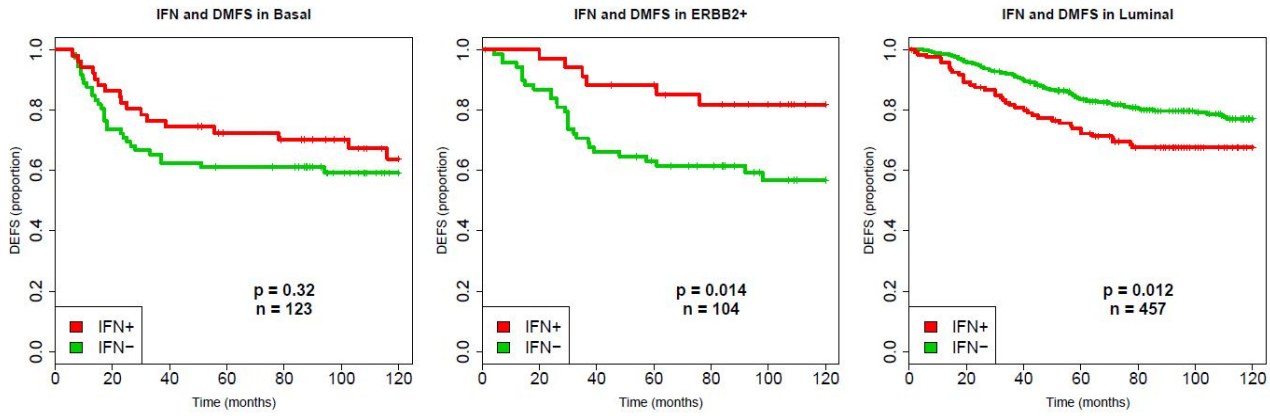

Figure 28: Kaplan-Meier curves according to the IFN metagene status in basal, ERBB2+ and luminal tumors.

Expression of IFN genes was protective in ERBB2+ tumors whereas the prognosis of the more aggressive basal tumors was not modified by IFN metagene expression levels. This suggests that ISGs may have opposite effects on tumor progression according to the specific biological background of each distinct molecular subtype, bestowing metastatic potential on luminal tumors while being protective for ERBB2+ tumors and irrelevant for basal ones.

ISGs are not only part of antiviral pathways but are also involved in tumor-immune cells interactions. Several studies have indicated a prognostic value of immune-function genes.

The paradoxical role of the immune system during cancer development (131) and metastatization (132) has been extensively documented for various tumors, but here we speculate based on our results that one possible explanation for the opposite effects of immune genes on prognosis may be related to the specific biological background of each distinct molecular subtype, like it happens in the case of the IFN metagene. The occurrence of genes related to immune response among prognostic genes predicting metastasis in ER+ tumors has already been reported (133).

In addition to eliciting anti-viral response through induction of ISGs genes, interferons are also key regulators of adaptive immunity and have emerged as central coordinators of tumour–immune-system interactions. Given the frequent involvement of immune response related genes in published breast cancer signatures with prognostic value, we analyzed, in the above defined breast cancer subtypes, the prognostic impact of a T-cell metagene (Table 13) in comparison with our IFN metagene.

T-cell cluster							
Gene	**Probesets**	**Gene**	**Probesets**	**Gene**	**Probesets**	**Gene**	**Probesets**
CCL5	213958_at	CD52	205798_at	LTB	213603_s_at	CD6	204923_at
SPOCK2	202524_s_at	IL10RA	204661_at	CORO1A	204057_at	PRF1	216250_s_at
HCLS1	203879_at	SASH3	34210_at	CD247	210031_at	LPXN	203416_at
CD53	213915_at	GZMA	207339_s_at	SH2D1A	38149_at	PLAC8	204912_at
PIK3CD	214617_at	IL7R	206337_at	ITK	206666_at	CD52	202957_at
IRF8	205488_at	CD2	204563_at	EVI2B	211339_s_at	ARHGAP25	209083_at
CD48	1405_i_at	CD27	219014_at	CD3D	204118_at		
SELL	204655_at	CCR7	206150_at	RAC2	205831_at		
CCL5	210116_at	GZMK	211742_s_at	NKG7	213539_at		

Table 13: T-cell metagene

T-cell metagene was composed by 22 genes (*ARHGAP15, CCL5, CD2, CD247, CD27, CD3D, CD48, CD53, CORO1A, EVI2B, GZMA, GZMK, HCLS1, IL10RA, IRF8, ITK, LPXN, LTB, PLAC8, RAC2, SELL, SH2D1A*), 13 of which involved in different aspects of innate and T-cell mediated adaptive immunity such as CD3/T cell receptor complex (*CD3D, CD247*) of T-lymphocytes, serine protease components necessary for lysis of target cells (*GZMA, GZMK*) by cytotoxic CD8+ T lymphocytes and natural killer (NK) cells and surface antigens providing costimulatory signals (*CD2, CD48*). Other molecules involved T cells and/or NK immunity are those encoded by CD48, CD27, Coro1A, IRF8 and finally CCL5 that, although described to have in given contexts pro-tumorigenic activity, is a potent chemotactic factor for inflammatory cells where it exerts major regulatory effects on CD4+ and CD8+ T cell-mediated immunity. Other genes included in the T-metagene like EVI2B have been poorly characterized and to date their function remains unknown.

Rody et al (134) observed that a T cell gene module was prognostic in patients with ER- tumors and with ER+/ERBB2+ tumors, which means that the protective effect of T cells seems to be confined to highly proliferating tumors only. In that dataset, B cell gene modules did not associate with the risk of metastasis, whereas a B-cells metagene did instead play an important role in highly proliferating tumors from distinct datasets analyzed by Schmidt (135). An immune module with prognostic relevance confined to ER- tumors was also reported by Teschendorff (136) who analyzed three different datasets highlighting that not all ER- tumors have a poor prognosis, and that down-regulation of a seven-gene module in such tumors attributes a doubling in metastatic risk. An IFN gene (STAT1 module) positively associated with positive clinical

outcome of basal tumors (ER-/ERBB2-) was instead reported by Abraham et al (137) using an approach based on gene sets rather than single genes.

In the validation dataset the T-cell metagene expression was associated to a reduced risk of distant metastases (Fig.29) both in ERBB2+ (HR=0.54, 95% CI 0.37-0.80, *P*=0.019) as well as in ER+ERBB2- tumors (HR=0.71, CI 0.56-0.89, *P*=0.0030).

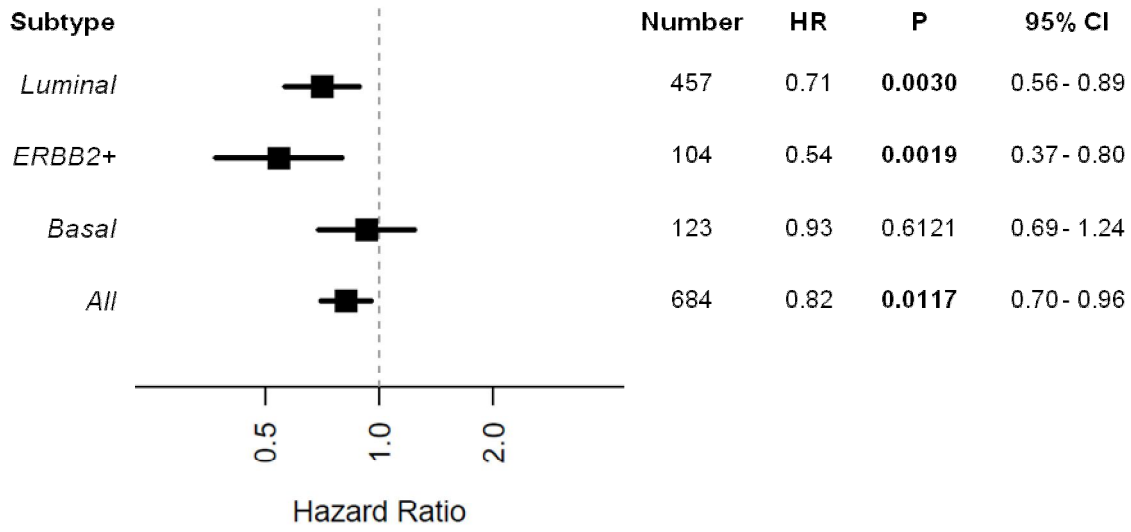

Figure 29: forest plots showing the HRs of the DMFS univariate Cox regression analyses for the T-cell metagene in the different molecular subtypes and in the overall population.

As also confirmed by life table analysis (Fig.30), high T-cell metagene expression was not able to affect the short DMFS in women with basal tumors (*P*=0.89, log-rank test, N=123), but it was associated with a longer DMFS in patients with ERBB2+ (*P*=0.0051, log-rank test, N=104) and with luminal tumors (*P*=0.0035,log-rank test, N=467).

Therefore, results suggest that T-cell and IFN metagenes impact similarly on prognosis in patients with basal and ERBB2 tumors, but they play instead opposite roles in luminal tumors.

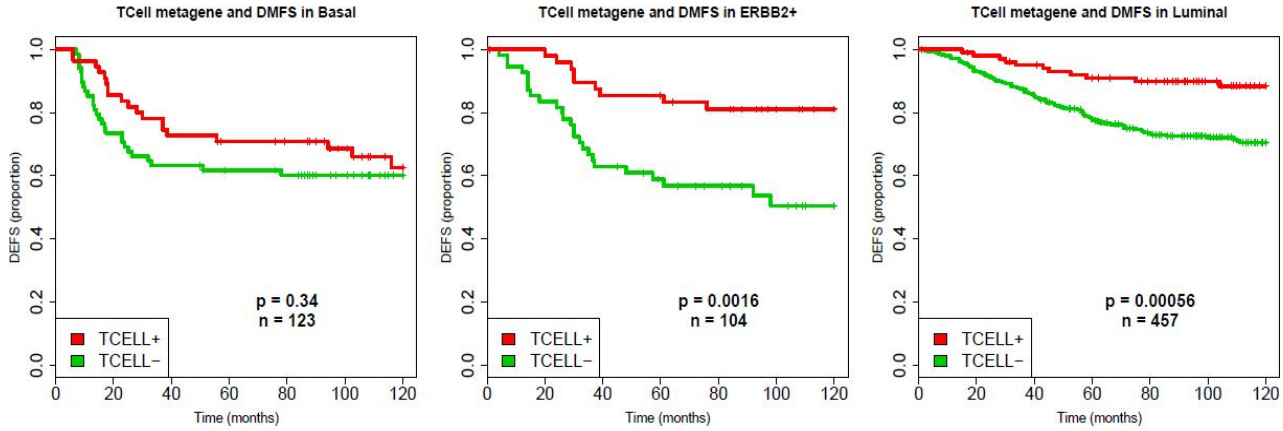

Figure 30: Kaplan-Meier curves according to the T-cell metagene status in basal, ERBB2+ and luminal tumors.

To directly compare the roles of these two metagenes, we performed multivariate analysis for T-cell and IFN metagenes in the three subtypes of tumors (Table 13). Only in women with luminal tumors the two metagenes maintained an independent but opposite prognostic relevance on outcome; the T-cell metagene was found to be associated to 1.6-fold reduction in metastasis risk (95% CI 0.50-0.80, *P*=0.001) and the IFN metagene was associated to 1.3 increased risk of relapse (95% CI 1.12-1.55, *P* =0.001).

		HR	P	95% CI
Basal				
	Tcell	1.03	0.8720	0.73 - 1.45
	IFN	0.85	0.2922	0.64 - 1.14
ERBB2+				
	Tcell	0.65	0.0636	0.42 - 1.02
	IFN	0.73	0.1260	0.49 - 1.09
Luminal				
	Tcell	0.63	**0.0001**	0.50 - 0.80
	IFN	1.32	**0.0010**	1.12 - 1.55

Table 14: IFN and T-cell metagenes multivariate Cox analysis.

Such result is in agreement with the different pattern of correlation between these two metagenes according to molecular subtype, with a stronger correlation in basal and ERBB2+ tumors (r=0.50, r=0.52) and weaker one in luminal (r=0.35), where high expression of the IFN metagene, but low expression of T-cell genes was observed, as reported in Figure 31. The combined effect of T-cell and IFN metagene on DMFS is reported in Figure 32.

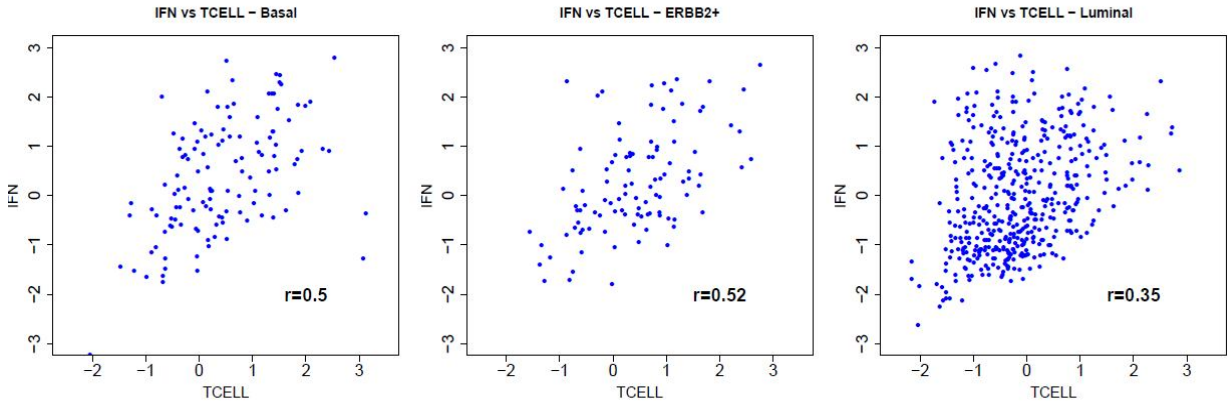

Figure 31: Scatter plots showing correlation between IFN metagene and T-cell metagene in basal, ERBB2+ and luminal tumors in a combined dataset derived from three publicly available datasets of node negative tumors (GSE2034; GSE7390;GSE11121).

As expected, in patients with basal tumors the 10-year DMFS was not affected by the expression of such metagenes, conversely in women with ERBB2+ and luminal tumors a high expression of T-cell metagene was associated with a longer DMFS, however if the T-cell metagene scored low, the outcome was in fact affected by the IFN metagene expression. The metastatization risk was reduced in ERBB2 tumors expressing high levels of IFN genes, but was increased in women with luminal tumors.

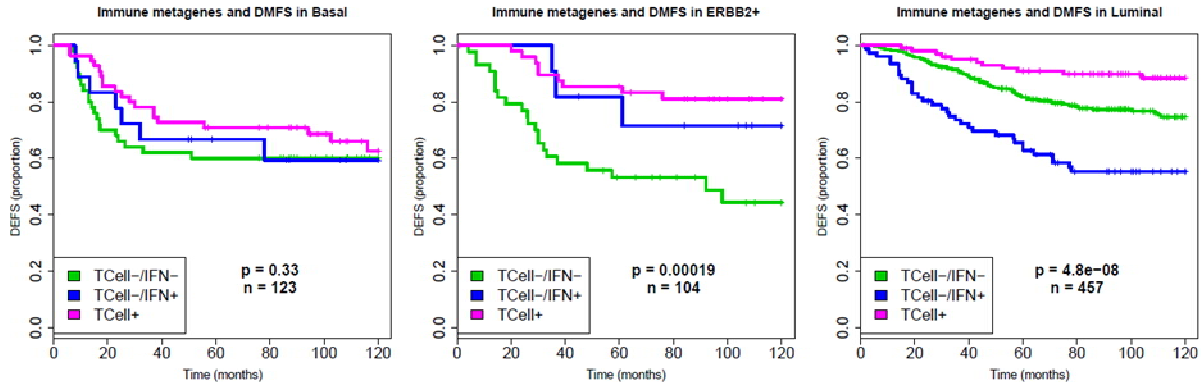

Figure 32: Kaplan-Meier curves according to the T-cell metagene and IFN-metagene status in basal, ERBB2+ and luminal tumors.

When T-cell metagene is expressed at low levels, high expression of the IFN metagene drives the bad prognosis. IFN-related genes seem therefore to play a metastasis promoting role only in luminal tumors in which T-cell related genes are scarcely expressed. At difference with previous reports however we do not support a role for innate and adaptive immunity in ER- tumors. This discordant result may be explained on the basis of wide variations, from one study to another, of gene signature composition.

To understand the biological basis for the different prognostic role of IFN metagene expression in distinct molecular subtypes, we selected from the validation dataset tumors with high (>4th quartile) versus low (<1st quartile) expression of IFN metagene and ran a class comparison analysis separately for each molecular subtype and for luminal tumors with low T-cell metagene expression.

Probesets both up- and down-regulated showing a fold change >1.5 and a FDR <1% were selected as differentially expressed (Table 15) and canonical pathways enriched in the differentially expressed genes compared with all tested genes were identified using Ingenuity Pathway Analysis.

Subtype	# of samples IFN+	# of samples IFN-	DE probesets	DE genes
Basal	42	17	392	286
ERBB2	25	12	263	181
Luminal	104	142	744	557
Luminal T-cell	65	138	631	469

Table 15: IFN multivariate Cox analysis.

By comparing the enrichments in all subtypes taken in account, we noticed that almost all enriched pathways included genes involved in adaptive and innate immunity (Fig.33) as already seen in our correlation data (Fig.31). However, most of such pathways were no more found among the significantly enriched gene terms when the analysis was limited to luminal tumors with low T-cell metagene expression. Interestingly, in the latter subgroup of tumors, where a high IFN gene expression predicts a worse distant metastases free survival (DMFS), genes

differentially expressed between tumors characterized by low or high IFN metagene expression showed an enrichment in a proliferation-related pathway '*Mitotic Roles of Polo-Like Kinase*', which was in fact also present among the enriched terms of luminal tumors, and a DNA damage pathway '*Cell Cycle: G2/M DNA Damage Checkpoint Regulation*' (Fig.33). This suggest once again the well known role of proliferation as driver of bad prognosis in luminal tumors, but also indicating that the trigger of that proliferative modulations may be the microenvironment with a still to be clarified molecular mechanism.

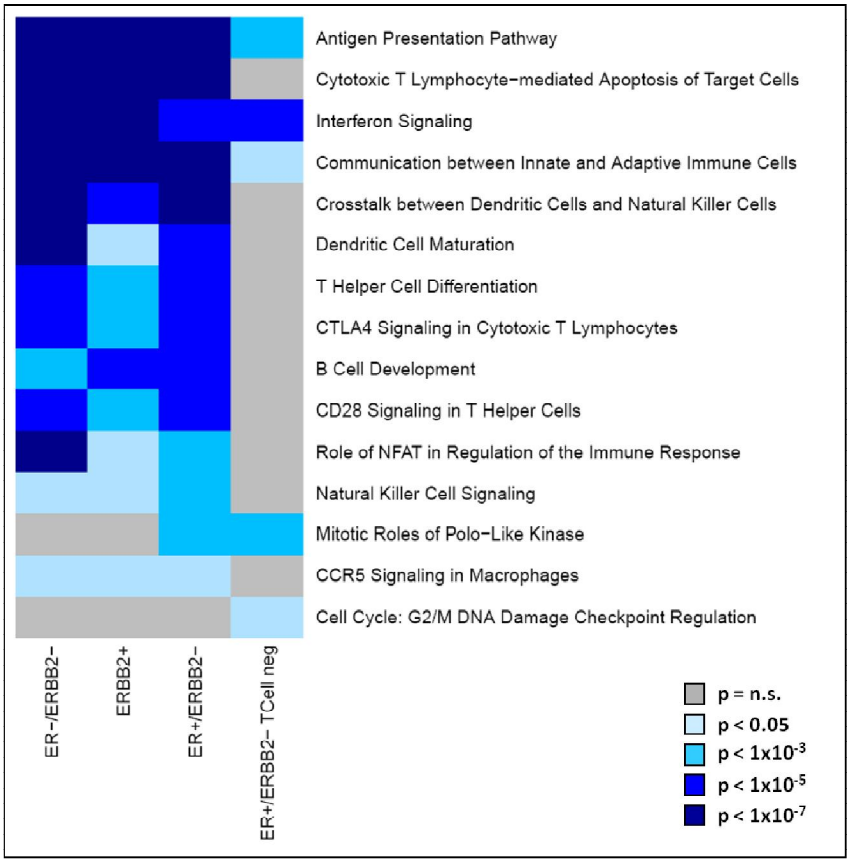

Figure 33: heatmap reporting *P* values referring to enrichment for selected *canonical pathways* as determined by IPA for genes found to be differentially expressed between tumors with high (>4th quartile) versus low (<1st quartile) IFN metagene expression.

Results from this part of study add therefore to the discordant data already reported in the literature, underlining the fact that the role of immune gene modules in breast cancer is far from being clear. Some confusion may derive from heterogeneity in treatments, from the use of meta-

analytical approaches in the literature, but also from the different methods used to identify molecular subtypes.

For instance in case of ERBB2 patients, the protective role of immune module in this subgroup (generally uniformly assigned to bad prognosis), appears only in those studies where ERBB2 positive patients were identified based on amplification of the gene rather than based on clustering techniques which do in fact fail to identify all HER2 cases, (138;139). Indeed in our analysis of the public datasets where HER2+ patients were identified based on ERBB2 gene expression, immune gene module expression was associated with a protective effect exactly opposite to what happens in the pure luminal (luminal tumors not contain any ERBB2+ cases) subclass.

Altogether our data confirm that it is of pivotal importance to analyze the contribution of prognostic variable in homogeneous patients subgroups taking into account the molecular subtype.

It is also important to underline that despite the 1:1 ratio between poor prognosis and good prognosis patients and the similar distribution of classical prognostic factors among the two groups, the poor prognosis clinical phenotype (IFN+, T cell–luminal tumors) associates to genes that are not directly involved in the metastatic process but track it indirectly due to a correlation with proliferation. On the contrary the good prognosis clinical group (IFN+, ERBB2+) is characterized by a strong activation of immune response pathways.

Results from our prognostic study lead to the paradoxical situation in which the same signature has opposite prognostic roles depending upon the molecular subtype. If we consider our IFN gene signature as an immune signature, the paradoxical role on the prognosis is not surprising, and we are supported by literature data reporting different effects of the immune axis according to the molecular subtype. However ISG genes can be induced in many different cell types and very different ways, and do not necessarily represent an activation of immune response. We therefore reasoned that it might be important to further characterize our profiled tumors with respect to the microenvironment to better understand the origin of the ISG signature.

Different cell types belonging to the stroma and the tumor microenvironment are known to produce opposite effects on tumorigenesis as summarized in the Table reported below.

Table 1. Noncancerous Cells of the Tumor Organ

Cell Type	Effect on Tumors	References
Normal epithelial cells	inhibit	Dong-Le Bourhis et al., 1997
Myoepithelial cells	inhibit (invasion, growth)	Gudjonsson et al., 2002; Hu et al., 2008
Fibroblasts	promote (proliferation, angiogenesis, invasion)	Bhowmick et al., 2004; Olumi et al., 1999; Orimo et al., 2005
Mesenchymal stem cells	promote (metastasis)	Karnoub et al., 2007
Adipocytes	promote (tumor growth, survival, angiogenesis)	Iyengar et al., 2005; Landskroner-Eiger et al., 2009
Endothelial cells	promote (angiogenesis, niche?)	Ausprunk and Folkman, 1977; Calabrese et al., 2007
Perivascular cells	promote (vascularization)	Song et al., 2005
	inhibit (metastasis)	Xian et al., 2006
Bone marrow-derived cells	promote (proliferation, invasion, angiogenesis)	Coussens et al., 2000; Du et al., 2008; Lyden et al., 2001
Dendritic cells	inhibit (stimulate antitumor immunity)	Knight et al., 1985; Mayordomo et al., 1995
Myeloid-derived suppressor cells and immature myeloid cells	promote (angiogenesis, metastasis, reduce antitumor immunity)	De Palma et al., 2005; Sinha et al., 2007; Yang et al., 2004, 2008b
Macrophages, M1-like	inhibit	Sinha et al., 2005
Macrophages, M2-like	promote (invasion, angiogenesis)	DeNardo et al., 2009; Lin et al., 2001, 2006
Mast cells	promote (angiogenesis)	Coussens et al., 1999; Soucek et al., 2007; Yang et al., 2008a
Neutrophils, N1	inhibit (stimulate antitumor immunity)	Fridlender et al., 2009
Neutrophils, N2	promote (angiogenesis, reduce antitumor immunity)	Nozawa et al., 2006; Schmielau and Finn, 2001; Shojaei et al., 2008
T cells, $CD4^+$, T helper 2	promote (metastasis)	DeNardo et al., 2009
T cells, $CD8^+$, cytotoxic	inhibit (tumoricidal)	Romero et al., 1998
T cells, $CD4^+CD25^+$ regulatory	promote (reduce antitumor immunity)	Casares et al., 2003; Curiel et al., 2004
T cells, gamma/delta	inhibit (stimulate antitumor immunity)	Girardi et al., 2001
T cells, Th17	promote (proliferation, angiogenesis)	Numasaki et al., 2005
	inhibit (stimulate T-cell antitumor immunity)	Hirahara et al., 2001
B cells	promote (reduce antitumor immunity)	Inoue et al., 2006
B cells, immunoglobulins	promote (stimulate inflammation-associated progression)	Andreu et al., 2010
Platelets	promote (metastasis)	Camerer et al., 2004; Nieswandt et al., 1999

Table 16: noncancerous cells of the Tumor Organ, Egeblad M. et al (140).

This prompted us to investigate directly on our clinical samples characterizing by IHC the leucocytes infiltrate, and attempting complementary *in vitro* co-culture experiments between cancer cell lines representative of the different subtypes and different type of fibroblasts.

i. Clinical evidence: infiltrating lymphocytes

To investigate if expression of the IFN metagene was associated to lymphocyte infiltration we performed a lymphocyte infiltration (LI) score on all samples.

There was no correlation between the LI score as determined on histological sections and the IFN metagene expression (P=0.6025, *Kruskal-Wallis* test, N=86). Luminal tumors with higher LI were more frequently metastasis free (P=0.1365, χ^2 test, N=86).

To establish the identity of cells expressing ISGs the subset of luminal tumors with the highest (3rd tertile) expression of the IFN metagene was stained for MX-1, ISG15, OAS2 and IFIT3 protein expression and also for STAT 1. This is involved in upregulating genes due to a signal by either type I, type II or type III interferons STAT1 forms a heterodimer with STAT2 that can bind the **ISRE** (**I**nterferon **S**timulated **R**esponse **E**lement) promoter element. In either case, binding of the promoter element leads to an increased expression of **ISG** (**I**nterferon **S**timulated **G**enes).

MX1 was almost always expressed by a higher percentage of tumoral cells compared to stromal cells, and only in 3 cases the stromal expression prevailed (Fig.34).

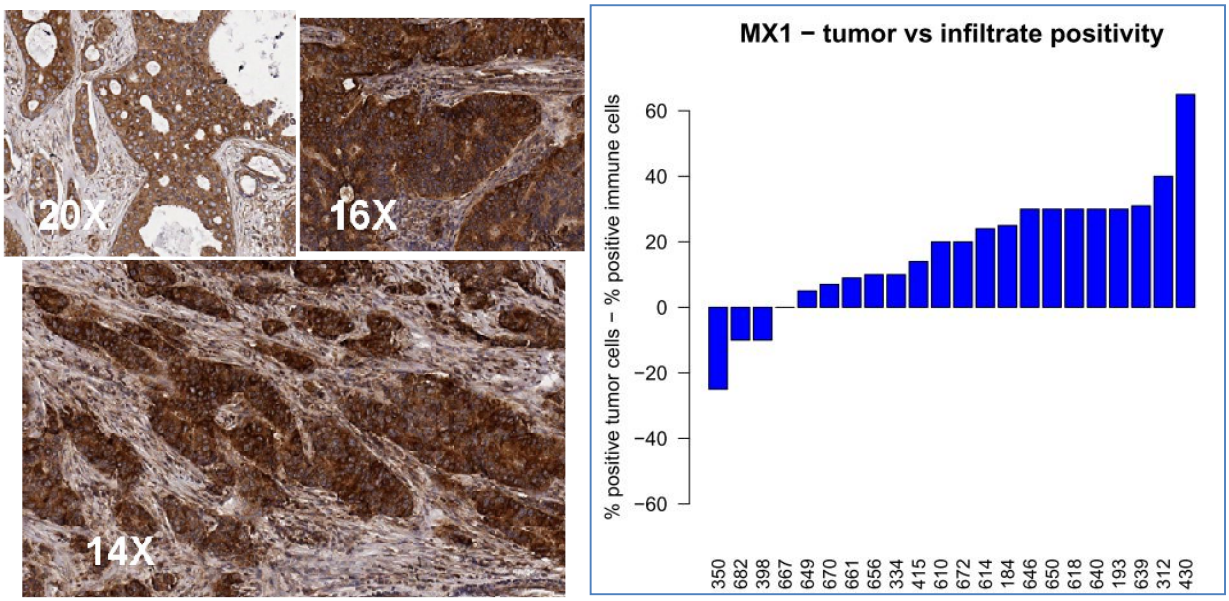

Fig.34: Strong positivity for MX1 in neoplastic cells in a case of breast invasive carcinoma, ductal type. Note the difference between cancer cells and immune cells of the stroma stained positively (left). Difference between percent of tumor and of immune cells stained positively for MX1 in FFPE sections from luminal tumors with high IFN metagene expression (3rd tertile) (right).

To further investigate the mechanism responsible for IFN stimulated gene up-regulation we performed IHC characterization of the different lymphocyte and myeloid sub/populations infiltrating tumor and tissue surrounding the tumor lesion to understand if particular sub-

populations with the leukocyte infiltrate could be positively correlated with the IFN metagene expression.

We used following antibodies: anti CD3, antigen expressed by T-cells and NK cells; anti CD4 expressed by T-helper lymphocytes, anti CD 8 expressed by cytotoxic T-lymphocytes; anti CD 68 expressed by monocytes and macrophages; anti CD56 expressed by T-cells and NK cells; anti CD57 expressed by NK cells; anti FOXP3 expressed by regulatory T-cell; anti CD45 expressed by T-cells and B-cells; anti CD20 expressed by mature B-cells; anti Granzyme expressed by T-cytotoxic cells and NK cells and anti HLADR for T-helper cell and B-cells.

By unsupervised analysis of IHC data, 4 clusters were identified with different expression pattern. For these clusters we evaluated the association with available clinic-pathological features. A significant association was found between the over-expression of HER-2 and the cluster 2, characterized mainly by the sub-population of CD8 (cytotoxic T-lymphocytes). However, expression of IFN metagene was not associated with any of the sub-groups of leukocyte cells (Fig.35).

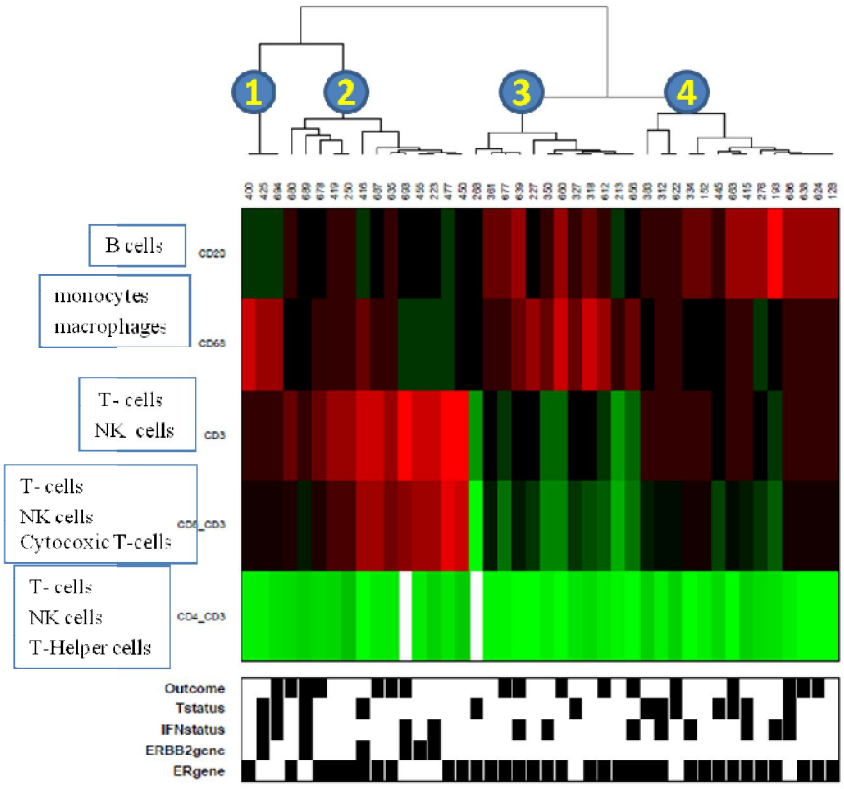

Fig.35: unsupervised analysis of IHC data.

We therefore conclude that genes are primarily expressed by the epithelial component of tumor and that none of the analyzed leukocyte sub-populations seen to implicated in their regulation.
We therefore decided to further analyze the interaction with the stroma looking fibroblast in *in-vivo* models using different combination of fibroblasts and cancer cells representing the three main molecular subtypes.

ii. Experimental evidence:

Stroma plays a critical role in epithelial proliferation and organization through production of extracellular matrix, paracrine signalling and direct cell contact-mediated effects.
Fibroblasts are a major component of stroma and their numbers are greatly enriched in tumors. Cancer associated fibroblast (CAFs) are different from normal tissue fibroblasts and can promote tumors progression affecting: proliferation, angiogenesis and metastasis by secreting a large number of growth factors, cytokines and extracellular matrix components. Breast CAFs can directly interact with cancer cells and immune cells, or indirectly interact with those cells through paracrine interactions. Such interactions can be reproduced *in vitro* in an artificially reconstituted microenvironment using heterotypic cell cultures.
The aim of this part of experiments was to study the interactions between epithelial and stromal cells growing in direct contact or simply interacting though secretion of soluble factors.
We used different *in vitro* models to stimulate tumor-stroma interaction by co-cultivating breast cancer cells with stromal fibroblasts of different origin. The biological effects that we proposed to evaluate were:
1. proliferation;
2. induction of IFN;
3. release of cytokines.

Initially, to simulate stroma-tumor interaction, the Transwell (Costar, Corning Life Science, NY, USA) co-culture system was used, testing two different conditions:

1. co-culture with direct contact between fibroblasts and epithelial cancer cells,
2. co-culture in which interaction is only mediated by secretion of soluble factors.

The effects of CAF and NAF were investigated in cell lines representative for the different breast cancer molecular subtypes.

We therefore focused our experiments on three different breast cancer cell lines: luminal MCF7, ERBB2+ SkBr3 , claudin-low MDA MB231. All cell lines were co-cultivated with fibroblasts of different origin: CCL-171 lung, HTB 125 breast stroma, HNDF normal derma and B-CAF MS132 (α-Sma+) isolated in our laboratory from clinical breast tumor. Molecular characterization of the isolated fibroblast is reported in (Fig.36).

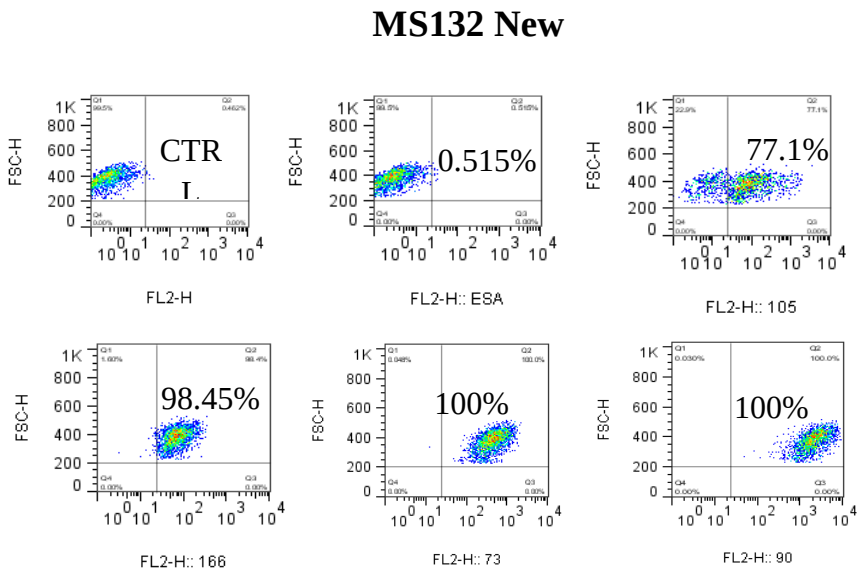

Figure 36: molecular characterization of B-CAF MS132 fibroblasts.

To investigate the possible roles of soluble factors or direct cell-cell contact in triggering the interferon response (observed in clinical tumors and associated to likelihood to develop distant metastases), we tested the ability of conditioned medium obtained from each co-culture to induce the response in a monoculture of the relative epithelial cell.

Real time PCR was performed to assess the expression of some interferon-stimulated genes (ISG), *OAS 2*(2'-5'-oligoadenylate synthetase 2), *IFIT 3* (interferon induced protein with tetratricopeptide repeats 1), *MX1* (gene encoding the mixovirus resistance proteins 1) and also *STAT 1*, an activator of transcription. All data were referred to co-culture control sample: epithelial cell/epithelial cell.

MDAMB 231 that represent an aggressive breast cancer cell line, showed an increased expression of ISG when in contact with all fibroblasts, except for HTB 125. ISG induction was stronger when cells were in direct contact.

For MCF7 instead, the two types of co-culture showed the same effects, in particular co-culture with HNDF determined a stronger up-regulation of ISG expression.

Indirect interaction between SkBr3 and HTB125 induced an up-regulation of ISG, while a down- regulation was observed with HNDF; the contact with B-CAF MS132 induce their down-regulation. On the average the effects observed with this Her2+ cell line were very variable compared to the luminal and the claudin-low cell lines.

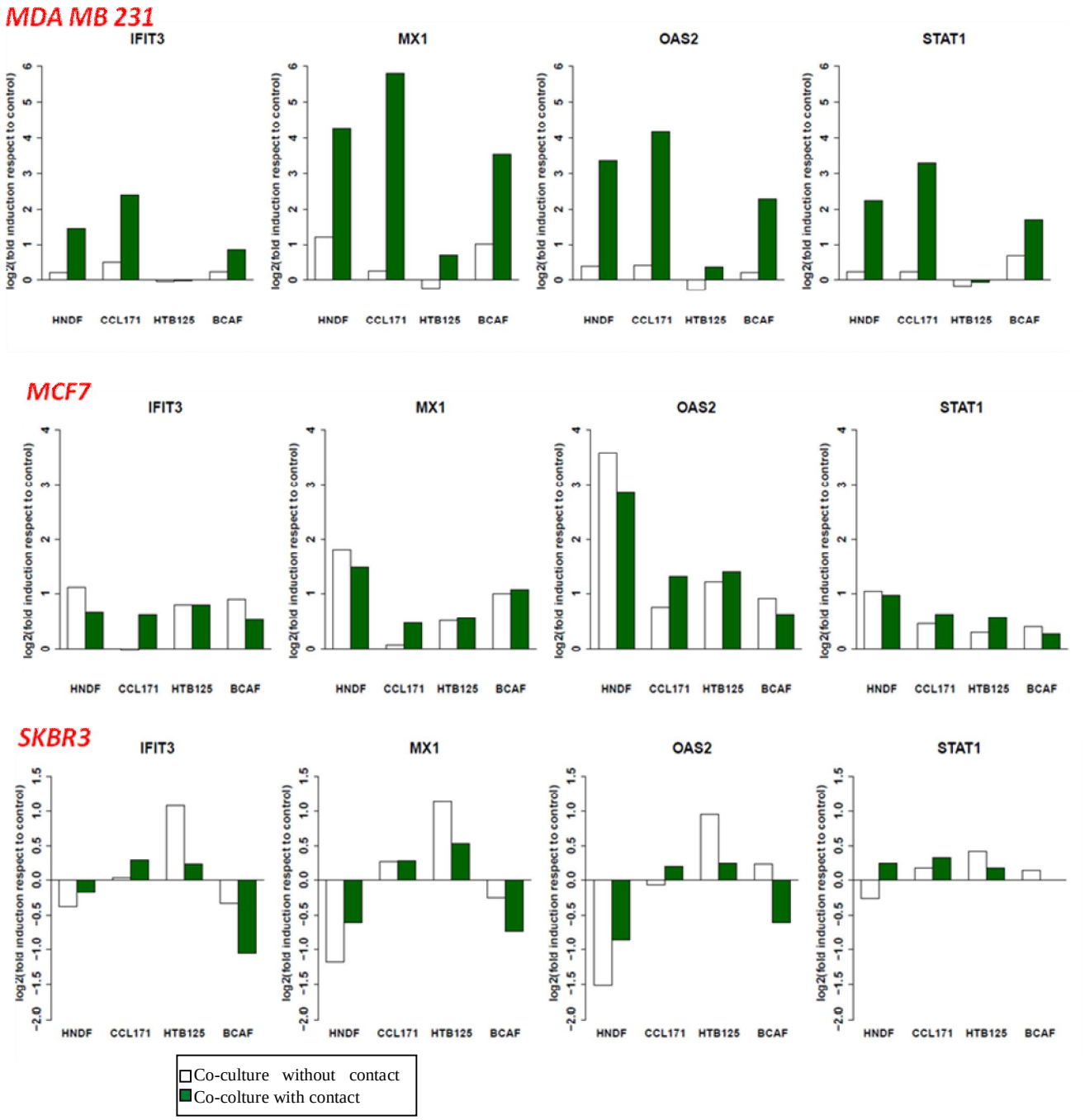

Figure 37: expression of interferon-stimulated genes (ISG) respect to different co-cultures.

We then investigated the conditioned medium after 96 h of co-culture using Bio-Plex Human Cytokine Assay to evaluate the cytokines reported in Fig.38a.

Unsupervised hierarchical clustering of samples according to cytokine content showed that in the MDA MB 231 cell line the cytokines expression pattern was not influenced by the type of fibroblasts. On the contrary, in the other two cell lines, cytokine expression appeared to be more fibroblast-dependent. Finally, cytokine expressions were very similar in two types of co-culture (Fig.38b).

From this first screening of cytokines, we identified four cytokines that showed a variation in all three epithelial cell lines, regardless of the type of fibroblast: IL-6, IL-8, HGF, SCF. These cytokine are known to be implicated in tumor progression and metastatization (34;34)(141;142).

a

Human Group I	Human Group II
IL-1β	IL-1α
IL-1ra	IL-2Rα
IL-2	IL-3
IL-4	IL-12 (p70)
IL-5	IL-16
IL-6	IL-18**
IL-7	CTACK
IL-8	GRO-α
IL-9	HGF
IL-10	
IL-12 (p70)	IFN-α2
IL-13	LIF
IL-15	MCP-3
IL-17A	M-CSF
Basic FGF	MIF
Eotaxin	MIG
G-CSF	β-NGF
GM-CSF	SCF
IFN-γ	SCGF-β
IP-10	SDF-1α
MCP-1 (MCAF)	TNF-β
MIP-1α	TRAIL
MIP-1β	VCAM-1
PDGF-BB	
RANTES	
TNF-α	
VEGF	

b

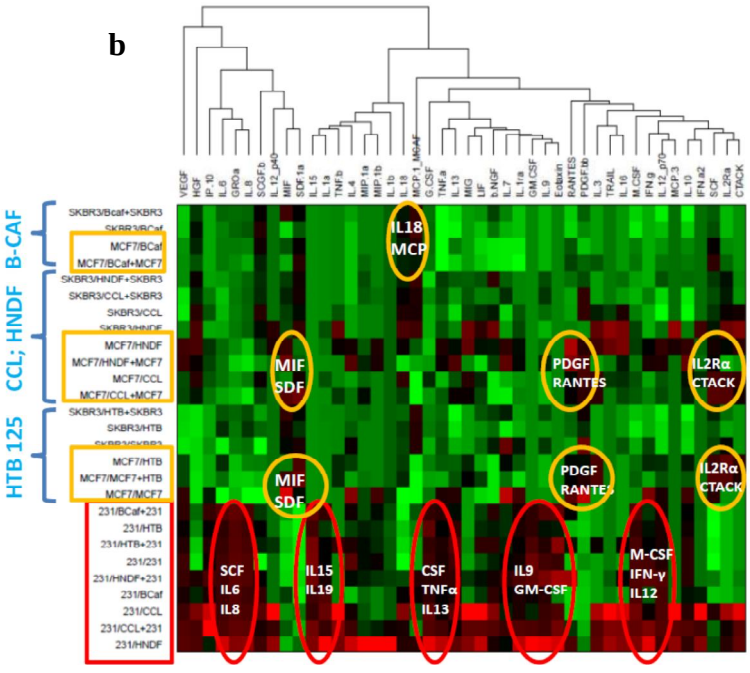

Figure 38: **a**. List of Bio-Plex Human Cytokine panel Assay ; **b.** Unsupervised hierarchical clustering between co-culture and cytokine expression.

Tumor invasion is a multi-step process. Tumor cells need to leave the primary site and get into contact with the normal environment. To maintain its normal tissue microenvironment, the body will mobilize various defensive measures to inhibit tumor growth and invasion. Through the direct contact with surface molecules or the indirect effects of cytokine secretion, tumor cells induce a shift in normal cells, which interferes with their ability to inhibit the tumor progression, and even allows to promote tumor growth and invasion (50;143).

The functional effect of co-culture conditioned medium (C.M.) on the migration and invasion activity of epithelial cells was tested by Transwell migration and invasion assay. Migration capacity was evaluated after 48 h of incubation, while invasion both after 48 h and 72h. Each test was performed in technical duplicate. The data were calculated as area pixel/µm.

We assayed three types of conditioned media:

1. condition medium obtained only from epithelial cells culture after 96 h.
2. condition medium obtained from epithelial cells co-cultivated with stromal cells for 96 h.
3. condition medium obtained only from stromal cells culture after 96 h.

Not unexpectedly, the picture of results that we obtain was complex, reflecting the different abilities of normal and malignant cells to respond to extrinsic signals.

Luminal MCF7, are known to have a small invasion and migration capacity *in vitro,* but several study, like Chen and co. (144) reported that chemokines released in the culture medium can promote the migration of this human breast carcinoma cell lines.

Our preliminary experiments confirmed on the average that migration and invasion capacity of epithelial cells, both MCF7 and SkBr3 was stimulated by factors released with fibroblast presence.

These early experiments suggested that after 48h MCF 7 migration was higher in presence of HNDF conditioned medium; similarly, invasion (evaluated at 72h), was more stimulated by C.M. derived from co-culture MCF7+HNDF. We can speculate that probably the presence of epithelial cancer cells contribute for activation of normal fibroblast, NAF that in turn start to release cytokines promoting this way the invasion process.

Also in the case of SkBr3 migration was more stimulated by CM of HNDF, while invasion (evaluated at 72 hrs) was stimulated by CM derived from co-culture of SKBR3 + CCL171.

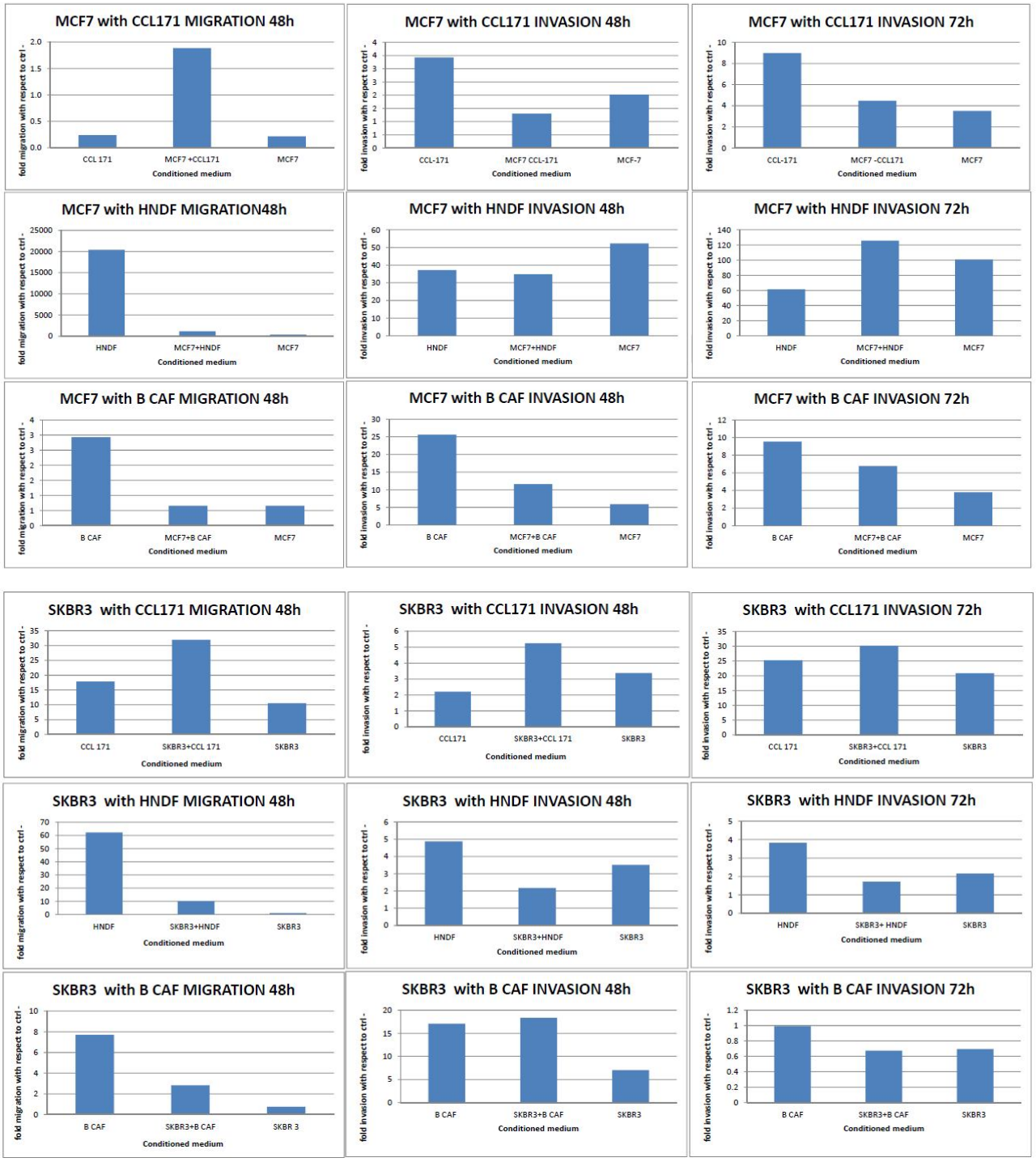

Figure 39: migration and invasion analysis

iii. Experiments in progress

To identify the best experimental setting that could respond to our question to study the interactions microenvironment-stroma, we began to evaluate and test new co-cultures approaches, also taking inspiration from the different systems that are showing in the literature (144-146).

Moreover, we decided also to evaluate a new experimental CAF- line dyed with PLVX-DS RED-EXPRESS2-N1 vector (CLONOTECH, Mountain View, CA, USA) a cell line derived from activated fibroblasts isolated from a patient. With the migration/invasion co-culture systems we evaluated the following setting:

1. MCF +HNDF.
2. MCF7 +B-CAF Red.

After 72h of starvation we evaluated:

a. the migration and invasion on the membrane filters used for the assay.
b. 4 cytokines (IL-6, IL-8, HGF, SCF) chosen based on the wide cytokine spectrum Bio-plex test; in the culture media.
c. Proliferation capacity of epithelial cells stimulated for 72h with media derived from co-culture experiments.

MCF7 migratory and invasive capacity was higher with HNDF fibroblast and such biological effect was paralleled by an increased secretion of IL-6, and IL 8 in the conditioned medium deriving from heterotypic co-cultures compared to homotypic cell cultures.

SCF and HGF were more stimulated with HNDF and this confirms the literature data. In fact co-culture with human breast cancer cells in a Transwell system induced NAF to secret HGF as well as to promote tumorigenicity (141).

The pattern of cytokines concentration in the conditioned media was similar between experiments run to evaluate migration and those run in the conditions used to evaluate invasion. The result is not surprising as the two types of experimental settings differ only for the presence of Matrigel.

MIGRATION/INVASION CO-CULTURE

MCF7

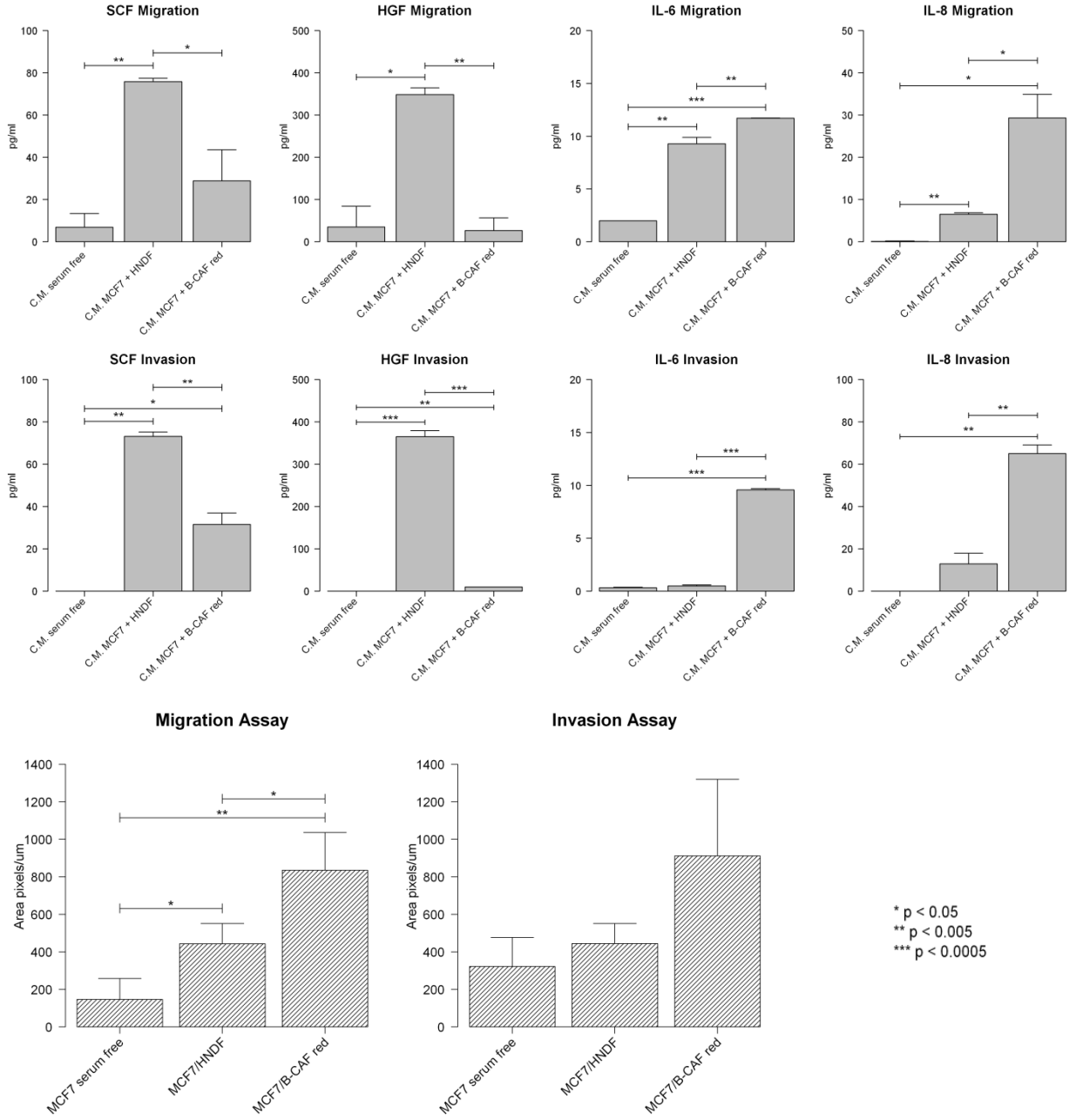

Figure 40: cytokine concentration evaluated with ELISA assay of conditioned medium and migration end invasion analysis of MCF7 stimulated by conditioned medium obtain from migration/invasion co-cultures.

In this type of experiment the direct contact between the fibroblasts and the tumor cells which exists in the clinical tumor is not taken in account. Therefore it is impossible to evaluate a possible effect on the proliferation. For this reason we will evaluate a further system of co-cultures defined flask co-cultured, in which the epithelial and stromal cells will be put in contact in the absence of serum for 72 h. The conditioned medium product will be evaluated in terms of cytokines present, and also used to stimulate the proliferation, migration and cell invasion.

Extracellular matrix is a key regulator of normal homeostasis and tissue phenotype (147). Important signals are lost when cells are cultured *ex vivo* on two-dimensional elastic substrata, many of these crucial microenvironmental cues be restored using three-dimensional (3D) cultures. Thus provides a more physiologically relevant approach to the analysis of gene function and cell phenotype *ex vivo.*

MCF7 transfected with GFP and fibroblast HNDF were co-cultivated to apply this new cell culture approach and after 10 co-culture days, the experiment was starved and with the ELISA assay we evaluated the concentration of IL-6 and IL-8 (Fig.41). We evaluated only these two cytokines because the media volumes were very low (~400µL).

Literature describes two 3D co-cultured types: “on top” assay, in which cells are sow on top of thin Matrigel matrix, and “embedded” assay in which cells are cultured embedded in Matrigel. The concentration of the two tested cytokines was similar in the two types of 3D co-culture systems. With confocal microscope it was possible to trace the cell morphology, interactions and the cells number (Fig.42).

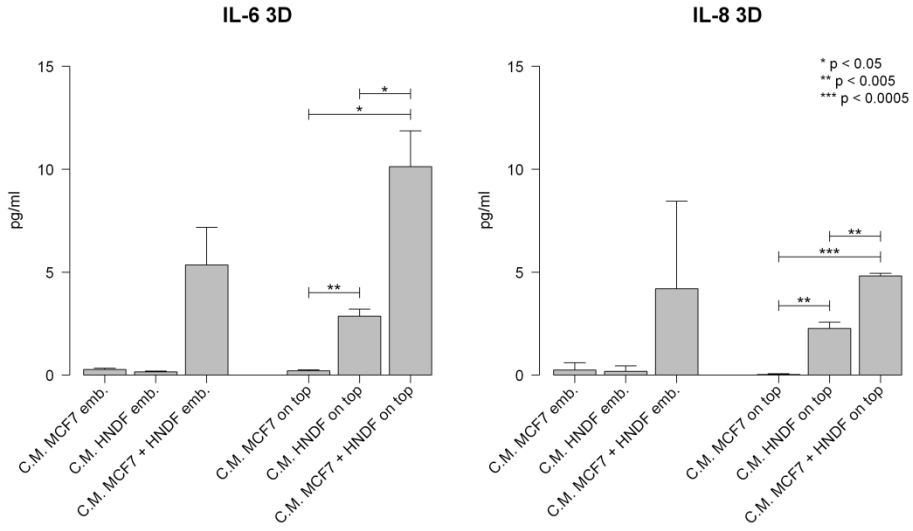

Figure 41: cytokine concentration evaluated with ELISA assay of conditioned medium of 3D co-cultures.

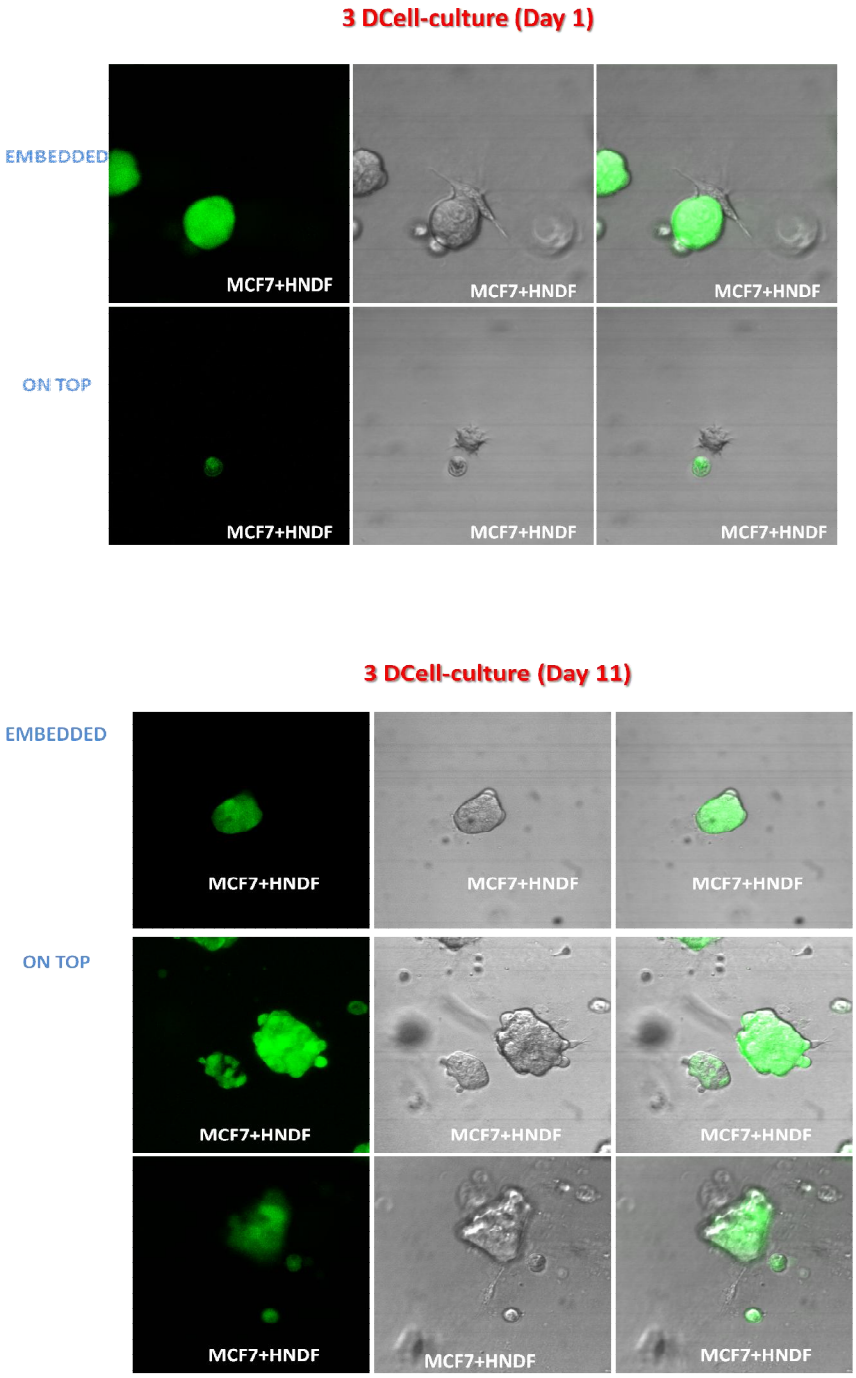

Figure 42: 3 D co-culture confocal microscope images

4.2 PREDICTING TREATMENT SENSITIVITY

4.2.1 EMERGING CHEMOTHERAPY RESPONSE PREDICTORS

The clinical importance of predicting who will or will not respond to chemotherapy is intuitively obvious. If a test could predict who will respond to a given drug, the treatment could be administered only to those patients who will benefit from it, and others could avoid unnecessary treatment and its toxicity. However, the practical development of chemotherapy response prediction tests poses several challenges. There are theoretical limits to the accuracy of any response predictor that measures the characteristics of the cancer only. Host characteristics that are not easily measured in cancer tissue, including the drug metabolism rate, can have an important impact on response to therapy. Also, there is considerable uncertainty as to what level of predictive accuracy would be clinically useful. In fact, different levels of predictive accuracy may be required for different clinical situations. For instance, the clinical utility of a chemotherapy response prediction test that has a 60% PPV (i.e., a 60% chance of response if the test is positive) and an 80% NPV (i.e., a 20% chance of response if the test is negative) will depend not only on these test characteristics but also on the availability and efficacy of alternative treatment options, the frequency and severity of adverse effects, and the risks of exposure to ineffective therapy (i.e., rapid disease progression with life-threatening complications). A test with the above performance characteristics may be of limited value in the palliative setting, when alternative treatment options are limited and generally ineffective. Patients and physicians may want to try a drug even if the expected response rate is only 10% (well within the range of test-negative cases), particularly if side effects are uncommon or tolerable. On the other hand, in the setting of potentially curative therapy, when multiple treatment options are available, a test with the same performance characteristics may be helpful in selecting the best regimen from the several treatment options. In addition, a test that was developed to predict response to a given treatment in previously untreated patients may not predict response sufficiently accurately when the same drug is used as second- or third-line treatment.

Considering these complexities, many of the recent predictive marker studies that use high-throughput analytic tools have not surprisingly focused on the pre-operative (neoadjuvant) treatment setting in breast cancer. Neoadjuvant chemotherapy provides a unique opportunity to

identify molecular predictors of response to therapy. Pathologic complete response (pCR) to chemotherapy indicates an extremely chemotherapy-sensitive disease and represents an early surrogate of long-term benefit from therapy. Histologic type, tumor size, nuclear grade, and ER status all influence the probability of response to neoadjuvant chemotherapy, and these clinical variables can be combined into a multivariable model to predict the probability of pCR (http://www.mdanderson.org/care_centers/breastcenter/dIndex.cfm?pn=448442B2-3EA5-4BAC-98310076A9553E63). However, these clinical variables lack regimen-specific predictive value and represent features of general chemotherapy sensitivity.

Several small studies have provided “proof-of-principle” that the gene expression profile of cancers that are highly sensitive to chemotherapy is different than that of tumors that are resistant to treatment (148). The largest study so far included 133 patients with stage I–III breast cancer who received preoperative weekly paclitaxel and 5-fluorouracil, doxorubicin, cyclophosphamide (T/FAC) chemotherapy (149). The first 82 cases were used to develop a multigene signature predictive of pCR, and the remaining 51 cases were used to test the accuracy of the predictor. The overall pCR rate was 26% in both cohorts. A 30-gene predictor correctly identified all but one of the patients who achieved pCR (12 of 13) and all but one of those who had residual cancer (27 of 28) in the validation set. It showed significantly higher sensitivity (92 vs. 61%) than a clinical variable-based predictor that included age, nuclear grade, and ER status. The high sensitivity indicated that the predictor correctly identified almost all of the patients (92%) who actually achieved pCR. The PPV of the pharmacogenomic predictor was 52% (30–73%); however, the lower bound of the 95% confidence interval did not overlap with the 26% pCR rate observed with this regimen in unselected patients. Thus, the predictor could define a patient population more likely to achieve pCR than unselected patients. The NPV of the test was also high at 96% (82–100%), indicating that <5% of test-negative patients (i.e., those predicted to have residual disease) achieved pCR. The NPV was similar to and the PPV better than those seen with ER immunohistochemical analysis or HER2 gene amplification as predictive markers for endocrine or trastuzumab therapies, respectively. However, to what extent this genomic predictor of sensitivity is specific to T/FAC therapy rather than being a generic marker of chemotherapy sensitivity has yet to be determined.

4.2.2 A THIRD TYPE OF MARKER: CONTEXT –SPECIFIC MARKER

Context specific markers provide information on time to event outcome in patients who receive a well-defined therapy ("context") without taking into account the distinction between prognostic and predictive contribution. The obvious question is whether we can derive predictive markers using time to event outcome in homogenously treated patients. There is not any difficulty in distinguishing benefit from non benefit, but things get more complicated when we aim at answering the question of whether a specific marker is predictive. Ideally we would like to be faced with a situation as described in the figure below (Fig.43).

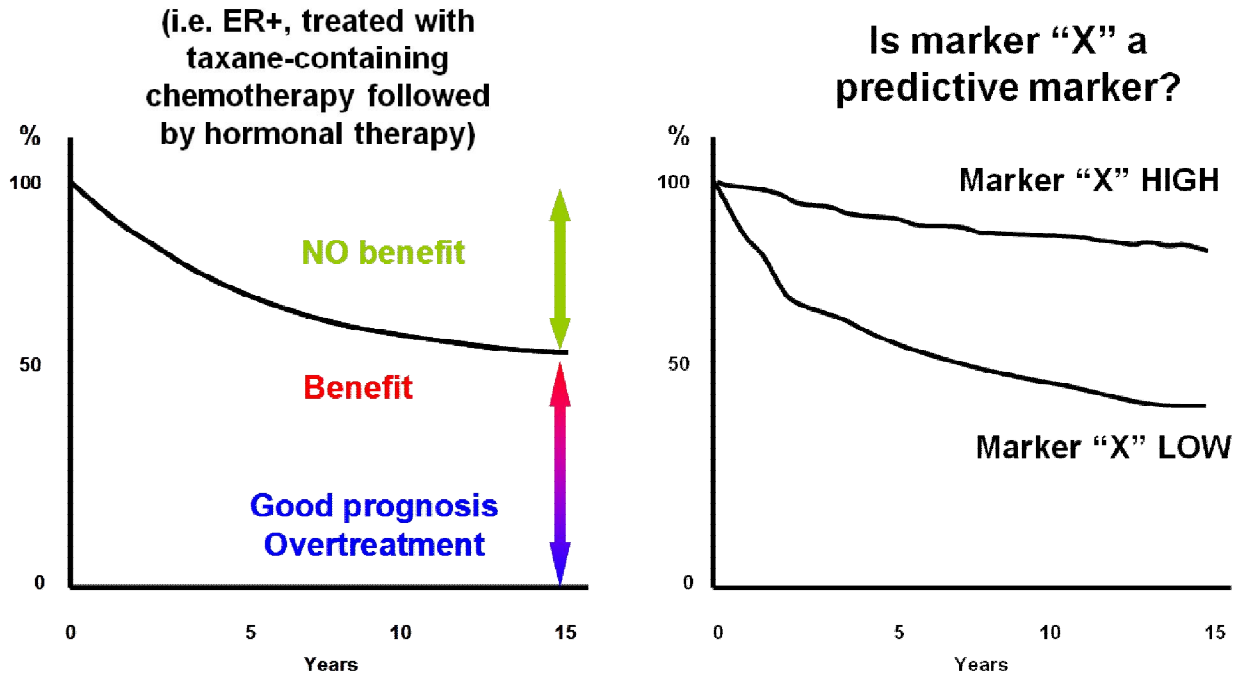

Figure 43: Can we derive predictive markers from time to event outcome in homogenously treated patients?

Which means we have a maker able to distinguish the time-based outcome. But the real problem is whether it is possible to derive such a time of marker using time to event outcome in homogeneously treated patients, which is the type of data sets that are available in our retrospective trials. In such a situation, like in the example referring to ER+ pts treated with chemotherapy and tamoxifen, it is very easy to be misled as show in the following example where we can erroneously think that a low genomic grade index (GGE) predicts a better

response. However if we look at the data stratified in a neoadjuvant context as residual cancer burden, (used to quantify pathological response) we clearly see that on the contrary it is the high GGI group that shows a better outcome.

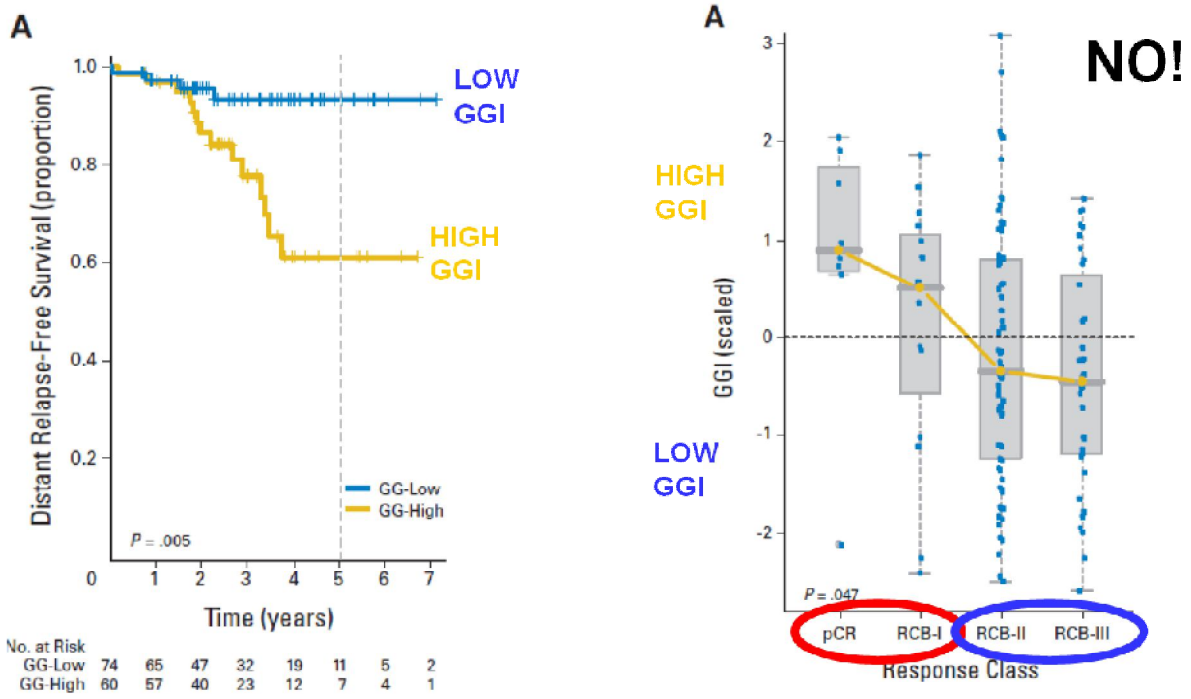

Figure 44: modified from Liedtke et al. (150)

This example clearly explains the difficulty of obtaining pure predictive markers in exploiting prospective-retrospective clinical trials.

The correct way for solving the problem is to perform a test for interaction between treatment and marker by stratifying the data according to the marker of interest.

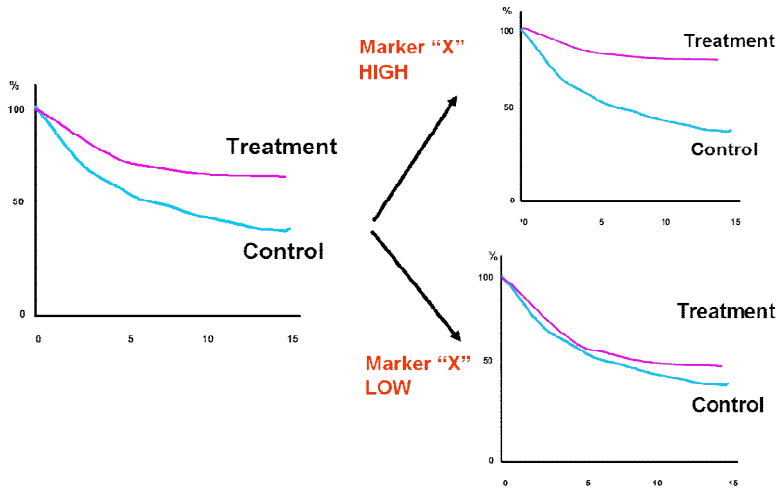

Figure 45: "Prospective-retrospective" clinical trial design. Test interaction between treatment and biomarker.

i. Available datasets for answering the clinically relevant questions

In this thesis we followed two approaches searching for a gene signature predictive of development of distant metastases in node negative patients receiving loco-regional treatment only, and trying to develop a genomic signature in the control arm (untreated) of node positive patients belonging to a historical chemotherapy trial run in our institution and setting the standards for future treatments worldwide. In such study of the early '70s the effects of CMF (cyclophosphamide, methotrexate, and fluorouracil) chemotherapy were evaluated as adjuvant treatment in 386 patients with operable breast cancer and histologically positive axillary lymph nodes (151). This pivotal randomized trial was the first to prove the benefit of adjuvant systemic treatment in breast cancer which was confirmed at 30 years' follow-up (152) and prompted the beginning of great improvement in breast cancer care. Adjuvant CMF administration benefit was confirmed also in a randomized trial included women with ER negative, node-negative disease (153).

In the attempt to improve the results of adjuvant CMF in patients with nodes positive breast cancer, two randomized studies introducing the use of the anthracycline doxorubicin were activated in the 1980's. In one of the studies restricted to patients with one to three positive axillary lymph nodes, a regimen of intravenous CMF for 12 cycles was compared to CMF for 8 courses followed by Doxorubicin for four courses on a total of 552 cases (154).

The studies of control versus CMF and the later study of CMF versus sequential administration of CMF and Doxorubicin have several interesting features that make them attractive for developing therapeutically relevant classifiers.

Both studies were conducted in a single institution and tumor specimens were collected and stored according to the same standard procedure. Patients were sufficiently homogeneous for stage of disease and standard category of risk, and were uniformly treated according to the same criteria for dose reduction, intervals of treatments and periodicity of follow-up. No adjuvant treatment other than chemotherapy was allowed (in particular, none of the patients received adjuvant tamoxifen). Either trials has been already used successfully for study conventional potential predictive biomarker (155;156). Moreover, a very long-term follow-up (157) confirmed quantitatively and qualitatively the initial findings, a feature that would allow for the generation of predictors of both short term and long term relapse. Finally the superior quality of the clinical data-base is internationally recognized.

Despite the strong reasons supporting the need of a control arm, which as described could only be available in the early pioneering studies, we run into a technical hurdle which was unfortunately an unresolved challenge. Historical samples in our Institution were fixed in Bouin, a picric acid fixative which preserves very well the histological morphology, but induces dramatic changes in the molecular structure of nucleic acids which appear degraded into small fragments and chemically modified interfering with the ability to retrotranscribe the RNA.

ii. The raise of a technical issue: Bouin

For preservation of tissue samples formalin fixation followed by embedding in paraffin has been the method of choice for decades. Other fixatives like Bouin have been quitted due to the poor performance in immunohistochemical reactions. With the development of molecular biology techniques there was a growing interest in the use of the vast archives of fixed paraffin-embedded (FFPE).

From a chemical point of view fixation induces degradation but also a chemical modification with the addition of methylol groups to the RNA bases (99).

This affects:

- *RNA amplification yields.*
- *Length of cDNAs derived from chemically modified RNA.*
- *Performance of qPCR* .

Despite these problems technical improvements and protocol amendments have allowed acquisition of biologically relevant gene expression data also from archival formalin-fixed paraffin-embedded (FFPE) tumors. Scanty data are instead available on Bouin-fixed paraffin embedded tumors (BFPE).

Since in our Institution Bouin fixation had been routinely used until 15 years ago, we attempted to develop protocol amendments which would allow the use of BFPE samples with results similar to those obtained in FFPE samples.

A great effort was spent on technical feasibility of the project especially concerning the possibility to obtain adequate RNA of a sufficient quality for obtaining non biased gene expression profiles.

The process of fixation and embedding itself, but also the long-time storage of tissue blocks in sub-optimal conditions, had a great impact on the quality of RNA affecting negatively the

outcome of GEP studies. We therefore addressed the two problems separately developing strategies to cope with fixation-induced artifacts and testing how far could we go with old samples without losing biological meaningfulness.

This was achieved through 3 consecutive steps:

- ❖ in **step one** we fixed good quality RNA extracted from MCF7 cells with either Bouin or buffered formalin and studied the effect of RNA chemical de-modification protocols on following technical endpoints.
  - RNA amplification yields.
  - Length of cDNAs derived from chemically modified RNA.
  - Performance of qPCR;
- ❖ in **step two** the same technical endpoints were evaluated for 20 RNAs from 30-years old BFPE breast tumors and for 6 RNA samples obtained from paired FFPE and BFPE tumors.
- ❖ Finally in **step three** the data quality and biological meaningfulness of gene expression profiles obtained with Affymetric U133 2.0 Plus chips and with the Illumina DASL assay were assessed.

Step 1: *restoration of ad hoc fixed RNA*

Fixation of isolated RNA with Bouin reduced RNA amplification yield by more than 90%, while fixation with formalin dropped the yield to about 50% of the control, unfixed isolated RNA treated with heat only (95°C), to mimic RNA degradation in the absence of chemical modification.

Heat treatment (60°; 70°; 80°C) with increasing temperatures for different time lengths (20 or 40 min) completely restored RNA amplification yields in the case of formalin fixation, while in the case of Bouin fixation the chemical de-modification protocol allowed only a partial restoration of amplification yields up to 50% of the control.

The size of the cDNA fragments obtained with the amplification protocol was measured using the RNA chip with the Agilent Bioanalyzer.

Fixation with Bouin dramatically reduced the cDNA product length which dropped to less than 40 nt, while it was around 100 nt after formalin fixation. The chemical de-modification protocol did not significantly improve cDNA length of Bouin fixed RNA, while it allowed the synthesis

of cDNA product similar in length to those obtained from heat-degraded unfixed RNA in the case of formalin fixation.

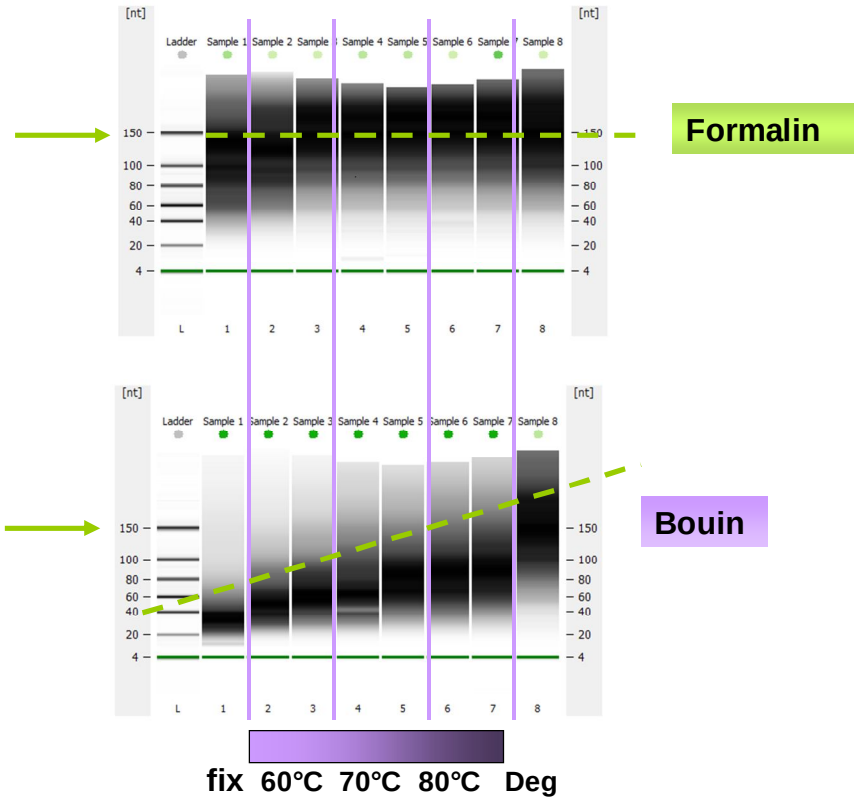

Figure 12: cDNA size: Bioanalyzer 2100, RNA chip

RNA fixed with formalin or with Bouin was used for carrying out TaqMan assays of highly expressed housekeeping genes. Amplification primers were chosen in order to obtain short amplification products, ie less than 80 bp.

The simple heat degradation (95°C) increased Ct values by about 1 cycle, formalin fixation caused approximately a 2 Ct increase, while under the same condition fixation with Bouin increased the Ct values by 12 cycles compared to heat-degraded RNA. The chemical de-modification protocol reduced Ct value, but never reached values comparable to those obtained on formalin-fixed RNA. Conversely, with short amplification products formalin fixed RNA did not “need” the chemical de-modification treatment.

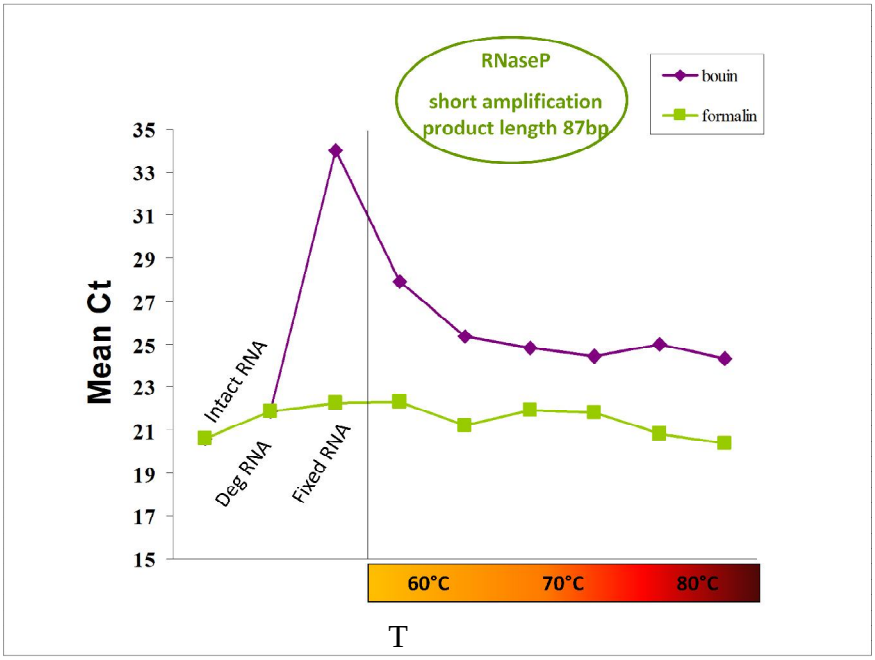

Figure 47: Ct variation for HK genes.

Chemical de-modification protocol based on heat treatment of RNA completely restores formalin-fixed RNA, but only partially restores Bouin fixed samples.

Step 2: *Application of 'restoration' protocol to archived samples (30 years old BFPE breast tumors and 20 years old matched FFPE and BFPE samples).*

When BFPE and FFPE matched samples were used for qPCR assays, Ct values were consistently lower for FFPE samples compared to BFPE samples, but again heat treatment did not always trigger a significant drop of Ct values.

Application of the chemical de-modification protocol to 30-year old samples did not allow a decrease of Ct values in all samples.

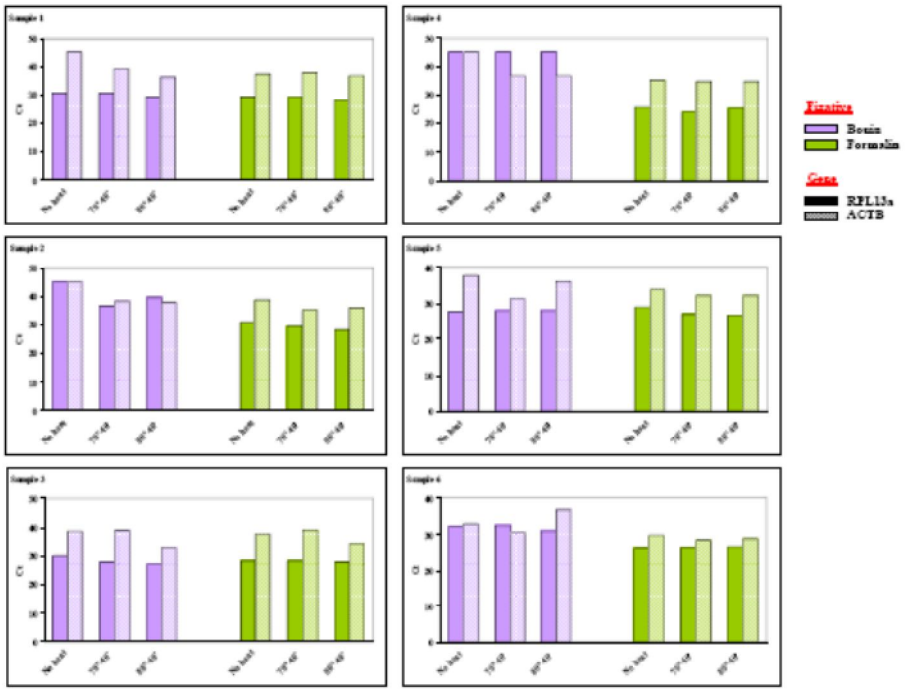

Figure 48: Ct variation after chemical de-modification.

Therefore, heat-treatment is not successful in restoring RNA obtained from old samples.

Step 3: *Gene expression profile from BFPE samples*

Sixteen RNA samples obtained from BFPE tissue and two samples from FFPE tissues were heat treated (80°C) and samples single-stranded c-DNA generated by WT-Ovation FFPE System (NuGEN) were optimal when hybridized on U133 2.0 Plus chips from Affymetrix (Fig.49a).

Despite the very low intensity values of the signal, controls gave good results indicating that the hybridization performed well. The two FFPE samples were characterized by higher present call percentages compared to BFPE samples. None of the Bouin fixed samples had however present calls above 8%, a value by far too low to obtain biologically meaningful results (Fig.49b).

The table summarizes the data.

a

ArrayID	Heat	quality	ER	Fix	% PRESENT
DNA9105-001	80	M	pos	Bouin	5.17
DNA9105-002	70	M	pos	Bouin	5.86
DNA9105-003	70	H	pos	Bouin	3.978
DNA9105-004	80	M	pos	Bouin	3.31
DNA9105-005	70	M	pos	Bouin	4.39
DNA9105-006	80	M	pos	Bouin	5.32
DNA9105-007	70	L	pos	Bouin	5.366
DNA9105-008	80	M	pos	Bouin	6.52
DNA9105-009	70	L	neg	Bouin	6.45
DNA9105-010	80	M	neg	Bouin	6.43
DNA9105-011	70	M	neg	Bouin	4.951
DNA9105-012	80	M	neg	Bouin	7.742
DNA9105-013	70	M	neg	Bouin	3.93
DNA9105-014	80	M	neg	Bouin	3.60
DNA9105-015	70	H	neg	Bouin	4.34
DNA9105-016	80	M	neg	Bouin	6.79
DNA9105-017	nT	H	neg	Form	16.35
DNA9105-018	nT	H	pos	Form	18.30

b

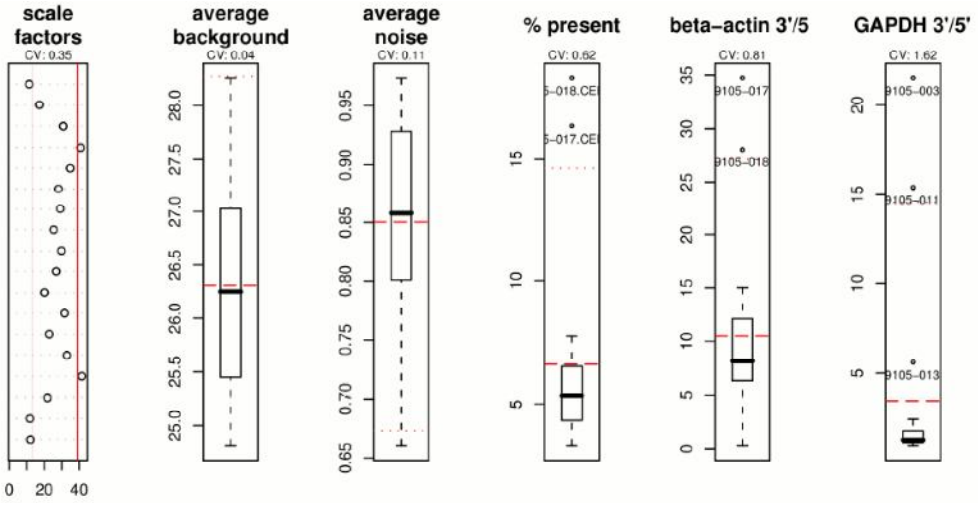

Figure 49: **a.** Present-Call of 18 samples hybridized on Affymetrix chip; **b.** hybridization quality control.

We therefore tried to us an alternative technical approach specifically designed for degraded samples: Illumina's cDNA-mediated annealing, selection, extension, and ligation assay-shortened to DASL is part of a powerful gene expression solution designed to generate reproducible gene expression profiles from degraded RNA samples. In twelve BFPE samples gene expression was determined with DASL and compared with the technical performance achieved on unfixed samples and in FFPE samples. These were characterized by correlation between duplicates around 0.9, while in BFPE samples R2 values ranged from 0.2 to 0.9. In

FFPE samples the number of detected probes ranged between 300 and 900, while for BFPE samples it was less than 300 and could be predicted by Ct values of housekeeping genes.

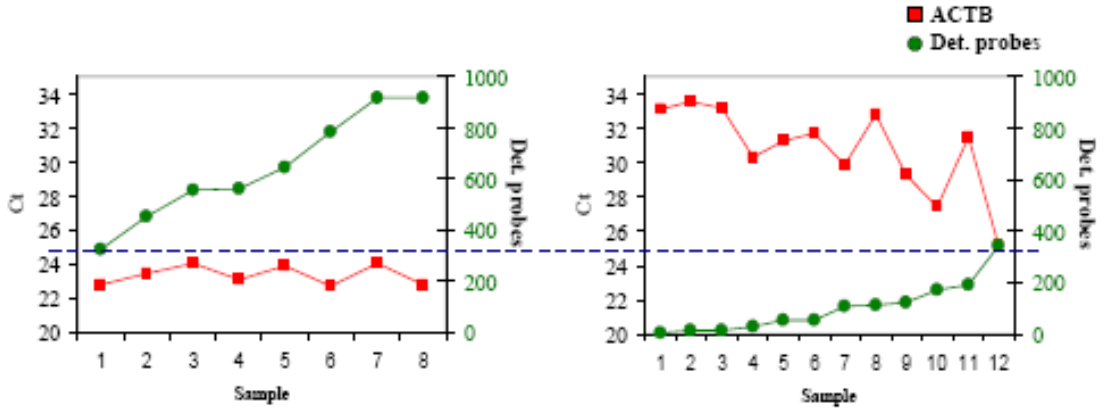

FFPE BFPE

Figure 50: 13 HK Ct *vs* detected probes

A closer look at the quality of data obtained with DASL using BFPE samples revealed dramatically dissimilar intensity signals (Fig.51a) and following unsupervised clustering many duplicates did not cluster together (Fig.51b).

a

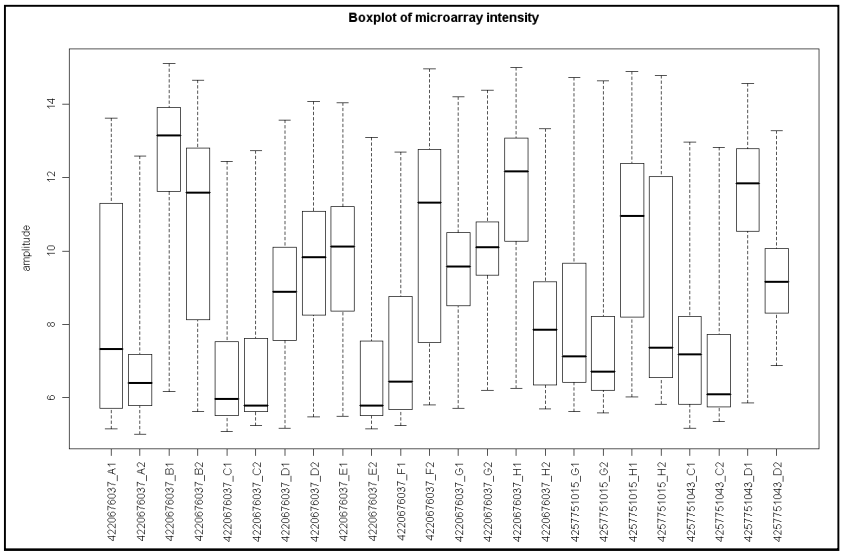

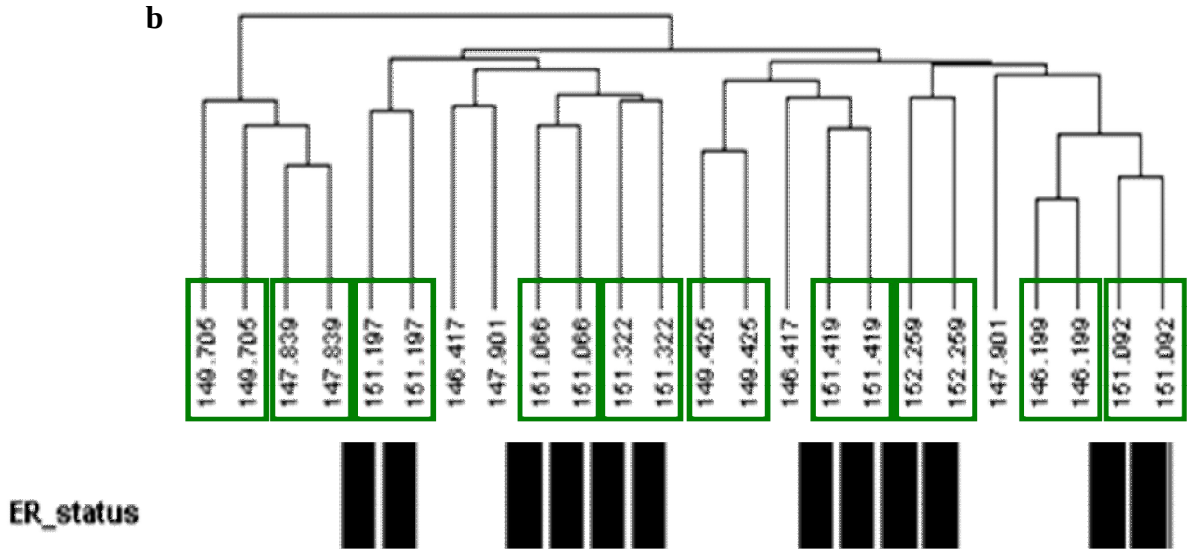

Figure 51: **a.** box plot of DASL intensity; **b**. unsupervised clustering of DASL data.

Furthermore, BFPE samples did not yield biologically meaningful results as can be seen from the fact that genes expected to be differentially expressed between samples with different ER status, did not differ significantly. This was also confirmed by cluster analysis which did not separate ER positive from ER negative samples (Fig.52).

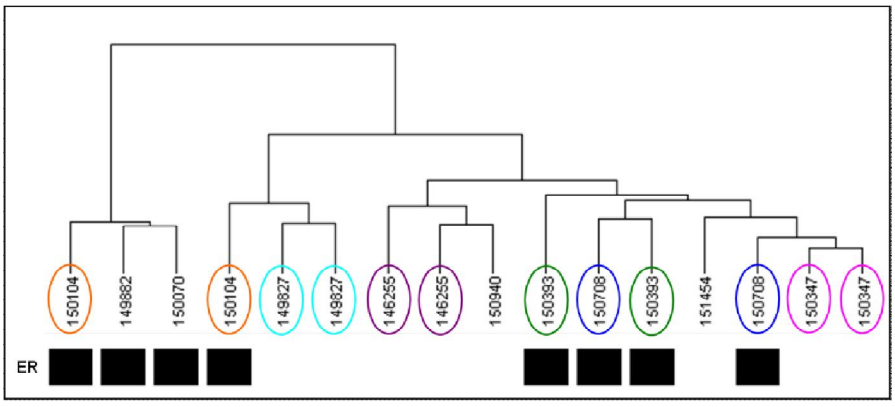

GENE	p-val
ESR1	0.33
GATA3	0.5
SCUBE2	0.2
BCL2	Filtered out
PGR	Filtered out
RERG	Filtered out

Figure 52: clustering analysis (left) and genes differentially expressed between ER+ and ER- (right).

These through experiments allowed us to conclude that while most of FFPE samples are suitable for gene expression analysis BFPE samples are of limiting value for gene expression analysis.

Partial restoration can be achieved by chemical de-modification protocol, but older samples do not allow obtaining neither technically satisfactory results nor biologically meaningful gene expression data by Affymetrix as well as by DASL.

As it was clear from our technical feasibility checks that aged BFPE samples are not suitable for obtaining GEPs, the project was redesigned in order to exploit a more recent trial where samples were fixed in formalin. In our preliminary experiments we had indeed demonstrated that formalin generates chemical modifications and crosslinks which do not interfere in reverse transcription, amplification and hybridization protocols used for obtaining a reliable expression profile.

iii. The ECTO data set

ECTO (European Cooperative Trial in Operable Breast Cancer) designed in 1996 is a multicenter, international, open-lab, three-arm, randomized phase III study conducted in 31 European centers.

It was designed to assess the effects of adding paclitaxel to an anthracycline-based regimen in patients with operable breast cancer, and to compare the same regimen given preoperatively and postoperatively.

A total of 1,355 patients with newly diagnosed unilateral, operable breast cancer larger than 2 cm at diagnosis, enrolled from November 1996 to May 2002, were randomly assigned to one of three treatments:

1. **Arm A:** surgery followed by adjuvant doxorubicin (A) (75 mg/m^2), every 3 weeks for 4 cycles, followed by cyclophosphamide, methotrexate, and fluorouracil (CMF) on days 1 and 8 every 4 weeks, for 4 cycles;
2. **Arm B**: surgery followed by adjuvant paclitaxel (T)(200 mg/m^2) plus doxorubicin (60mg/m^2), every 3 weeks for 4 cycles followed by CMF, on days 1 and 8 every 4 weeks, for 4 cycles;
3. **Arm C:** paclitaxel (200mg/m^2) plus doxorubicin (60mg/m^2) every 3 weeks for 4 cycles followed by CMF, on days 1 and 8 every 4 weeks, for 4 cycles and then surgery.

This study had two co-primary objectives:

1) to assess the effects on relapse-free survival (RFS) of the addition of paclitaxel to postoperative chemotherapy (arm B *vs* arm A);

2) to assess the effects of the primary chemotherapy versus adjuvant chemotherapy (arm B *vs* arm C).

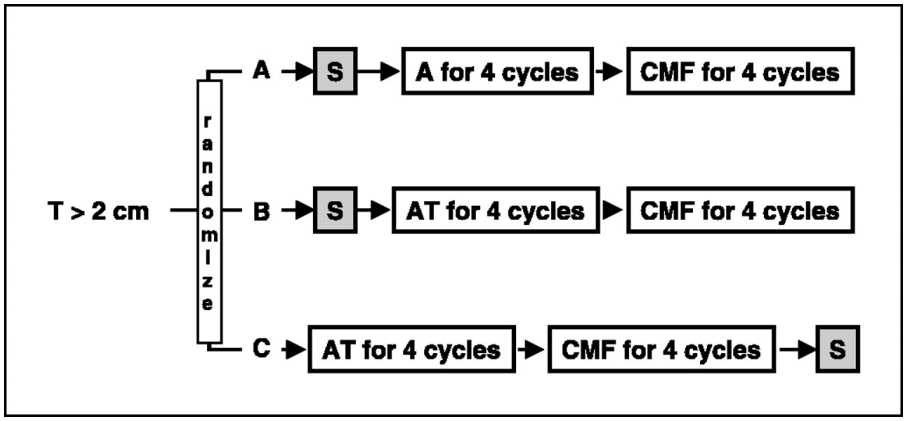

Figure 53: ECTO clinical trial design.

The ECTO study concluded that doxorubicin plus paclitaxel followed by CMF was well-tolerated as adjuvant or as primary chemotherapy. The addition of paclitaxel to adjuvant doxorubicin followed by CMF significantly improved RFS compared with adjuvant doxorubicin alone followed by CMF (hazard ratio (HR),0.73; *P*=0.03).

There was no significant difference in RFS when the paclitaxel/doxorubicin/CMF chemotherapy was given before surgery compared with the same treatment after surgery (HR, 1.21; *P*=0.18).

Finally when paclitaxel was given as primary systemic therapy it allowed breast-sparing surgery in the majority of patients without increasing local recurrence or compromising survival (158).

Based on our premises it appears clear that for a true individualized treatment it must be possible to predict the high probability to survive from standard cancer treatments. In line with such a concept the main purpose of the multifaceted work of this thesis was to define genomic predictors of survival following the actually best standard of treatment (Taxane antracycline chemotherapy followed by hormonetherapy), it means define a pure **context-specific predictor** to be able to

- identify patients who will do well with standard treatments;
- identify patients who should receive more intense treatments or new drugs.

As explained it is therefore important to consider both pure prognostic aspects as well as specific drug sensitivity markers.

vi. New technical challenge

Formalin fixation and paraffin embedding is the standard procedure used to preserve tissue morphology and for tissue archiving. Samples collected and preserved during decades of work are an extremely rich source of material for clinical studies. On the contrary few repositories exist where frozen samples have been collected.

Processing of FFPE samples is however affected by many confounding factors linked to the extreme variability in the tissue handling and fixation times. The obtained RNA is highly degraded and chemically modified by the chemical cross linking promoted by formalin. Most of times short RNA fragments lack the polyA tail and are not very efficient templates for reverse transcription.

Additional variability derives from the length of storage with older samples usually yielding worse results.

Despite all the listed problems, formalin, according to our preliminary results, did not generate such chemical modifications and cross-links as observed with Bouin, which were limiting for the reverse transcription, amplification and hybridization protocols used for obtaining a reliable GEP. If successful, the development of a technical protocol to obtain reliable GEPs from FFPE would open the access to many other patient series (beyond the one analyzed for the purpose of our study) accelerating biomarkers discovery not only in breast cancer, but also in other tumor types.

Nonetheless, attempting to obtain clinically useful GEPs from archived samples over 10 years old and multicenter collected not an easy task and therefore we went through an extensive technical assessment by comparing different microarray platforms, by running a pilot study on a limited number of samples and by assessing the biological reliability of our samples.

4.3 TECHNICAL INSERT

4.3.1 EXPLORATIVE STUDY TO ASSESS FEASIBILITY OF MEASURING GENE EXPRESSION ON FFPE SAMPLES WITH ARRAY PLATFORMS

As frozen samples represent the golden standard in array methods our initial assessment focused on 10 matched fresh frozen (FF) and FFPE samples. Frozen samples were processed with the Illumina platform (HT12, 48,000 genes), and compared to FFPE paired samples processed with either the specific low quality/low input RNA approach DASL (Cancer Panel, allowing assessment of the expression levels of 502 cancer genes) or processed with the standard Illumina Ref8 assay allowing assessment of 24,000 genes following linear amplification with the NuGEN WT- Ovation FFPE V2 kit.

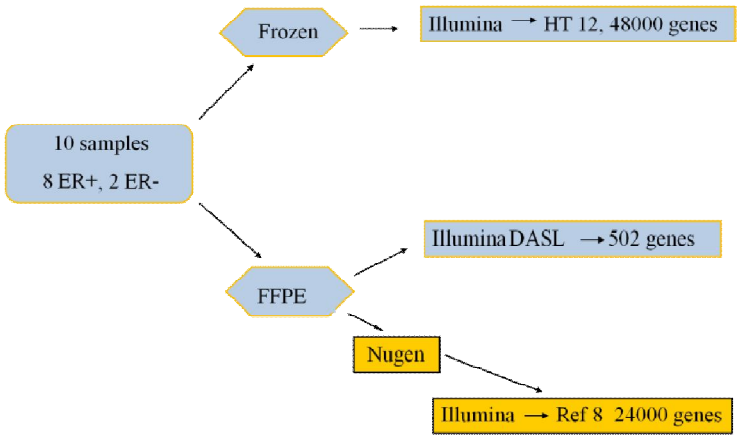

Figure 54: scheme of 10 samples study.

In the FF samples the probe detection rate ranged from 0.45 to 0.55, while with FFPE samples it hardly reached 0.35. Clustering analysis with 6074 probes common between frozen and FFPE samples (analyzed with the Ref 8 Illumina platform), yielded the expected separation between estrogen receptor positive (ER+) and ER negative (ER-) samples only for FF samples and not for FFPE samples. On the average the correlation between gene expression evaluated with the two methods was rather low (median value=0.31).

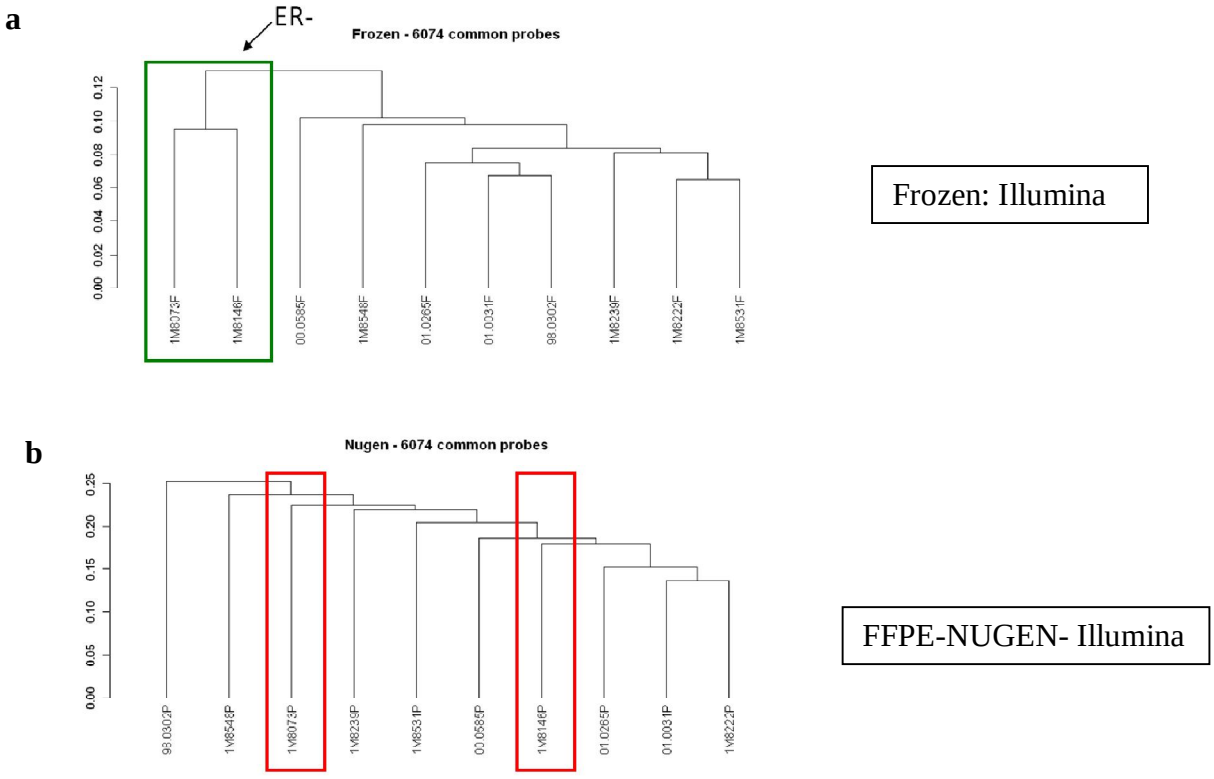

Figure 55: **a.** clustering analysis for frozen samples after hybridization on Ref8 Illumina platform; **b.** clustering analysis for FFPE samples after hybridization on Ref8 Illumina platform.

On the contrary, when FFPE samples were processed with the DASL arrays the two ER- samples clustered together either based on the expression of 999 DASL probes or based on the expression of 198 genes in common between all three tested procedures.

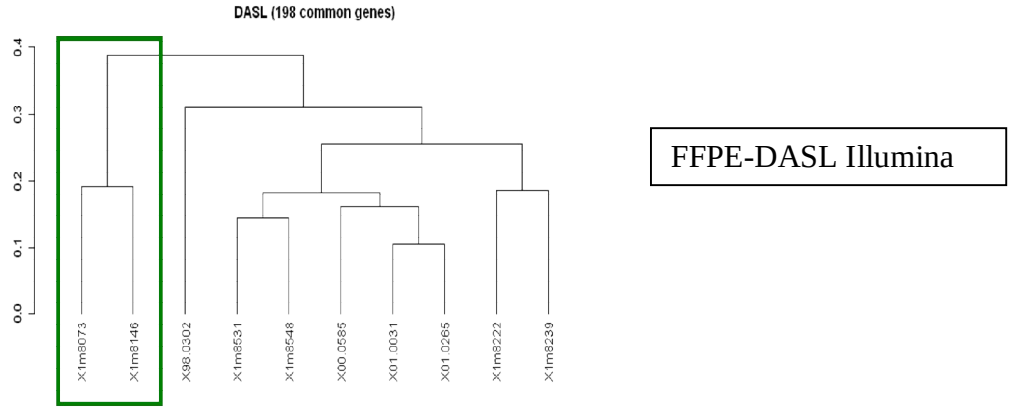

Figure 56: clustering analysis for FFPE samples after hybridization on DASL Illumina platform.

Despite the suboptimal results obtained with the Illumina platform with respect to the DASL platform, the DASL was discarded due to a low dynamic range (data not shown), and a second experiment was run using 12 breast cancer samples where only FFPE blocks were available. The samples were chosen in order to have 6 ER+ and 6 ER- cases to allow class comparison analysis, as this could be useful for choosing between different technical approaches based on the obtained DE genes. The figure below reports the experimental design.

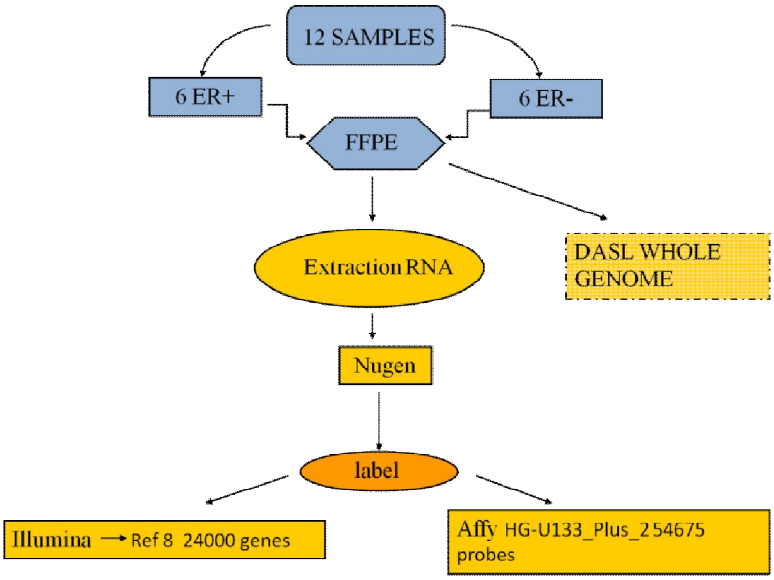

Figure 57: scheme of 12 samples study.

As can be seen RNA was amplified and labelled using two distinct strategies to be used with the Illumina platform and the Affy HG U133 Plus chips. The Affymetrix chips were chosen as they represent the most commonly used gene expression chips in clinical studies with frozen samples and therefore, obtaining GEPs on this platform would assure a better comparability of the data with the literature.

Clustering results are reported hereafter using 6535 probes from the Illumina platform.

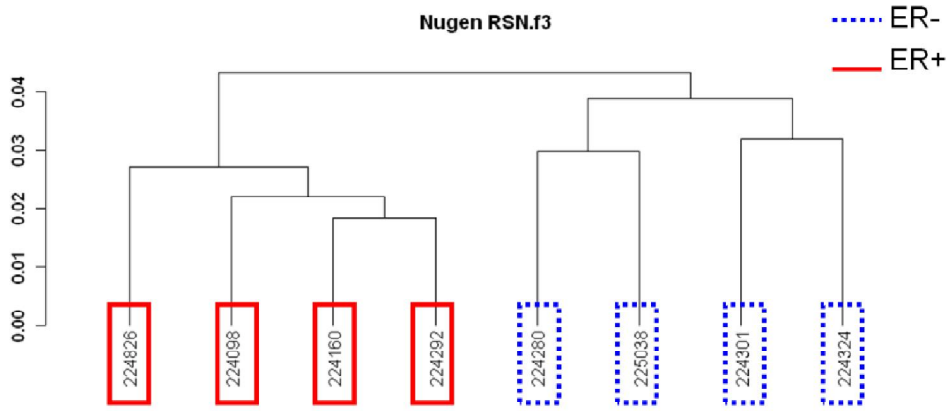

Figure 58: clustering analysis for FFPE samples after hybridization on DASL Illumina platform.

Despite the fact that samples were FFPE, using the Illumina platform it was possible to separate the samples according to the ER status. However, some of the probes raised concerns, like the *BCL2* and the GATA3 genes, expected to be strongly correlated to *ESR1*, and showing instead a correlation R^2= 0.05 and R^2=0.19 respectively. This suboptimal performance was also noticed looking at the genes DE between ER+ and ER- samples. Some of the genes expected to be DE (GATA3, BCL2) did not reach statistical significance.

GENE	P-val
ESR1	0.0496
GATA3	0.2649
SCUBE2	-
BCL2	0.1120
PGR	-
RERG	0.0643
GREB1	0.0024

Table 17: different expression genes between ER+ and ER- samples.

Affymetrix data were also extensively evaluated. The box plots indicated low signal intensities and some variability among the samples. The present calls were rather low on the average, ranging from 17% to 40%. The same type of variability was confirmed by the degradation plots which suggested that some samples did not pass quality controls.

In order to set up a pre-analytical quality control for future studies, the obtained Present Calls (PC) were correlated with a Ct value obtained with a standard protocol for qPCR of the *RPL13a* gene on a small aliquot of sample after the first step of the amplification procedure.

As can be seen in the graphs below there was a good correlation between the two measures (Ct and PC) and we arbitrary chose the Ct value of 37 as cutoff for sample pre-assessment as samples with Ct values higher than 37 had PC% under 20%.

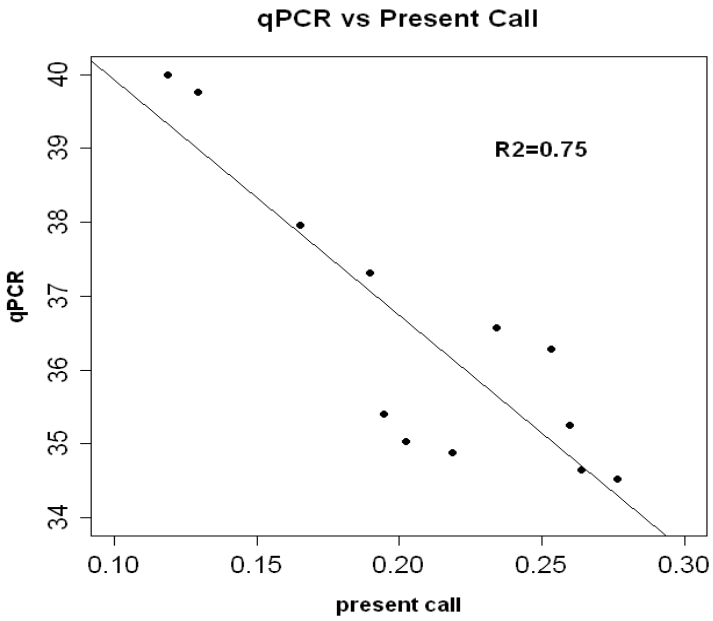

Figure 59: scatter plot of RPL13a qPCR as a function of present call

Also after removing samples of bad quality, the clustering analysis did not allow to separate ER+ (dotted blue line) from ER- (solid red line) samples.

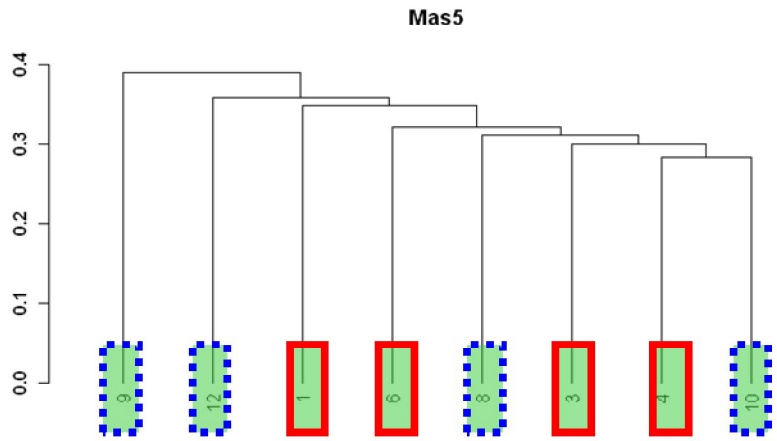

Figure 60: clustering analysis for FFPE samples after hybridization on Affymetrix platform.

However, in the case of GEPs obtained with the Affymetrix platform correlations between expression of genes expected to be correlated were higher compared to those reported for Illumina (GATA3 *vs* ESR1, R^2=0.61; RERG *vs* ESR1, R^2= 0.56; BCL2 *vs* ESR1, R^2= 0.31).
The genes expected to be DE among the two ER subgroups were actually found and were statistically significant. On the average looking only at the 8 samples which passed QC, 134 probes were found to be DE at $p<0.01$ and the top genes were biologically reasonable.
Due to its better performance and to its wide use in clinical studies, we chose to use the Affymetrix U133 2.0 plus chips for our further analyses.

4.3.2 THE PILOT STUDY

The pilot study was carried out to:

1. assess on a testing series of adequate size the proportion of retrospectively clinical samples effectively suitable for GEPs with our standardized protocol;
2. evaluate the quality and biological meaning of the derived GEPs by comparing these results (e.g. comparison between ER+ and ER-) with those expected with similar GEPs derived from frozen samples (confirmatory analysis)

with the final aim of applying the technically and biologically verified protocol on samples collected within a clinical trial.

Sixty clinical samples from patients with breast cancer who underwent radical mastectomy at the Fondazione IRCCS Istituto Nazionale dei Tumori of Milan, and were treated with adjuvant chemotherapy (A→CMF) similarly to the ECTO I patients approximately in the same time lapse (1998-2002) were used to estimate the proportion of successful GEPs. Sixty-five % of patients were ER+.

After pathological assessment to assure that the tissue blocks were representative 5 samples (8.3%) were lost. RNA was extracted from 2 sections (20µm each) and quantified. Mean yields were 17±9 µg/ sample.

A pre-analytical sample assessment was implemented to avoid to profile bad quality RNA on expensive chips. It consisted in two steps: qPCR for the housekeeping gene RPL13A and capillary electrophoresis of the obtained aDNA to remove samples with too short amplicons.

The size of the aDNA was found to be very critical for obtaining high present calls with the Affymetrix chips and had to be considered in association to the Ct value cutoff already described. In fact samples with similar cutoff values could still yield variable present calls once hybridized on the chip.

An example is reported for 6 samples with the same Ct value but with

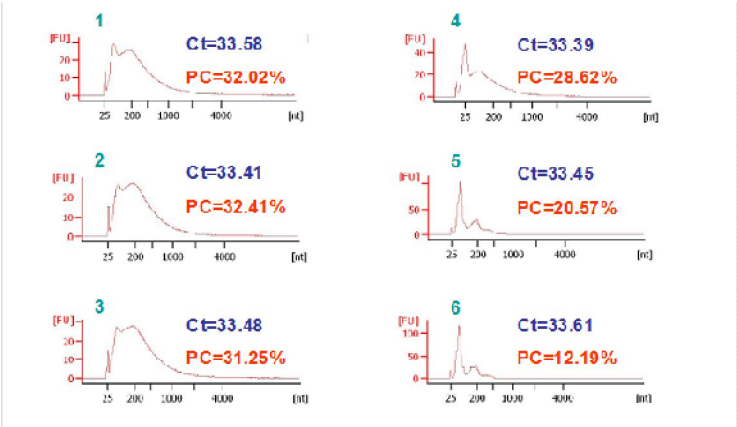

Figure 61: output of bioanalyzer analysis

Therefore based on the two combined criteria further 7 samples were excluded from the analysis, and thus a total of 55 amplified samples were hybridized on Affymetrix U133 2.0 Plus chips.

A post hybridization QC reveled that 2/46 samples presented abnormal intensity levels as shown in the box plot and the same samples clustered separately showing low correlation with the rest of the samples. They were therefore excluded.

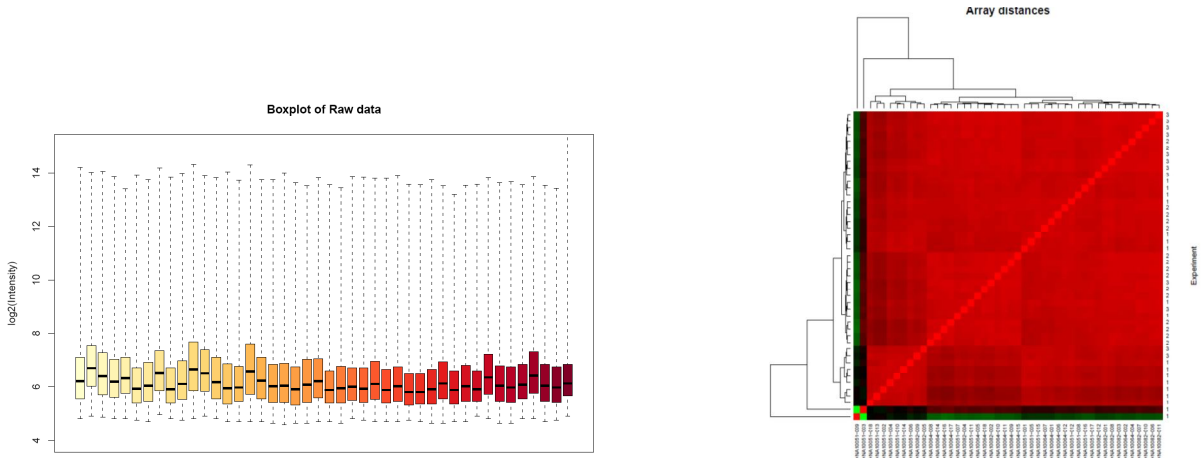

Figure 62: quality control of data from 46 FFPE samples. Box plot (left) and reciprocal correlation of samples (right).

The remaining GEPs which passed the quality control showed a uniform distribution of intensities and a relatively high PC rate (median PC=30%).

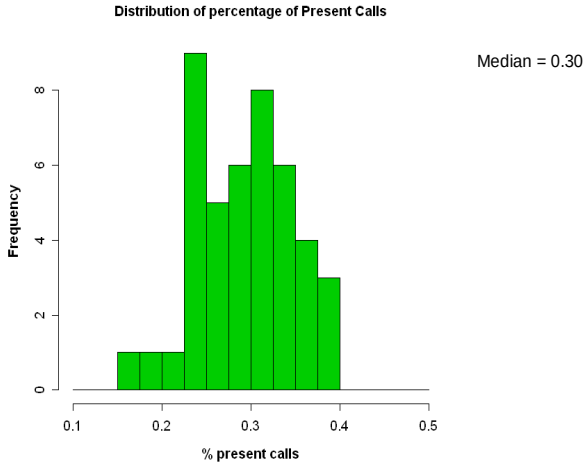

Figure 63: distribution of percentage of Present Call

In order to check if the type of information provided by GEPs obtained from FFPE samples was comparable to that of frozen samples, a set of 8 genes consistently found to be differentially

expressed between ER+ and ER- samples was used to cluster our samples. Tumors separated into two groups according to the ER status. Only two samples were incorrectly classified.

Such results confirm the technical feasibility to produce gene expression profiles technically ***reliable*** and ***biologically meaningful*** on about 75% of unselected FFPE archival material from patients enrolled in clinical trials using the developed protocol. As expected the use of archival material leads **to loss** of part of the samples:

- 8% due to poor pathological sampling during preparation of tissue blocks;
- 13% due to poor quality RNA which interferes with the amplification process.
- Finally, as estimated on the basis of this series, an additional 2% of gene expression profiles obtained may be unreliable due to low PC.

A sample pre-assessment step is mandatory to identify critical samples not worth to hybridize on chips.

4.3.3 BIOLOGICAL RELIABILITY OF FFPE DATA

Our pilot study, allowed us to identify the best and robust technical strategy applicable to ECTO I samples. The identified strategy was therefore applied to samples derived from the arm B (adjuvant) and their biological meaningfulness was evaluated and later was applied to samples derived from arm C (neoadjuvant).

Pre-analytical sample assessment led to a higher loss of samples compared to the pilot study probably due variations in tissue handling and processing (length of fixation in formalin, type of buffer incorporated in the fixative) as expected in a multicentric study (99).

Indeed 272 initially selected surgery samples dropped to 162 after pathological assessment of samples and technical pre-assessment of aDNA and core biopsy samples dropped from 192 to 121(ranging from around 26% to 40%) (Table 17a Fig. 64). Table 17b show ER and grading characterization of ECTO sample profiled.

a	Pilot study	Adjuvant arm Surgery	Neo-adjuvant arm Core biopsy
Total samples	60	272	192
Pathological assessment	55	234	173
Technical Pre-assessment +Total samples profiled on Affymetrix chip HG-133_PLUS_2	44	162	121

b	Neo-adjuvant arm Core biopsy	Adjuvant arm Surgery
ER		
pos	50	56
neg	71	105
missing	0	1
Grade		
1	9	16
2	70	100
3	41	41
missing	1	5

Table 17: **a.** loss of samples for pre-analytical and analytical factors; **b**. ER and grading characterization of ECTO sample profiled.

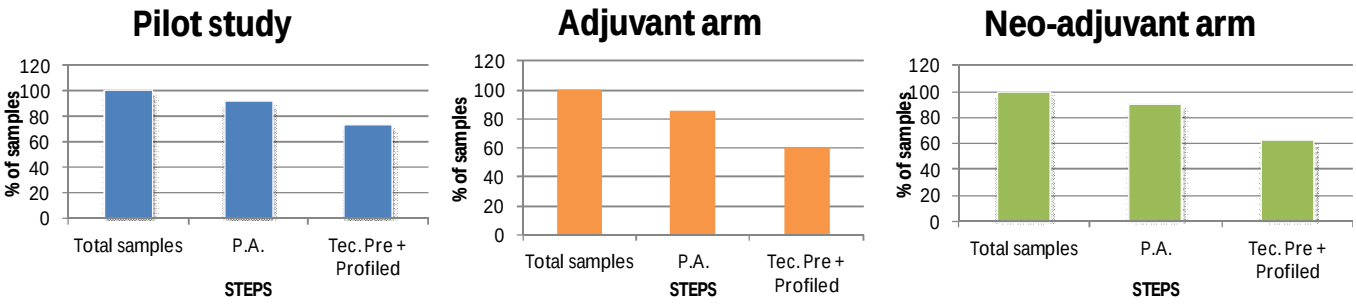

Figure 64: loss of samples for pre-analytical and analytical factors.

162 obtained from ECTO arm B and 44 from the pilot study (matched with ECTO I samples by year at diagnosis) were used to check the biological and technical reliability of the obtained GEPs.

The median Present call (PC) obtained was quite low (PC=26.2) with a wide distribution, essentially in agreement with literature data for FFPE samples. In fact the higher PC values obtained in FFPE samples were comparable to the lowest ones derived from frozen samples.

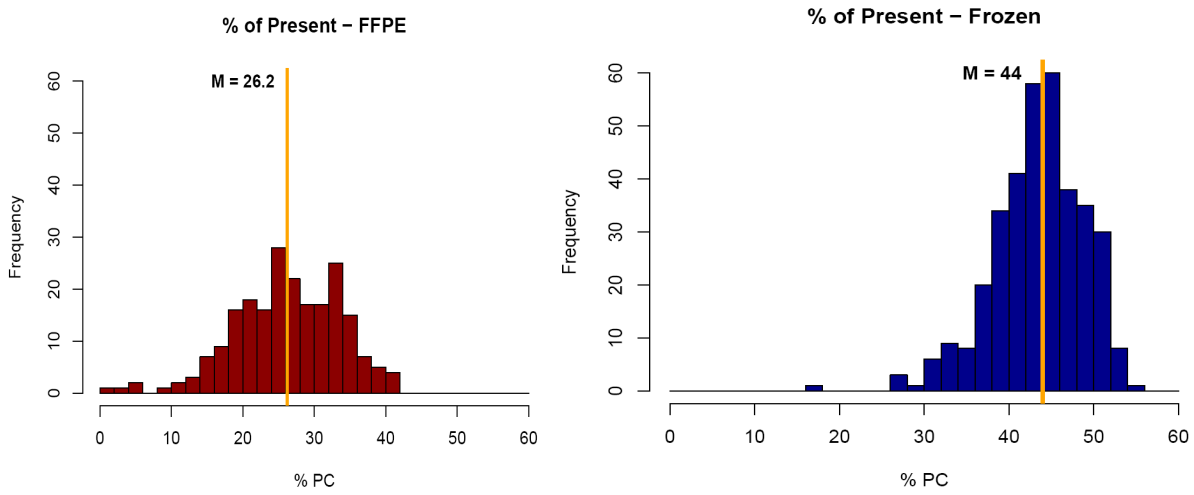

Figure 65: distribution of percentage of Present Call. FFPE samples (left) and Frozen samples (right).

An inverses and still good correlation between PC% and Ct values for the housekeeping gene RPL13, as observed in the pilot study, was confirmed also in this larger data set.

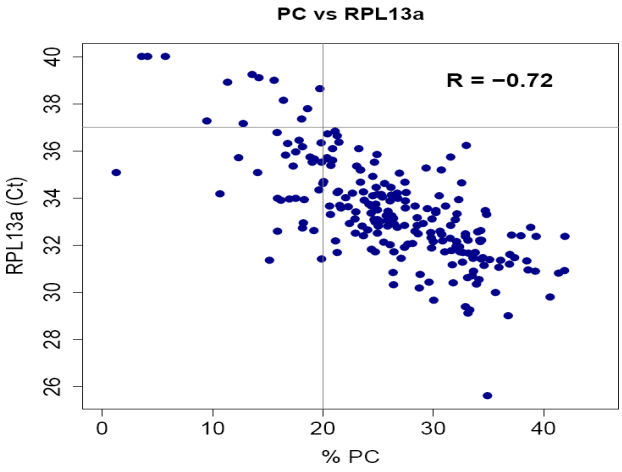

Figure 66: scatter plot of RPL13a qPCR as a function of Present Call

To specifically evaluate the biological meaningfulness of our data we used two main criteria:

a) correct clustering according to ER and ERBB2 status;

b) suitability to develop clinically relevant predictors.

a) After array quality control we were left with 204 samples which we clustered using 12 probe sets targeting genes from the ERBB2 amplicon (GRB7, ZNFN1A3, PPP1R1B, NEUROD2,

STARD3, PERLD1, CRKRS and ERBB2). For each sample a label referring to HER2 status obtained by IHC was available. Label are reported at the bottom of the figure considering either HER3+ cases alone a HER2+and HER3+ cases together. The two clusters defined by GEP data showed a good agreement with IHC data, indirectly confirming the good quality of the data.

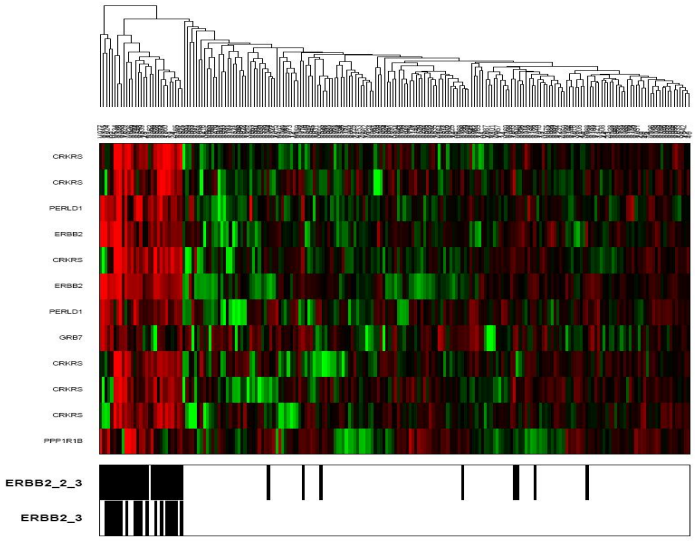

Figure 67: clustering of 204 samples using ERBB2 amplicon genes and compared with IHC data.

To further asses the biological reliability of the GEPs obtained from FFPE, 167 samples (for which ER status defined by IHC was available) were clustered using ER-related genes (GATA3, CA12, SCUBE2, RERG, GREB1, PGR, NAT 1).

Again, the two obtained clusters were in good agreement with ER status determined either by IHC or by ESR1 gene expression (ESR1 was not included among the ER-related genes).

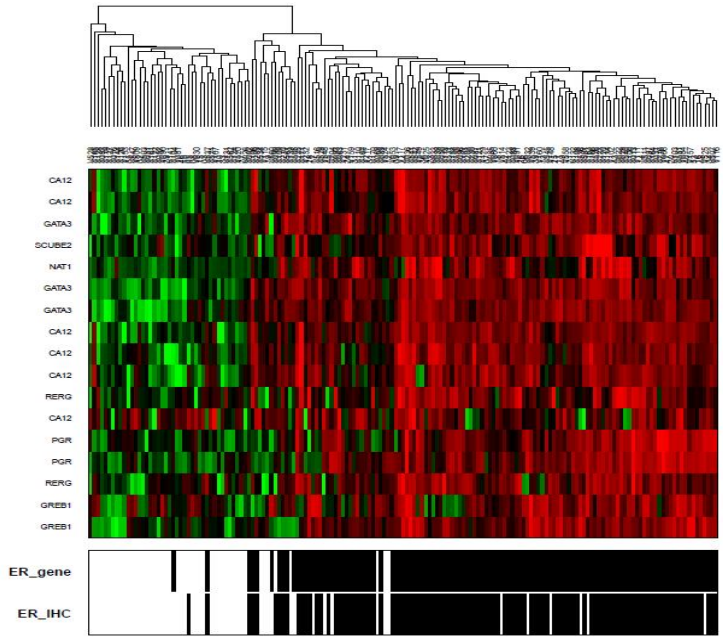

Figure 68: clustering of 2167 samples using ER related genes and compared with IHC data.

b) To evaluate the suitability of our GEP data obtained from FFPE samples to build classifiers we used a publicly available data set (GSE2109) of frozen samples obtained from different tumors and selected 165 breast cancer samples where there was an agreement between ER status determined by ESR1 gene expression and by IHC (119ER+ and 46ER-).

On such training set an ER status classifier was developed by Prediction Analysis of Microarrays (PAM) using the Set Index gene list (159). The classifier was then challenged on two independent frozen datasets of 127 (160) and 684 (pooled from (GSE2034, GSE7390, and GSE11121) samples and on our FFPE data set of 204 samples.

In the Lu dataset of 127 samples (77 ER+ and 50 ER-) profiled by *Affymetrix chip HG-U133_PLUS_2*, using our classifier we obtained a prediction accuracy of 0.96 (0.91-0.99) with a Cohen's k 0.92 (0.85-0.99) with either the IHC- or gene-determined ER status.

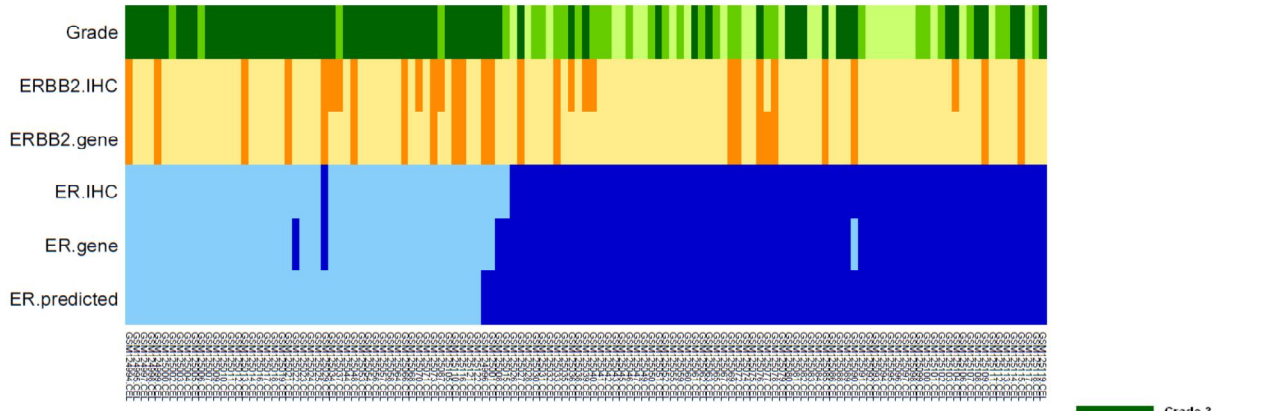

	Accuracy	Cohen's k
Gene	0.96	0.92
IHC	0.96	0.92

Figure 69: graphical representations of classifier performance on Lu dataset.

In the second pooled dataset of 684 samples (514 ER+ and 170 ER-), profiled with *Affymetrix chip HG-U133A*, the prediction accuracy was 0.96 (0.95-0.98) with a Cohen's k of 0.91(0.87-0.94) when the ER label derived from gene expression was used and 0.90 (0.87-0.92) with a Cohen's k 0.75 (0.69-0.82) when using ER status defined by IHC.

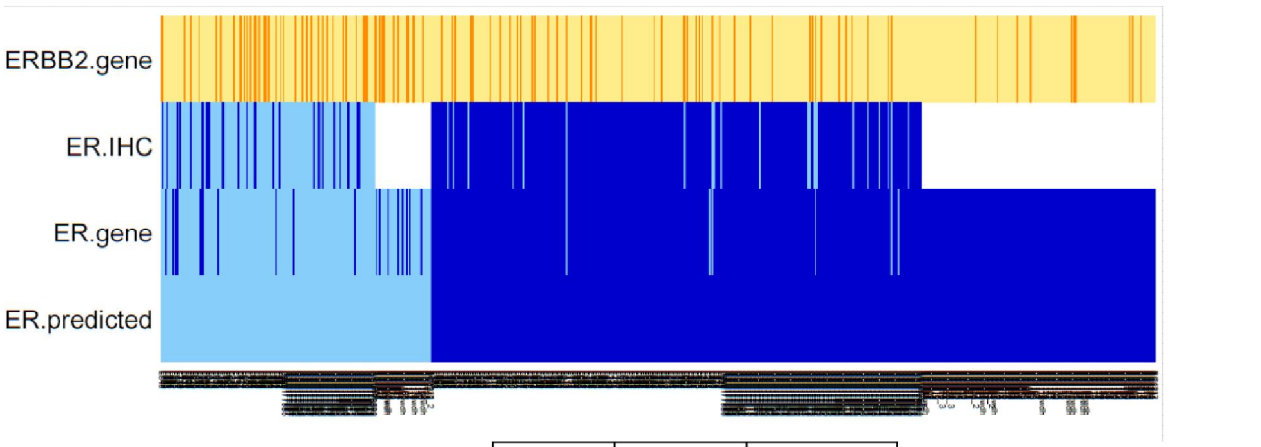

	Accuracy	Cohen's k
Gene	0,96	0,91
*** IHC**	0,90	0,75

* Computed on 484 samples with available IHC.

Figure 70: graphical representations of classifier performance on pooled dataset.

Using our ECTO FFPE data set of 206 samples (146 ER+ end 170 ER-) profiled by our technical protocol we obtained a prediction accuracy of 0.96 (0.92-0.98) with a Cohen's k of 0.89 (0.82-0.96) with respect to ER status defined by gene expression and of 0.90 (0.67-0.79) with a Cohen's k 0.76 (0.66-0.89) with respect to ER status defined by ICH. Prediction accuracies obtained in our FFPE data set using GEP determined with an improved technical protocol were therefore not different from the ones obtained on frozen datasets. This is an indirect proof of the good quality of our gene expression data.

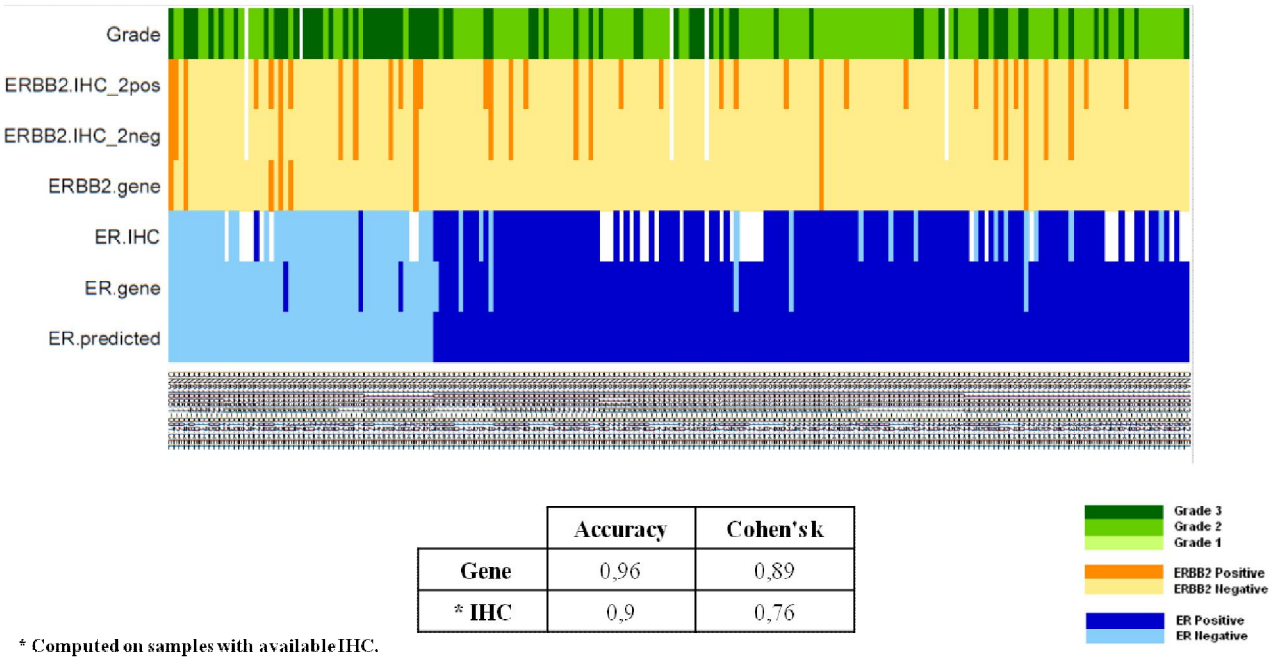

	Accuracy	Cohen's k
Gene	0,96	0,89
*** IHC**	0,9	0,76

* Computed on samples with available IHC.

Figure 71: graphical representations of classifier performance on ECTO FFPE dataset.

It is therefore fair to conclude that gene expression data obtained from FFPE are biologically reliable as gene expression data obtained from frozen samples. FFPE samples can definitely be used to generate GEP data to be used for clinical prediction purposes, especially if an accurate sample pre/assessment procedure is applied to discard samples predicted to be unreliable. The low PC rates obtained in FFPE samples do not preclude the possibility to gain biological information.

4.4 THE DATA ANALYSIS ISSUE

4.4.1. DEVELOPMENT OF AN OPTIMIZED PROCESSING PIPELINE FOR AFFYMETRIX GENE EXPRESSION DATA DERIVED FROM FFPE SAMPLES

As demonstrated before, ad hoc optimized protocols using the Affymetrix HGU133 Plus 2.0 microarray platform following amplification with the NuGEN WT-Ovation FFPE System proved to yield biologically meaningful gene expression profile data from FFPE clinical samples. Nevertheless, high frozen-FFPE discrepancies remain in expression data. In their dataset (GSE19246), Williams et al. (161) processed 59 matched frozen and formalin-fixed DLBCL patient samples belonging to two distinct prognostic subgroups and, after standard data processing procedures, reported 1428 genes as differentially expressed (DE) with a false discovery rate (FDR) <5% between the two subgroups when expression data from frozen samples were used; however only 289 genes were found to be DE when using expression data from corresponding FFPE samples at the same FDR threshold. Moreover, only 35 of the top-100 differentially expressed genes were in common.

We therefore developed a data analysis pipeline able to improve expression data obtained with the Affymetrix platform in FFPE samples. In the Affymetrix platform, each gene can be measured by different probesets and the signal of each probeset is obtained by combining the signals coming from 11 independent probes. Between the time where the probes for a given chip were designed, and the time an analysis is made, the transcript annotation might have changed. As a consequence, probe re-annotation was demonstrated to improve data quality. This can be practically done by creating alternative Chip Description Files (aCDFs) where only probes of interest are used and probesets are redefined (162).

An alternative Chip Description File (CDF) where only probes unambiguously mapping RefSeq transcripts were retained was created, thus removing poorly informative probes and creating a single probeset for each gene (hereafter we refer to this alternative CDF as RefSeq_all). A total of 16,991 probesets were generated and about half of them (45.3%) contains more than the 11 probes present in standard Affymetrix probesets (Fig.72), thus increasing the statistical power in measuring expression levels.

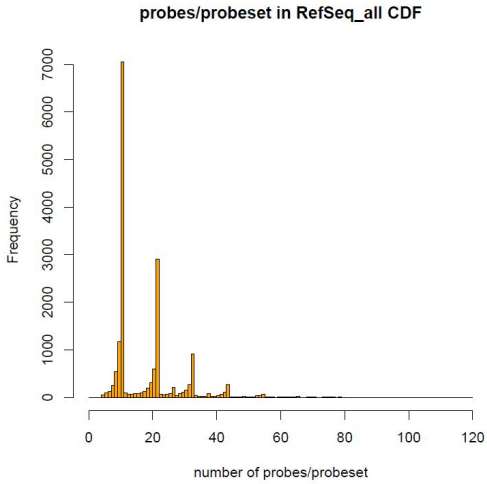

Figure 72: Number of probes in each probeset in the *RefSeq_all* CDF

Using the standard Affymetrix CDF and looking at the 11 probes in each probeset taking into account their distance from the 3'-end, we had noticed a decay in their signal intensity moving toward the 5' also in frozen data. But this effect was much more marked in FFPE data (Fig.73).

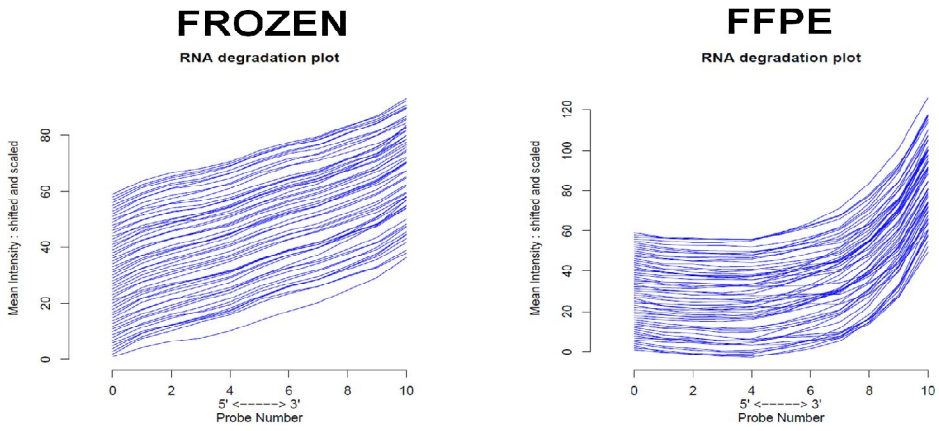

Figure 73: RNA degradation plot for the frozen (left) and FFPE (right) data

This was not surprising since, despite the use of a combination of random primers and oligo-dT in the amplification step, a 3'-biasis still expected as a consequence of fixation and RNA degradation. We therefore hypothesized that probes nearer to the 3'-end could be the more informative and reliable in FFPE data.

To verify it, after the probe re-annotation described before, we computed the distance from the probe to the 3'-end of the transcript. The correlation between frozen and FFPE data turned out to be inversely correlated with such distance (Fig.74).

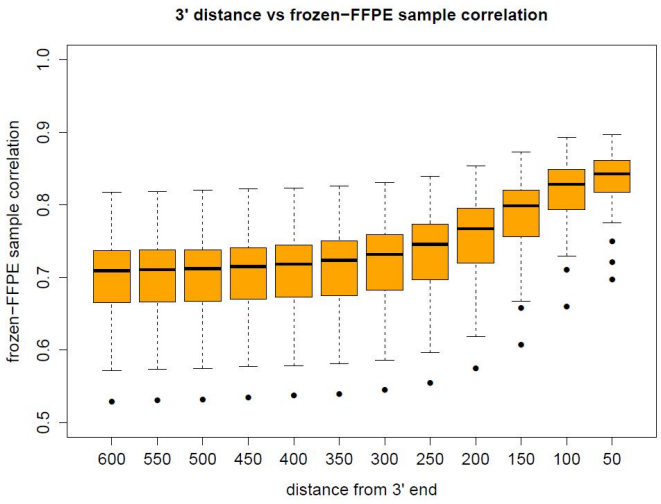

Figure 74: Frozen-FFPE correlation and distance of the probes from 3'-end.

Based on this observation, we created a second CDF using for each transcript only the five probes closest to the 3'-end and in any case mapping within 300 bp from the 3'-end (this alternative CDF was called RefSeq_dist). Using such criteria it was possible to define 8,263 probesets, in which the reliability of each probe was likely to be increased, despite the number of probes measuring each gene was reduced.

To verify the utility of our alternative data analysis approach, we tested the agreement between Frozen and FFPE data in the William's dataset, after processing the raw data with one of the Affimetrix standard CDF, the RefSeq_all CDF or the RefSeq_dist CDF. As processing methods we considered MAS5 and RMA, the two most commonly used algorithms for Affymetrix data, together with fRMA, a recently developed method that allows single array processing (118), which is important in biomarker development studies where the final goal is to obtain the gene-based classification of a single sample.

Three out of 59 matched samples were removed from our analysis due to poor quality of FFPE data.

We considered the results obtained from frozen samples as the gold standard, and rated the processing pipelines based on various measures of concordance between frozen and FFPE samples. Specifically we measured the following quantities: a) frozen-FFPE sample correlation

and frozen-FFPE probeset correlation; b) frozen-FFPE fold change correlation and slope; c) percentage of DE genes in data from frozen samples called as DE in FFPE data; d) number of common genes among top-100 DE genes in frozen and FFPE data. Results obtained for each combination of processing algorithm (MAS5, RMA, fRMA) and CDF (standard, RefSeq_all and RefSeq_dist) are reported in Table 18. From the data processed with the standard CDF, we also extrapolated the subset of probesets mapping on genes targeted in the RefSeq_all and RefSeq_dist aCDFs, in order to undertake a fair comparison.

CDF	Number of probesets	Number of genes	median frozen-FFPE sample correlation	median frozen-FFPE probeset correlation (50% higher IQR)	Frozen-FFPE Fold change correlation			Frozen-FFPE Fold change slope			Percentage of DE probesets in Frozen data called as DE in FFPE data	Number of common genes among top-100 DE genes in Frozen and FFPE data
					Value	CI lower 5%	CI upper 95%	Value	CI lower 5%	CI upper 95%		
CDF standard - MAS5	54675	19798	0.691	0.116	0.407	0.400	0.414	0.442	0.434	0.451	20.7	35
CDF standard - RMA	54675	19798	0.792	0.333	0.696	0.691	0.700	0.525	0.520	0.529	28.4	37
CDF standard - fRMA	54675	19798	0.784	0.347	0.717	0.713	0.721	0.627	0.622	0.632	31.5	38
CDF standard common with RefSeq_all - MAS5	36727	16991	0.709	0.135	0.430	0.422	0.438	0.472	0.462	0.482	23.1	39
CDF standard common with RefSeq_all - RMA	36727	16991	0.777	0.359	0.706	0.701	0.712	0.543	0.537	0.548	29.8	44
CDF standard common with RefSeq_all - fRMA	36727	16991	0.773	0.371	0.726	0.721	0.731	0.637	0.631	0.643	32.2	41
CDF standard common with RefSeq_dist - MAS5	18517	8263	0.713	0.131	0.413	0.401	0.425	0.461	0.446	0.476	20.8	39
CDF standard common with RefSeq_dist - RMA	18517	8263	0.783	0.36	0.695	0.688	0.703	0.550	0.542	0.558	29.2	42
CDF standard common with RefSeq_dist- fRMA	18517	8263	0.776	0.371	0.715	0.708	0.722	0.649	0.640	0.659	32.4	46
CDF RefSeq_all - MAS5	16991	16991	0.759	0.228	0.566	0.556	0.576	0.526	0.514	0.537	30.9	44
CDF RefSeq_all - RMA	16991	16991	0.79	0.42	0.737	0.730	0.744	0.526	0.519	0.533	35.9	52
CDF RefSeq_all - fRMA	16991	16991	0.782	0.43	0.761	0.755	0.767	0.634	0.626	0.642	41.7	53
CDF RefSeq_dist - MAS5	8263	8263	0.736	0.178	0.468	0.451	0.484	0.491	0.471	0.511	18.5	30
CDF RefSeq_dist - RMA	8263	8263	0.795	0.349	0.688	0.676	0.699	0.626	0.611	0.640	26.7	47
CDF RefSeq_dist - fRMA	8263	8263	0.801	0.359	0.694	0.683	0.705	0.694	0.678	0.709	24.7	44

Table 18: Frozen-FFPE comparison results for each combination of processing algorithm.

Independently from the CDF used, MAS5 gave the poorest agreement between Frozen and FFPE data while fRMA slightly outperformed RMA. When using the RefSeq_dist CDF we obtained the best frozen-FFPE sample correlation and the best frozen-FFPE fold change slope, confirming that, as hypothesized, the probes nearer to 3'-end are those giving the most similar signals in frozen and FFPE data. Nevertheless, using this aCDF we did not obtained an improvement in frozen-FFPE probeset correlation or in the agreement of genes called as differentially expressed. On the opposite, the best agreement was obtained using the RefSeq_all CDF in combination with the fRMA method. For example, 41.7% of genes identified as DE in frozen data were found DE in FFPE data at the same significance threshold, about twice the value obtained with MAS5 method and the standard CDF (20.7% looking at all probesets or 23.1% looking at probesets targeting the same pool of genes). Similarly, the number of common top-100 genes increased from 35 to 53.

4.4.2 VALIDATION OF THE DEVELOPED DATA PROCESSING PIPELINES ON BREAST CANCER DATASETS

The robustness of the results was verified by applying the different processing pipelines to the GSE5460 dataset (163) from 127 frozen breast cancers and to our FFPE data (data from the pilot-study of 44 FFPE breast cancers and data from the surgery arm of ECTO1 trial (see §4.3). As described in the scheme (Fig.75), in the frozen dataset we performed a class comparison between ER positive and ER negative samples and 5% of probesets with lowest p-values were selected. Then in our FFPE data we computed the same class comparison for such selected probsets and looked at the distribution of their p-values. The same analysis was carried out using MAS5 with the standard CDF as well as using fRMA and the RefSeq_all CDF.

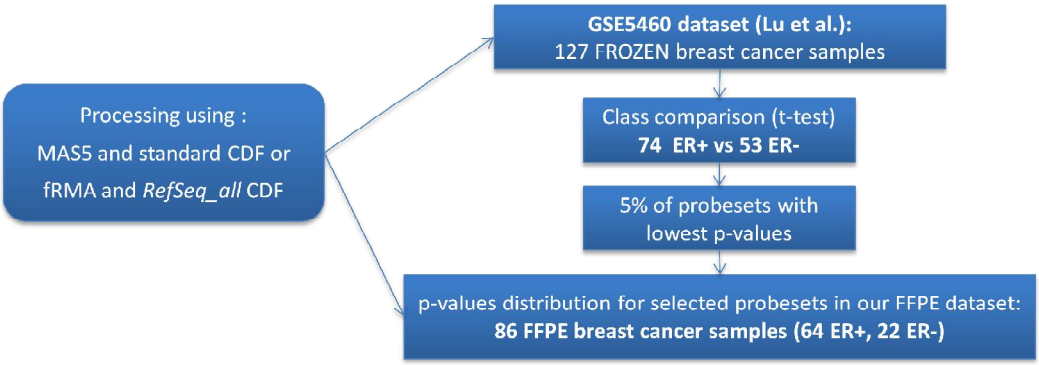

Figure 75: Flow chart of the analysis to evaluate the improvement in data reliability using independent datasets and ER status.

As shown in the figure, p-values shifted towards lower values, thus the number of probesets keeping to be significantly DE in the FFPE dataset increased from about 40% to more than 70% when using our processing method (Fig.76).

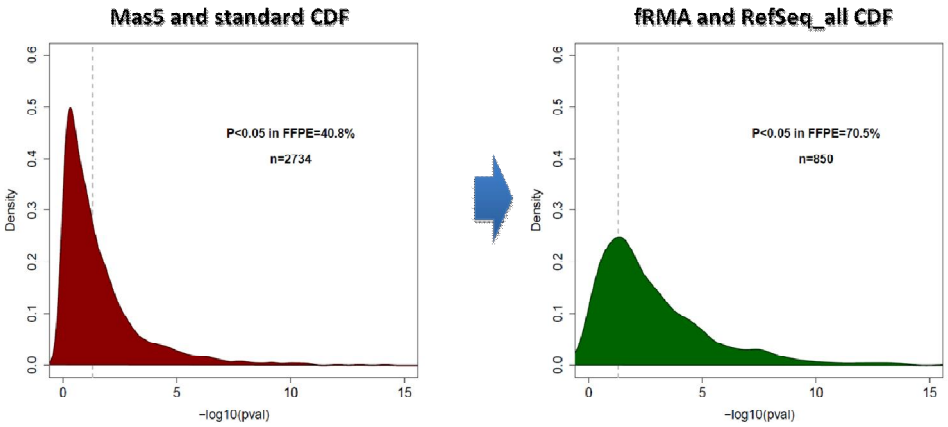

Figure 76: Distribution of p-values in the INT FFPE dataset for top 5% of probesets identified as differentially expressed in the GSE5460 Frozen dataset. The analysis was performed on data processed using MAS5 and the standard CDF (left), fRMA and the standard CDF (center) or fRMA and the RefSeq_all CDF (right).

The utility of our data analysis pipeline was further tested looking at pathological features of the tumor, like grade and lymphocyte infiltration. We compared tumors with high or low lymphocyte infiltration looking this time at the expression of a set of Tcell specific genes previously described (see § 4.1.1) (Fig.77).

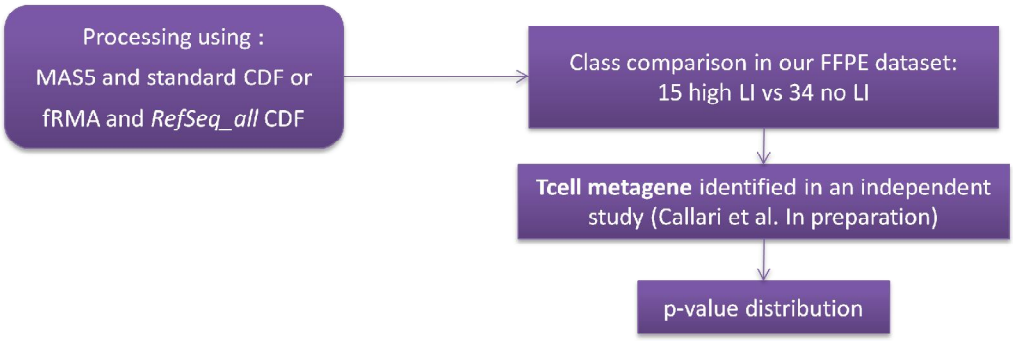

Figure 77: Flow chart of the analysis to evaluate the improvement in data reliability using independent datasets and lymphocytes infiltration (LI).

By processing our data with the standard or with the method developed by us, we could observe that the percentage of significant probesets rose from 48% to 67% (Fig.78).

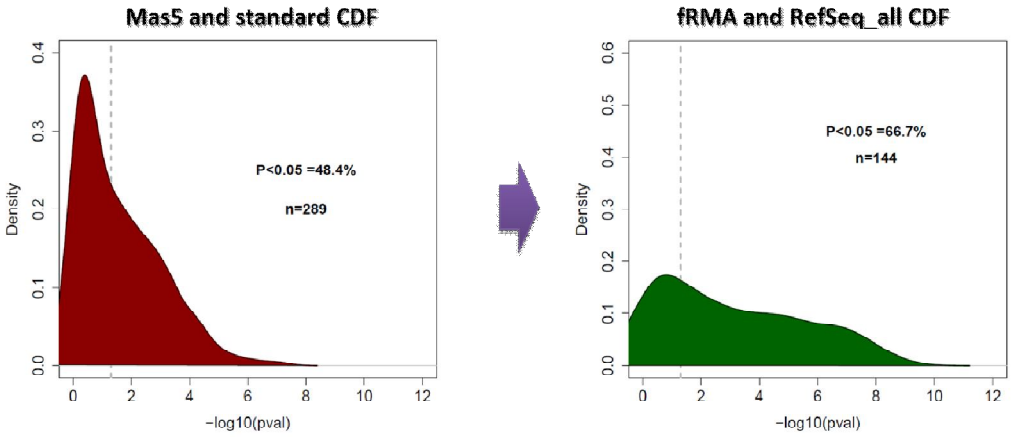

Figure 78: Distribution of p-values in the INT FFPE dataset for top 5% of probesets identified as differentially expressed in the GSE5460 Frozen dataset. The analysis was performed on data processed using MAS5 and the standard CDF (left), fRMA and the standard CDF (center) or fRMA and the RefSeq_all CDF (right).

Similarly, we performed in our data the class comparison between grade 3 and grade 2 tumors looking at p-values of the genes of the GGI developed by Sotiriou and colleagues (164) (Fig.79).

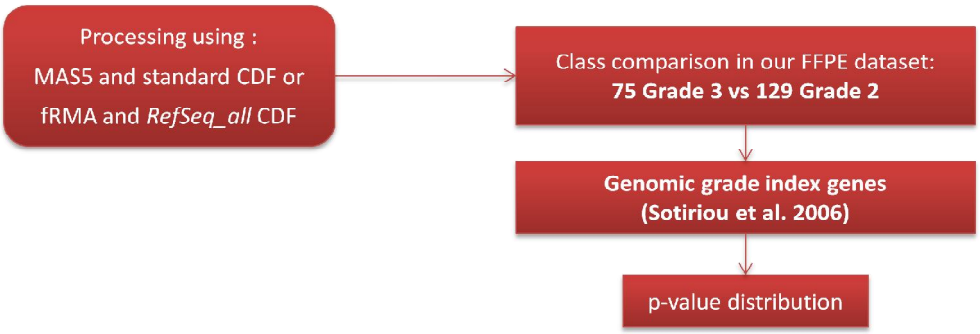

Figure 79: Flow chart of the analysis to evaluate the improvement in data reliability using independent datasets and grade.

This time the percentage of significant probesets rose from 54% to 82% (Fig.80).

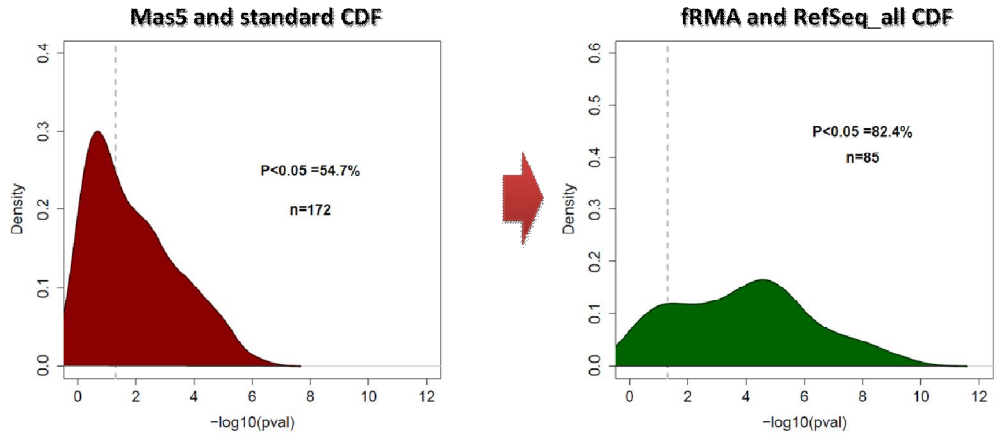

Figure 80: Figure 78: Distribution of p-values in the INT FFPE dataset for top 5% of probesets identified as differentially expressed in the GSE5460 Frozen dataset. The analysis was performed on data processed using MAS5 and the standard CDF (left), fRMA and the standard CDF (center) or fRMA and the RefSeq_all CDF (right).

Our data demonstrate that optimized processing of FFPE Affymetrix data leads to a sizable improvement of their reliability. In particular a significant advantage is obtained by using custom CDFs based on current transcript annotation (RefSeq_all and Refseq_dist) together with fRMA normalization.

4.4.3 USING GENE EXPRESSION PROFILES TO PREDICT TREATMENT SUCCESS FOR STANDARD TREATMENTS IN BREAST CANCER

Developing predictors of response and survival from standard chemotherapy for patients with newly diagnosed invasive breast cancer is a crucial issue in attaining a treatment personalization. In the present thesis we have developed a strategy to obtain optimal treatment response prediction by

- combining information from already published signatures,
- using publicly available data set,
- developing predictors and biomarkers based on metagenes rather than single genes and
- exploiting data obtained within a multicentric clinical trial with a high clinical relevance

to **validate** the developed strategy.

A similar strategy has been used in a recent study by Hatzis et al (REF, Jama 2011) to develop genomic predictors of response and survival following Taxane-Anthracyclin therapy. Treatment

sensitivity was predicted using a combination of signatures independently for ER+ and ER- tumors.

The general strategy used by Hatzis et al is illustrated in the following graph (Fig.81):

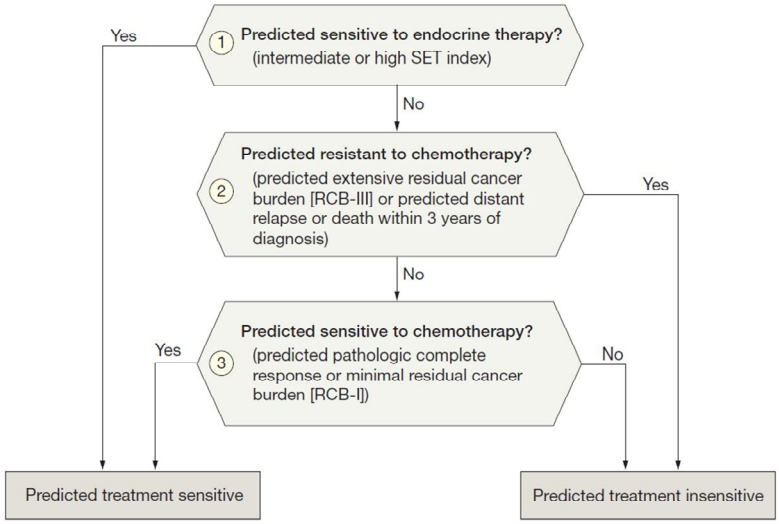

Figure 81: Hatzis et al. (165)

ER+ patients were evaluated with respect to signature predicting endocrine sensitivity, and if sensitive endocrine treatment was considered the best choice treatment for those women. If insensitive, based on the signature, a signature predicting chemotherapy resistance was used to sort patients. Those predicted to be chemo-resistant were considered insensitive to conventional treatment and allocated to new alternative treatments. The patients not predicted to be chemo-resistant were instead evaluated for chemo sensitivity and allocated to conventional treatments if defined as sensitive or diverted to alternative new treatments if predicted as insensitive according to their gene profile.

This type of algorithm applied to a validation cohort of patients showed that the outcome for patients predicted as sensitive based on the genomic predictor was as good as those in patients actually achieving a pCR (an in vivo sensitivity test).

We built our prediction strategy taking the strengths of Hatiz paper (a specific clinical question aim as aim; the fact that a patients cannot be cured twice, i.e. patients cured by endocrine therapy

do not need to be assessed for chemosensitivity, and the development of separate genomic predictors according to ER status).

However, in our prediction model we tried to overcome following limitations:

- Hatzis et al consider only patients with HER-2 negative tumors.
- Only a small proportion of patients is predicted to be treatment sensitive (28%).
- The prognostic issue was not considered as no pure prognostic genomic predictor was included in the model.
- The model was not compared with conventional prognostic/predictive models.
- Follow up time was relatively short.

Overcoming of the above limitations was possible thanks to the use of gene expression profiles obtained within the ECTO1 trial as validation cohort. Such data represent internationally recognized high quality clinical data which warrant the relevance of the developed predictors.

One of the central issues of this thesis work was to overcome the technical hurdles intrinsic in obtaining biologically and clinically relevant gene expression profiles from FFPE samples using array platforms widely used for frozen samples, allowing this way to unlock the valuable clinico-biological information of the ECTO I samples.

As stated above we collected publicly available data sets with distinct features suitable to answer the different type of prediction questions. All collected data set had in common the fact that they were available in GEO and that their gene expression data had been obtained using the Affymetrix platform either with the HG-U133A or the HG-Plus 2.0 chips.

The table below summarizes the main features of our dataset collection

Definition	Suitable samples	Features
GENERIC	1366	GEP of untreated primary breast cancers beloging to all subtypes
PROGNOSTIC	826	GEP of untreated primary breast cancers from node negative patients receiving any adjuvant sistemic treatment. All subtypes. 10-years follow-up available.
TAM	962	GEP of ER+ (IHC) untreated primary breast cancers from patients receiving hormonal adjuvant therapy. 10-years follow-up available.
CHEMO	508	GEP of untreated primary breast cancers from patients receiving chemo and hormonal (ER+) therapy in both neoadjuvant or adjuvant setting. All subtypes. 3-years follow-up available.

Table 19: description of collected public dataset.

The so-called **generic dataset** (including gene expression profiles obtained from 1366 fresh frozen breast cancer samples) was used to derive metagenes. Metagenes were defined as a group of highly correlated genes and whose expression level was computed as the average expression level of each single gene belonging to the metagene. The metagene-strategy was chosen to attain more robust data especially in the event of the necessity to switch to a different platform. Probes for single genes are in fact likely to perform differently on different platforms, whereas the average expression level of a metagene is likely to be more stable.

The **prognostic dataset** (including gene expression profiles obtained from 826 fresh frozen breast cancer samples from node negative breast cancer patients not receiving any type of adjuvant treatment) was used to derive a pure prognostic genomic predictor. It is important to mention that such dataset included all breast cancer subtypes and that the follow up time was up to 10 years long.

The **TAM dataset** (including gene expression profiles from 962 ER+ tumors from breast cancer patients receiving hormonal adjuvant therapy only) was used to derive an endocrine sensitivity predictor.

The **chemo dataset** (including 508 gene expression profiles from primary breast cancer patients receiving chemotherapy alone or in combination with endocrine treatment either in the neoadjuvant or adjuvant setting) was used to derive a chemosensitivity predictor.

By looking closer at the selected datasets we noticed that there may exist for certain genes a chip-associated bias despite the use of a CDF including only RefSeq common to the U133A (22283 probesets) and the Plus 2.0 (54675 probesets). A possible interpretation is that even the same probesets can perform differently depending on the 'environment' (more or less dense chip).

An example is reported in the graph below

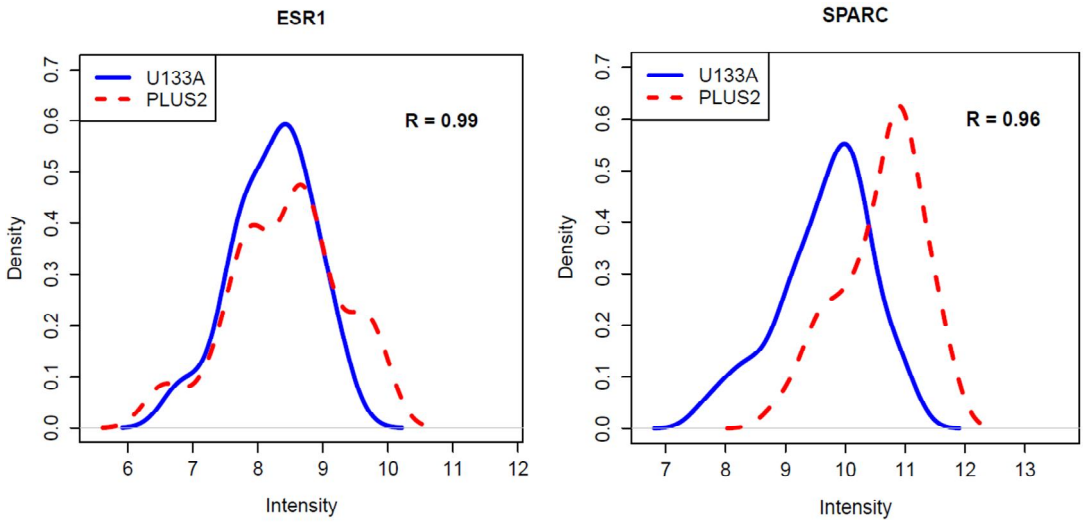

Figure 82: density plot of ESR1 and SPARC genes.

As can be seen even in the presence of high correlations (r>0.95) for certain genes, as for example *SPARC* there may be a shift in the intensity levels depending upon the used chip.

This is one more reason for choosing the metagene-strategy which counteracts such effects through averaging.

As already stated, one of the main points of our prediction strategy was the development of genomic predictors separately for patients with ER+ and ER- tumors.

To do so, it was important to have a way, as uniform as possible, to classify ER status of our tumors. This was achieved by selecting within the generic dataset (as the latter was not used for other predictor developments) 317 samples where the ER status had been defined by IHC using the same criterion, i.e. 1% positivity as threshold.

Within such datasets ER related genes were selected and genes having the highest AUC were used for ER-status metagene computation.

The selected genes and their relative AUC values are reported hereafter:

Symbol	AUC
TBC1D9	0.965
SLC39A6	0.964
SCUBE2	0.963
GATA3	0.953
CA12	0.953
ESR1	0.95

Table 20: genes with the highest Area Under ROC Curve (AUC)

Once the genes belonging to the ER-status metagene were selected, we defined a threshold mainly looking at the bimodal distribution of the ER-metagene in the population and confirming the choice by comparing with the IHC-defined ER status, as illustrated below

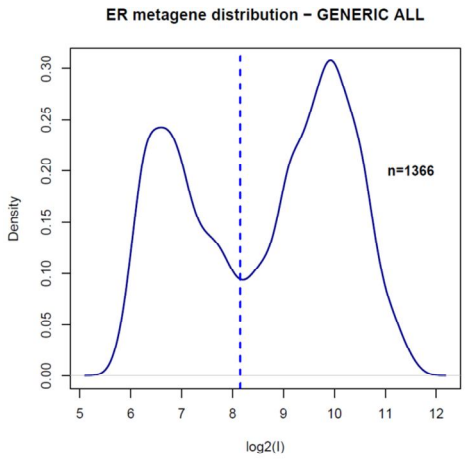

Generic N=317 K= 0.930		ER_IHC	
		0	1
ER_mg	0	141	7
	1	4	165

Figure 83: density plot of ER metagene (left) and agreement with IHC ER status.

The ER-status metagene defined this way was thereafter validated. We know from the literature that ER status is predictive of response to endocrine treatment.

To validate the predictive significance of our ER-status metagene, in a combined dataset of 934 HT treated ER+ patients, a subgroup was ER- according to the ER-metagene and showed worse outcome (p=4.8E-08) (Fig. 84).

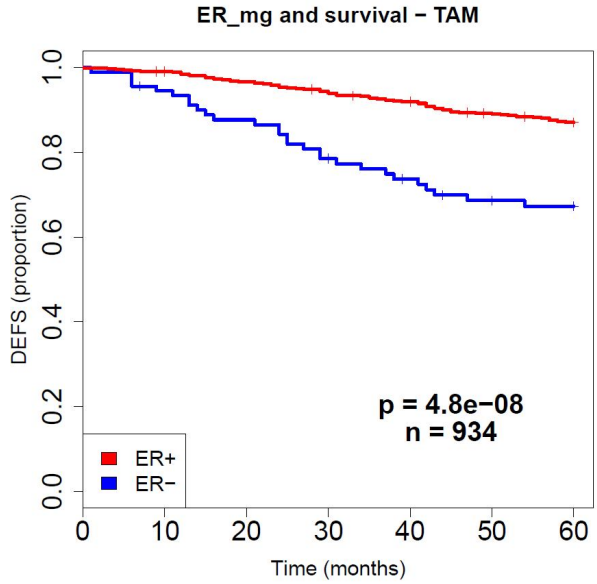

Figure 84: Kaplan Meier curve for ER+ and ER- patients

The same type of strategy was applied also to the HER2 status definition.
A dataset of 490 cases with Her2 positivity defined by IHC (as 3+) or by FISH was identified. The following genes, all mapping on chromosome 17, were identified based on the AUC and used for metagene computation.

Symbol	Chr	AUC
PGAP3	17	0.902
PNMT	17	0.817
ERBB2	17	0.805

Table 21: genes with the highest Area Under ROC Curve (AUC).

A threshold was arbitrarily selected based on the distribution of the metagene expression levels and the chosen cut-off was validated comparing with the IHC or FISH –defined HER2 status.

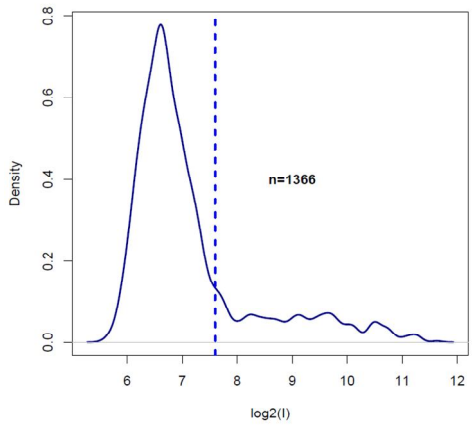

Generic N=490 K=0.729		HER2 FISH+ or 3+	
		0	1
HER2_mg	0	396	18
	1	17	59

Figure 85: density plot of Her2 metagene (left) and agreement with IHC/FISH Her2 status.

Once uniform genomic predictors of ER and HER2 status were available the next step was to classify all samples with follow up data in the three groups:

- HER2 negative/ER negative
- HER2 positive
- ER+/HER2 negative

which were separately investigated for defining subtype-specific genomic predictors.

At the same time the generic dataset was used to identify metagenes (eg. Proliferation, immune axis, etc) with specific biological significance.

The choice of using metagenes presented several advantages over the use of single genes to build prediction signatures. One of the main advantages is the possibility to identify prognostic and predictive biomarkers based on biological knowledge. This could be done also with single genes, but with metagenes we obtain more complete information for biological features or pathways which are regulated by many genes. A single gene could in fact hardly represent a biological property like proliferation which derives from the interaction of many genes at different levels, from cell membrane signals, to kinase cascades transducing the external signal to transcription factors acting on specific gene involved in regulation of cell cycle.

An additional advantage of metagenes is the possibility to perform an easier cross-platform analysis which is very important in this thesis which considers gene expression profiles obtained

from both frozen and FFPE samples and combines the two types of information 'jumping' from one setting to the other.

Once a cluster of correlated genes is identified in a specific platform, when moving to another platform some of the genes could not correlate with the others anymore but, after excluding them we will be able to plausibly evaluate the same biological process in the second platform.

The metagene identification was attained with the following strategy. We used 1366 gene profiles from the generic dataset which was split into two parts. The first part (including 683 samples) was used to cluster all genes and to identify clusters of genes showing a correlation >0.4 and including more than 25 genes. A re-clustering was performed on the second group and clusters containing genes with a correlation coefficient superior to 0.4 were identified. To assure the reproducibility of the data on FFPE samples, an additional re-clustering was done on the 44 FFPE samples belonging to the pilot study. After clustering and re-clustering, 36 clusters containing at least 12 genes were retained for following analyses.
The following chart illustrates the strategy for metagene identification:

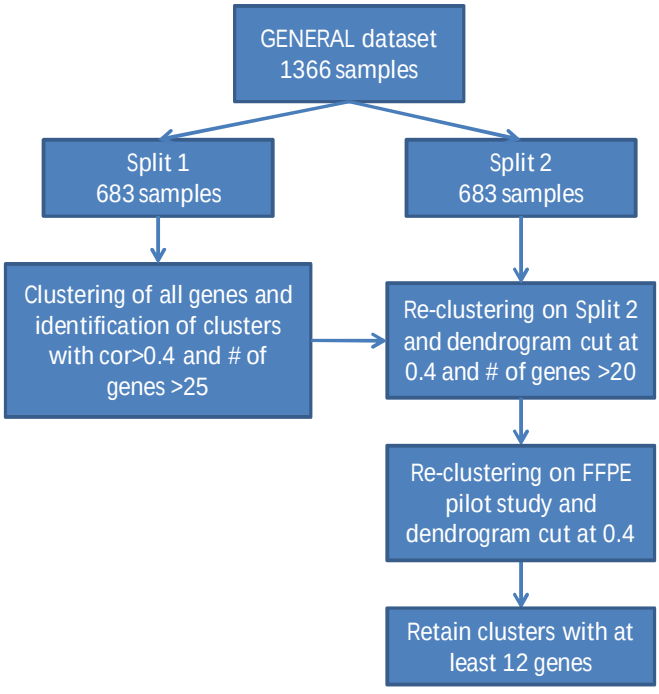

Figure 86: Flow chart of metagene identification strategy.

And the following table show some examples of the identified metagenes:

Metagene	Name
15	Proliferation
26	ER axis
39	STAT1/ISGs
40	Immune
41	Dendritic cells
42	T-cell
44	ECM
46	ECM/SPARC
47	ECM/TFGBR2
48	ECM/PLAU

Table 22: biological function for selected metagenes.

Once equipped with metagenes we could continue our strategy for genomic predictor definition.

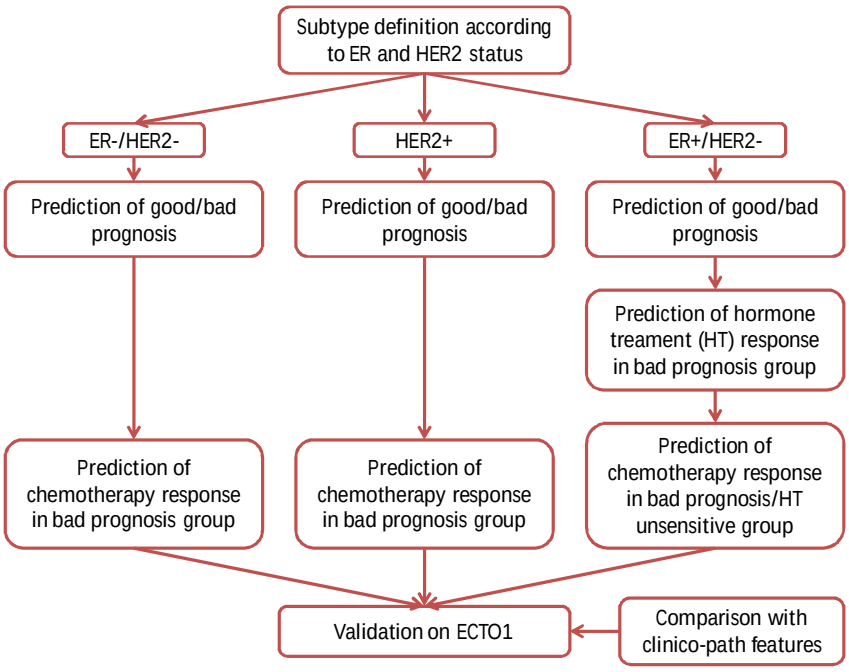

Figure 87: flow chart of the strategy to identify a genomic predictor.

We first concentrated on prediction of good and bad prognosis for patients with ER+/HER2- tumors. Based on previous knowledge and literature data, **proliferation** and **immune axis** genes

were chosen in order to be defined/refined on our prognostic datasets and to be further validated out of context using the TAM dataset.

The proliferation metagene identified as previously described was now refined with respect to its prognosis predictive power. The refinement was done using 495 ER+/HER2- cases from the prognostic dataset. The originally defined metagene contained 88 genes, and to attain a refinement each of them was tested in univariate analysis using a Cox model with regard to association with prognosis. Then genes were ordered according to their Cox p-value and the number used to compute the metagene was gradually reduced. Simultaneously, the fraction of patients defined as at low risk was varied between 10 and 90%. All the procedure was performed in a 10-fold cross validation setting iterated 100 timed. The top 25 genes with the lowest p-values were chosen.

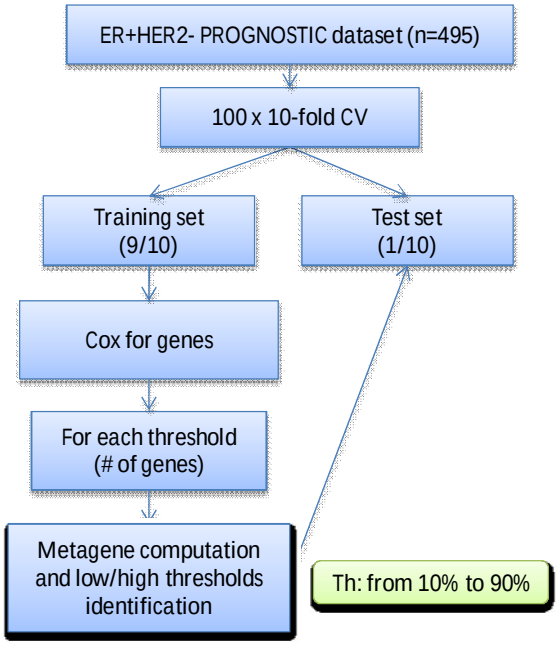

Figure 88: metagene refinement procedure.

Using the newly refined proliferation metagene 60% of patients were defined as having low-proliferating tumors and more than 90% of those patients were disease-free at 5 years.

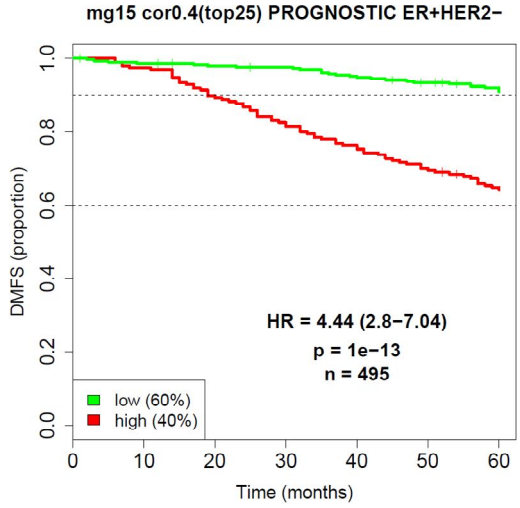

Figure 89: Kaplan Meier curve for patients with high or low proliferation.

A similar strategy was then applied to the identified immune axis metagene which originally contained 20 genes. Refinement was carried out as described for the proliferation gene performing an univariate analysis for each gene but using only cases defined as highly proliferating. The refined gene contained the top 16 genes and was significantly (p=0.016) associated with prognosis in tumors characterized by high proliferative activity as shown in the following plot:

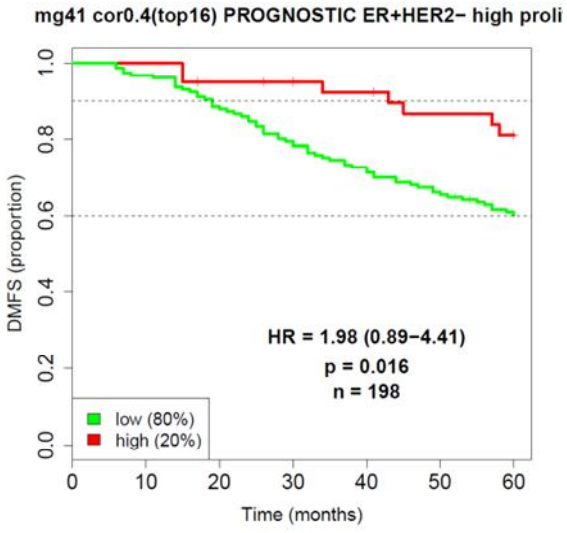

Figure 90: Kaplan Meier curve for high proliferation patients with high or low immune cells infiltration.

The immune axis gene however maintained its prognostic relevance also in the whole population not subdivided according to proliferation (p=0.00083), and the two variables were independent as they remained significantly associated with outcome in a multivariate analysis.

Variable	hazard ratio	Multivariate Cox p-value
Proliferation mg	4.16	0
Immune mg	0.58	0.000842

Table 23: multivariate Cox analysis in the prognostic dataset.

The 20% of patients with the highest expression of the immune genes were disease-free after 5 years from surgery in 90% of cases.

For an optimal prediction of prognosis proliferation and immunity were combined and a prognostic score (PS) was defined using the β-coefficients derived from the multivariate Cox analysis. As can be seen from the plot, the 60% of patients with the lowest PS had a 5 years disease free survival higher than 90%.

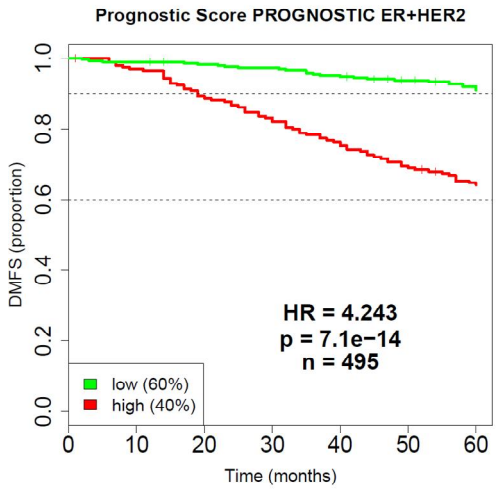

Figure 91: Kaplan Meier curve for patients with high or low prognostic score.

The thresholds defined in the prognostic dataset were then applied to the TAM data set separately for node positive and node negative patients. The predictive value of the PS was

validated in both subsets. More than 95% of women with negative nodes treated with tamoxifen were disease free 5 years after surgery.

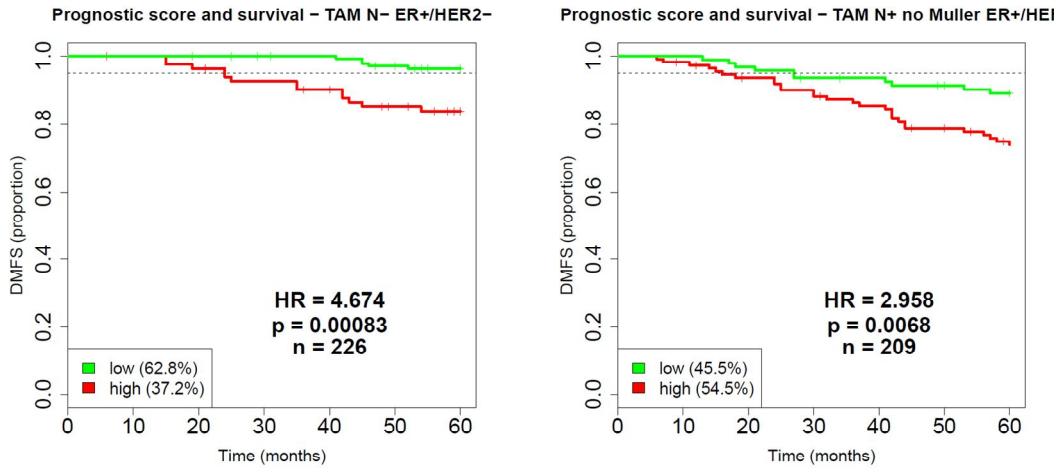

Figure 92: Prognostic score validation in N- (left) and N+ (right) tamoxifen treated patients.

The strategy consisted in defining an ER-axis metagene exploiting the TAM dataset and in validating the defined metagene out of context in the chemo datasets.

The originally defined ER metagene contained 42 genes and the top 16 genes obtained after refinement in the bad prognosis group were used. More than 95% of patients with high ER-metagene values in the third tertile were disease free after 5 years from surgery, independently from prognosis and from nodal status. Data are reported in the following plots.

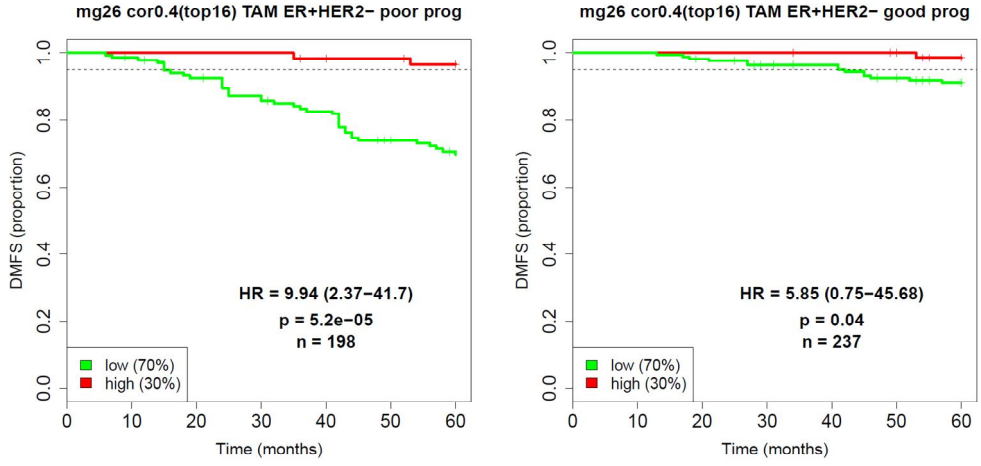

Figure 93: Kaplan Meier curves for patients with high or low expression of ER-axis genes in poor (left) or good (right) prognostic groups.

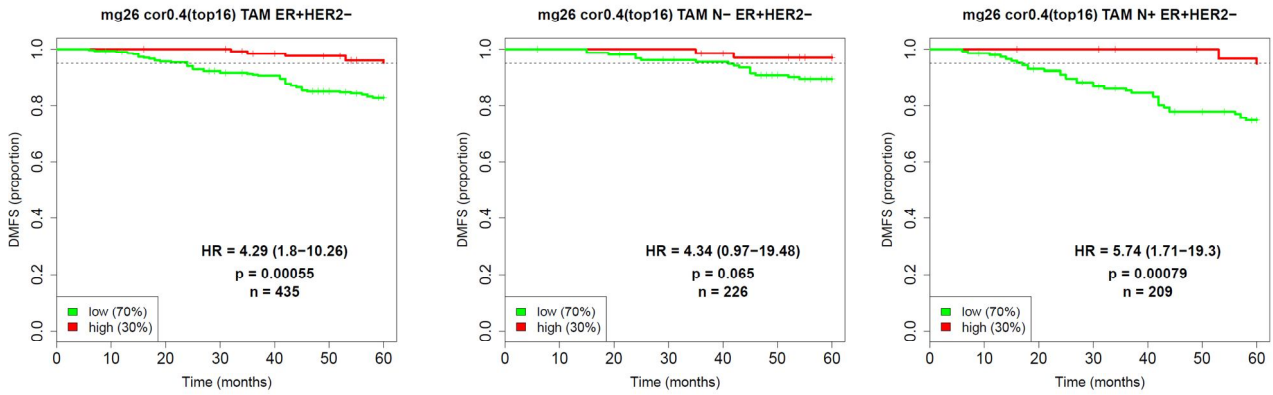

Figure 94: Kaplan Meier curves for patients with high or low expression of ER-axis genes (from the left: all, N- and N+ patients).

The PS, ER metagene and nodal status were combined to define a **hormone score** (HS). A 5-year DFS superior to 95% was attained in the 45% of patients with the highest HS values.

The HS score was therefore subjected to a validation on chemo datasets. Analyses are still ongoing.

Results so far obtained are very promising and will acquire additional value from the validation on the ECTO1 series, thanks to the technical success achieved in obtaining biologically reliable gene expression profiles from FFPE samples.

5. CONCLUSION

As stated in the chapter 'purpose of this thesis' our main aim was to **provide a genomic based-tool for on optimal treatment planning of breast cancer**.

The initial hypothesis was that the more accurate the prognostic and response predictions, the more personalized treatment recommendation can be made for an individual.

Presently available treatments based on hormones and on chemotherapy are very effective, but have two major drawbacks:

- Over-treatment, with unnecessary exposure to toxicity for patients who would have been treated without chemotherapy.
- Difficulty in identification treatment insensitive and resistant patients who are likely to mostly benefit from newly developed anticancer drugs, rather than receive conventional treatment which is ineffective for them.

Presently available treatment predictors fail from provide optimal identification of patients based on their likelihood to respond.

We therefore built our own treatment prediction strategy

- based on previous knowledge mostly developed using gene expression profess obtained from frozen samples and combining available predictors
    1. with a hierarchical approach
    2. using metagenes
    3. developing specific predictors according to the molecular subtype
- and developed a robust technical protocol with an improved data analysis pipeline allowing to finally unlock the biological information locked in FFPE samples derived from clinical trials

with such tools it was possible to identify *a priori* in the ER+/Her2- a subset of patients who were predicted (and confirmed by external validation) to have a 95% 5-year disease free survival. Such accurate (and validated) prediction was achieved by combining optimized metagenes with clear biological roles in proliferation, ER signaling and immunity and separately analyzing prognostic and predictive information.

Work is still in progress for the other molecular subtypes (Her2+ and ER-/Her2-).

We reported in the results a detailed dissection of all technical hurdles arising with FFPE samples and solutions to minimize or overcome the technical problems. We also extensively analyzed *pro* and *cons* of several different approaches suitable for gene expression studies in FF and FFPE samples.
The impossibility to utilize with the presently available technologies, samples which were fixed in Bouin (an important issue which dramatically affected our treatment predictor development strategy as it prevented us from being able to use data obtained in untreated arms from old clinical trials) was also extensively demonstrated and supported by comparative data with formalin-fixed samples.

The role of the immune system in affecting breast cancer prognosis was separately studied not only from a clinical point of view, but also to better understand the biological base for the tumor-promoting and tumor-inhibiting effects of the immune axis. We started from clinical data including a series of 127 untreated node negative breast cancer, and showed that the ISG expression was associated to the likelihood to develop distant metastases.
During the external validation of such piece of information we surprisingly noticed that the ISG expression had a distinct role in impacting distant metastases development based on the molecular subtype of the tumor: positive association with metastasis in patients with ER+/Her2- tumors, positive association in patients with Her2+ tumors and non association in women with ER-/Her2- tumors.
We also noticed that in clinical samples there was no association between the expression levels of ISG and either lymphocyte infiltration or specific type of infiltrates defined using IHC with several antibodies specific for different cell subpopulations of immune system (anti CD3, anti CD4, anti CD8, anti CD 68, anti CD56, anti CD57, anti FOXP3, anti CD45, anti CD 20, anti GRANZYME and anti HLADR). Furthermore IHC approaches clearly demonstrated that ISG genes were mostly expressed by the epithelial cells. Such data add to other controversial data on the prognostic role of the immune axis in breast cancer, already available in the literature, but, most importantly, underline the importance of evaluating genomic prognostic (and treatment predictive) factors distinctly for each molecular subgroup.
To further search for biological mechanism justifying the prognostic role of ISG expression we switched to *in vitro* co-cultures of epithelial cells with normal fibroblasts of different origin or

CAFs. Many different experimental setting either 2D or 3D were adopted and described in detail. The experimental setting played a major role on the experimental results. On the average basal-like cells were more sensitive to fibroblasts promoted effects in terms of cytokine secretion in the culture medium and up-regulation of ISG genes in the epithelial cells. Those cells were characterized by high intrinsic migratory and invasive ability which did not change much upon co-cultures.

On the contrary luminal cells were stimulated to growth and gained invasive and migratory abilities after stimulation with fibroblasts and CAFs.

Our experiments showed a complicated and sometimes controversial interplay between fibroblasts and epithelial cells which fully justifies the paradoxical role of the immune system in clinical

REFERENCE LIST

(1) Hennighausen L, Robinson GW. Information networks in the mammary gland. Nat Rev Mol Cell Biol 2005 Sep;6(9):715-25.

(2) Kardinal CG, Yarbro JW. A conceptual history of cancer. Semin Oncol 1979 Dec;6(4):396-408.

(3) Ford D, Easton DF. The genetics of breast and ovarian cancer. Br J Cancer 1995 Oct;72(4):805-12.

(4) Dite GS, Jenkins MA, Southey MC, Hocking JS, Giles GG, McCredie MR, et al. Familial risks, early-onset breast cancer, and BRCA1 and BRCA2 germline mutations. J Natl Cancer Inst 2003 Mar 19;95(6):448-57.

(5) Henderson BE, Ross R, Bernstein L. Estrogens as a cause of human cancer: the Richard and Hinda Rosenthal Foundation award lecture. Cancer Res 1988 Jan 15;48(2):246-53.

(6) Brown P, Allen AR. Obesity linked to some forms of cancer. W V Med J 2002 Nov;98(6):271-2.

(7) Hirose K, Tajima K, Hamajima N, Takezaki T, Inoue M, Kuroishi T, et al. Association of family history and other risk factors with breast cancer risk among Japanese premenopausal and postmenopausal women. Cancer Causes Control 2001 May;12(4):349-58.

(8) Friedenreich CM, Bryant HE, Courneya KS. Case-control study of lifetime physical activity and breast cancer risk. Am J Epidemiol 2001 Aug 15;154(4):336-47.

(9) Bernstein L, Henderson BE, Hanisch R, Sullivan-Halley J, Ross RK. Physical exercise and reduced risk of breast cancer in young women. J Natl Cancer Inst 1994 Sep 21;86(18):1403-8.

(10) Miller BA, Kolonel LN, Bernstein L, Young JL, wanson GM, West D, Key CR, Liff JM, Glover CS, Alexander GA. Racial/Ethnic Patterns of Cancer in the United States 1988-1992. Miller BA, Kolonel LN, Bernstein L, Young JL, wanson GM, West D et al., editors. 1996. Bethesda, MD, National Cancer Institute.
Ref Type: Serial (Book,Monograph)

(11) Polanska UM, Acar A, Orimo A. Experimental generation of carcinoma-associated fibroblasts (CAFs) from human mammary fibroblasts. J Vis Exp 2011;(56):e3201.

(12) Weaver VM, Fischer AH, Peterson OW, Bissell MJ. The importance of the microenvironment in breast cancer progression: recapitulation of mammary tumorigenesis using a unique human mammary epithelial cell model and a three-dimensional culture assay. Biochem Cell Biol 1996;74(6):833-51.

(13) Kelsey JL, Gammon MD. The epidemiology of breast cancer. CA Cancer J Clin 1991 May;41(3):146-65.

(14) Wu SC, Hotes J, Fulton JP, Chen VW, Howe HL, Correa C. Cancer in North America, 1995-1999. Wu SC, Hotes J, Fulton JP, Chen VW, Howe HL, Correa C, editors. [Volume III: NAACCR Combined Cancer Incidence Rates]. 2013. Springfield, IL, Noth American Association of Central Cancer

Registries.
Ref Type: Serial (Book,Monograph)

(15) Russo IH, Russo J. Pregnancy-induced changes in breast cancer risk. J Mammary Gland Biol Neoplasia 2011 Sep;16(3):221-33.

(16) Familial breast cancer: collaborative reanalysis of individual data from 52 epidemiological studies including 58,209 women with breast cancer and 101,986 women without the disease. Lancet 2001 Oct 27;358(9291):1389-99.

(17) Venkitaraman AR. Cancer susceptibility and the functions of BRCA1 and BRCA2. Cell 2002 Jan 25;108(2):171-82.

(18) Narod SA. Early-onset breast cancer: what do we know about the risk factors?: A Countercurrents Series. Curr Oncol 2011 Oct;18(5):204-5.

(19) Helmrich SP, Shapiro S, Rosenberg L, Kaufman DW, Slone D, Bain C, et al. Risk factors for breast cancer. Am J Epidemiol 1983 Jan;117(1):35-45.

(20) Kelsey JL, Gammon MD, John EM. Reproductive factors and breast cancer. Epidemiol Rev 1993;15(1):36-47.

(21) Calle EE, Rodriguez C, Walker-Thurmond K, Thun MJ. Overweight, obesity, and mortality from cancer in a prospectively studied cohort of U.S. adults. N Engl J Med 2003 Apr 24;348(17):1625-38.

(22) Ewertz M, Jensen MB, Gunnarsdottir KA, Hojris I, Jakobsen EH, Nielsen D, et al. Effect of obesity on prognosis after early-stage breast cancer. J Clin Oncol 2011 Jan 1;29(1):25-31.

(23) Berclaz G, Li S, Price KN, Coates AS, Castiglione-Gertsch M, Rudenstam CM, et al. Body mass index as a prognostic feature in operable breast cancer: the International Breast Cancer Study Group experience. Ann Oncol 2004 Jun;15(6):875-84.

(24) Lorincz AM, Sukumar S. Molecular links between obesity and breast cancer. Endocr Relat Cancer 2006 Jun;13(2):279-92.

(25) Iyengar P, Combs TP, Shah SJ, Gouon-Evans V, Pollard JW, Albanese C, et al. Adipocyte-secreted factors synergistically promote mammary tumorigenesis through induction of anti-apoptotic transcriptional programs and proto-oncogene stabilization. Oncogene 2003 Sep 25;22(41):6408-23.

(26) Rose DP, Gilhooly EM, Nixon DW. Adverse effects of obesity on breast cancer prognosis, and the biological actions of leptin (review). Int J Oncol 2002 Dec;21(6):1285-92.

(27) Smith-Warner SA, Spiegelman D, Yaun SS, van den Brandt PA, Folsom AR, Goldbohm RA, et al. Alcohol and breast cancer in women: a pooled analysis of cohort studies. JAMA 1998 Feb 18;279(7):535-40.

(28) Kwan ML, Kushi LH, Weltzien E, Tam EK, Castillo A, Sweeney C, et al. Alcohol consumption and breast cancer recurrence and survival among women with early-stage breast cancer: the life after cancer epidemiology study. J Clin Oncol 2010 Oct 10;28(29):4410-6.

(29) Dumitrescu RG, Shields PG. The etiology of alcohol-induced breast cancer. Alcohol 2005 Apr;35(3):213-25.

(30) Etique N, Chardard D, Chesnel A, Flament S, Grillier-Vuissoz I. Analysis of the effects of different alcohols on MCF-7 human breast cancer cells. Ann N Y Acad Sci 2004 Dec;1030:78-85.

(31) Tezak Z, Kondratovich MV, Mansfield E. US FDA and personalized medicine: in vitro diagnostic regulatory perspective. Personalized Medicine 2010 Sep 1;7(5):517-30.

(32) Ludwig JA, Weinstein JN. Biomarkers in cancer staging, prognosis and treatment selection. Nat Rev Cancer 2005 Nov;5(11):845-56.

(33) Sawyers CL. The cancer biomarker problem. Nature 2008 Apr 3;452(7187):548-52.

(34) Place AE, Jin HS, Polyak K. The microenvironment in breast cancer progression: biology and implications for treatment. Breast Cancer Res 2011;13(6):227.

(35) Radisky D, Hagios C, Bissell MJ. Tumors are unique organs defined by abnormal signaling and context. Semin Cancer Biol 2001 Apr;11(2):87-95.

(36) Weinberg R, Mihich E. Eighteenth annual pezcoller symposium: tumor microenvironment and heterotypic interactions. Cancer Res 2006 Dec 15;66(24):11550-3.

(37) Allinen M, Beroukhim R, Cai L, Brennan C, Lahti-Domenici J, Huang H, et al. Molecular characterization of the tumor microenvironment in breast cancer. Cancer Cell 2004 Jul;6(1):17-32.

(38) Shao ZM, Nguyen M, Barsky SH. Human breast carcinoma desmoplasia is PDGF initiated. Oncogene 2000 Sep 7;19(38):4337-45.

(39) Kalluri R, Zeisberg M. Fibroblasts in cancer. Nat Rev Cancer 2006 May;6(5):392-401.

(40) Orimo A, Weinberg RA. Stromal fibroblasts in cancer: a novel tumor-promoting cell type. Cell Cycle 2006 Aug;5(15):1597-601.

(41) Orimo A, Gupta PB, Sgroi DC, renzana-Seisdedos F, Delaunay T, Naeem R, et al. Stromal fibroblasts present in invasive human breast carcinomas promote tumor growth and angiogenesis through elevated SDF-1/CXCL12 secretion. Cell 2005 May 6;121(3):335-48.

(42) Witz IP. Tumor-microenvironment interactions: dangerous liaisons. Adv Cancer Res 2008;100:203-29.

(43) Mbeunkui F, Johann DJ, Jr. Cancer and the tumor microenvironment: a review of an essential relationship. Cancer Chemother Pharmacol 2009 Mar;63(4):571-82.

(44) Devy L, Blacher S, Grignet-Debrus C, Bajou K, Masson V, Gerard RD, et al. The pro- or antiangiogenic effect of plasminogen activator inhibitor 1 is dose dependent. FASEB J 2002 Feb;16(2):147-54.

(45) Hu M, Polyak K. Microenvironmental regulation of cancer development. Curr Opin Genet Dev 2008 Feb;18(1):27-34.

(46) Swartz MA, Iida N, Roberts EW, Sangaletti S, Wong MH, Yull FE, et al. Tumor microenvironment complexity: emerging roles in cancer therapy. Cancer Res 2012 May 15;72(10):2473-80.

(47) Hanahan D, Weinberg RA. Hallmarks of cancer: the next generation. Cell 2011 Mar 4;144(5):646-74.

(48) Balkwill F, Mantovani A. Inflammation and cancer: back to Virchow? Lancet 2001 Feb 17;357(9255):539-45.

(49) Balkwill F, Charles KA, Mantovani A. Smoldering and polarized inflammation in the initiation and promotion of malignant disease. Cancer Cell 2005 Mar;7(3):211-7.

(50) Mantovani A, Allavena P, Sica A, Balkwill F. Cancer-related inflammation. Nature 2008 Jul 24;454(7203):436-44.

(51) Coussens LM, Werb Z. Inflammation and cancer. Nature 2002 Dec 19;420(6917):860-7.

(52) Moustakas A, Pardali K, Gaal A, Heldin CH. Mechanisms of TGF-beta signaling in regulation of cell growth and differentiation. Immunol Lett 2002 Jun 3;82(1-2):85-91.

(53) Smyth MJ, Dunn GP, Schreiber RD. Cancer immunosurveillance and immunoediting: the roles of immunity in suppressing tumor development and shaping tumor immunogenicity. Adv Immunol 2006;90:1-50.

(54) Haque SJ, Williams BR. Signal transduction in the interferon system. Semin Oncol 1998 Feb;25(1 Suppl 1):14-22.

(55) Stark GR, Kerr IM, Williams BR, Silverman RH, Schreiber RD. How cells respond to interferons. Annu Rev Biochem 1998;67:227-64.

(56) Zhou A, Paranjape JM, Der SD, Williams BR, Silverman RH. Interferon action in triply deficient mice reveals the existence of alternative antiviral pathways. Virology 1999 Jun 5;258(2):435-40.

(57) Shi L, Reid LH, Jones WD, Shippy R, Warrington JA, Baker SC, et al. The MicroArray Quality Control (MAQC) project shows inter- and intraplatform reproducibility of gene expression measurements. Nat Biotechnol 2006 Sep;24(9):1151-61.

(58) Driouch K, Landemaine T, Sin S, Wang S, Lidereau R. Gene arrays for diagnosis, prognosis and treatment of breast cancer metastasis. Clin Exp Metastasis 2007;24(8):575-85.

(59) Lu X, Lu X, Wang ZC, Iglehart JD, Zhang X, Richardson AL. Predicting features of breast cancer with gene expression patterns. Breast Cancer Res Treat 2008 Mar;108(2):191-201.

(60) Bild AH, Potti A, Nevins JR. Linking oncogenic pathways with therapeutic opportunities. Nat Rev Cancer 2006 Sep;6(9):735-41.

(61) Perou CM, Sorlie T, Eisen MB, van de RM, Jeffrey SS, Rees CA, et al. Molecular portraits of human breast tumours. Nature 2000 Aug 17;406(6797):747-52.

(62) Sorlie T, Perou CM, Tibshirani R, Aas T, Geisler S, Johnsen H, et al. Gene expression patterns of breast carcinomas distinguish tumor subclasses with clinical implications. Proc Natl Acad Sci U S A 2001 Sep 11;98(19):10869-74.

(63) Sorlie T. Molecular portraits of breast cancer: tumour subtypes as distinct disease entities. Eur J Cancer 2004 Dec;40(18):2667-75.

(64) Robison JE, Perreard L, Bernard PS. State of the science: molecular classifications of breast cancer for clinical diagnostics. Clin Biochem 2004 Jul;37(7):572-8.

(65) Cappelletti V, Gariboldi M, De CL, Toffanin S, Reid JF, Lusa L, et al. Patterns and changes in gene expression following neo-adjuvant anti-estrogen treatment in estrogen receptor-positive breast cancer. Endocr Relat Cancer 2008 Jun;15(2):439-49.

(66) Toffanin S, Daidone MG, Miodini P, De CL, Gandellini P, Cappelletti V. Clusterin: a potential target for improving response to antiestrogens. Int J Oncol 2008 Oct;33(4):791-8.

(67) Smith IE, Dowsett M, Ebbs SR, Dixon JM, Skene A, Blohmer JU, et al. Neoadjuvant treatment of postmenopausal breast cancer with anastrozole, tamoxifen, or both in combination: the Immediate Preoperative Anastrozole, Tamoxifen, or Combined with Tamoxifen (IMPACT) multicenter double-blind randomized trial. J Clin Oncol 2005 Aug 1;23(22):5108-16.

(68) Ellis MJ, Coop A, Singh B, Mauriac L, Llombert-Cussac A, Janicke F, et al. Letrozole is more effective neoadjuvant endocrine therapy than tamoxifen for ErbB-1- and/or ErbB-2-positive, estrogen receptor-positive primary breast cancer: evidence from a phase III randomized trial. J Clin Oncol 2001 Sep 15;19(18):3808-16.

(69) Bild AH, Yao G, Chang JT, Wang Q, Potti A, Chasse D, et al. Oncogenic pathway signatures in human cancers as a guide to targeted therapies. Nature 2006 Jan 19;439(7074):353-7.

(70) Badve S, Nakshatri H. Oestrogen-receptor-positive breast cancer: towards bridging histopathological and molecular classifications. J Clin Pathol 2009 Jan;62(1):6-12.

(71) Perou CM, Sorlie T, Eisen MB, van de RM, Jeffrey SS, Rees CA, et al. Molecular portraits of human breast tumours. Nature 2000 Aug 17;406(6797):747-52.

(72) Sorlie T, Tibshirani R, Parker J, Hastie T, Marron JS, Nobel A, et al. Repeated observation of breast tumor subtypes in independent gene expression data sets. Proc Natl Acad Sci U S A 2003 Jul 8;100(14):8418-23.

(73) van ', V, Dai H, van d, V, He YD, Hart AA, Mao M, et al. Gene expression profiling predicts clinical outcome of breast cancer. Nature 2002 Jan 31;415(6871):530-6.

(74) Hu Z, Fan C, Oh DS, Marron JS, He X, Qaqish BF, et al. The molecular portraits of breast tumors are conserved across microarray platforms. BMC Genomics 2006;7:96.

(75) Wennmalm K, Calza S, Ploner A, Hall P, Bjohle J, Klaar S, et al. Gene expression in 16q is associated with survival and differs between Sorlie breast cancer subtypes. Genes Chromosomes Cancer 2007 Jan;46(1):87-97.

(76) Bergamaschi A, Kim YH, Wang P, Sorlie T, Hernandez-Boussard T, Lonning PE, et al. Distinct patterns of DNA copy number alteration are associated with different clinicopathological features and gene-expression subtypes of breast cancer. Genes Chromosomes Cancer 2006 Nov;45(11):1033-40.

(77) Roylance R, Gorman P, Papior T, Wan YL, Ives M, Watson JE, et al. A comprehensive study of chromosome 16q in invasive ductal and lobular breast carcinoma using array CGH. Oncogene 2006 Oct 19;25(49):6544-53.

(78) Balint EE, Vousden KH. Activation and activities of the p53 tumour suppressor protein. Br J Cancer 2001 Dec 14;85(12):1813-23.

(79) Bergh J, Norberg T, Sjogren S, Lindgren A, Holmberg L. Complete sequencing of the p53 gene provides prognostic information in breast cancer patients, particularly in relation to adjuvant systemic therapy and radiotherapy. Nat Med 1995 Oct;1(10):1029-34.

(80) Berns EM, Foekens JA, Vossen R, Look MP, Devilee P, Henzen-Logmans SC, et al. Complete sequencing of TP53 predicts poor response to systemic therapy of advanced breast cancer. Cancer Res 2000 Apr 15;60(8):2155-62.

(81) Nakopoulou LL, Alexiadou A, Theodoropoulos GE, Lazaris AC, Tzonou A, Keramopoulos A. Prognostic significance of the co-expression of p53 and c-erbB-2 proteins in breast cancer. J Pathol 1996 May;179(1):31-8.

(82) Armes JE, Trute L, White D, Southey MC, Hammet F, Tesoriero A, et al. Distinct molecular pathogeneses of early-onset breast cancers in BRCA1 and BRCA2 mutation carriers: a population-based study. Cancer Res 1999 Apr 15;59(8):2011-7.

(83) Grushko TA, Blackwood MA, Schumm PL, Hagos FG, Adeyanju MO, Feldman MD, et al. Molecular-cytogenetic analysis of HER-2/neu gene in BRCA1-associated breast cancers. Cancer Res 2002 Mar 1;62(5):1481-8.

(84) Fan S, Wang J, Yuan R, Ma Y, Meng Q, Erdos MR, et al. BRCA1 inhibition of estrogen receptor signaling in transfected cells. Science 1999 May 21;284(5418):1354-6.

(85) Curtis C, Shah SP, Chin SF, Turashvili G, Rueda OM, Dunning MJ, et al. The genomic and transcriptomic architecture of 2,000 breast tumours reveals novel subgroups. Nature 2012 Jun 21;486(7403):346-52.

(86) Herrmann H, Strelkov SV, Burkhard P, Aebi U. Intermediate filaments: primary determinants of cell architecture and plasticity. J Clin Invest 2009 Jul;119(7):1772-83.

(87) allo-Danebrock R, Ting E, Gluz O, Herr A, Mohrmann S, Geddert H, et al. Protein expression profiling in high-risk breast cancer patients treated with high-dose or conventional dose-dense chemotherapy. Clin Cancer Res 2007 Jan 15;13(2 Pt 1):488-97.

(88) Matos I, Dufloth R, Alvarenga M, Zeferino LC, Schmitt F. p63, cytokeratin 5, and P-cadherin: three molecular markers to distinguish basal phenotype in breast carcinomas. Virchows Arch 2005 Oct;447(4):688-94.

(89) Honrado E, Osorio A, Milne RL, Paz MF, Melchor L, Cascon A, et al. Immunohistochemical classification of non-BRCA1/2 tumors identifies different groups that demonstrate the heterogeneity of BRCAX families. Mod Pathol 2007 Dec;20(12):1298-306.

(90) Golub TR, Slonim DK, Tamayo P, Huard C, Gaasenbeek M, Mesirov JP, et al. Molecular classification of cancer: class discovery and class prediction by gene expression monitoring. Science 1999 Oct 15;286(5439):531-7.

(91) Bhattacharjee A, Richards WG, Staunton J, Li C, Monti S, Vasa P, et al. Classification of human lung carcinomas by mRNA expression profiling reveals distinct adenocarcinoma subclasses. Proc Natl Acad Sci U S A 2001 Nov 20;98(24):13790-5.

(92) Shipp MA, Ross KN, Tamayo P, Weng AP, Kutok JL, Aguiar RC, et al. Diffuse large B-cell lymphoma outcome prediction by gene-expression profiling and supervised machine learning. Nat Med 2002 Jan;8(1):68-74.

(93) Krafft AE, Duncan BW, Bijwaard KE, Taubenberger JK, Lichy JH. Optimization of the Isolation and Amplification of RNA From Formalin-fixed, Paraffin-embedded Tissue: The Armed Forces Institute of Pathology Experience and Literature Review. Mol Diagn 1997 Sep;2(3):217-30.

(94) Bresters D, Schipper ME, Reesink HW, Boeser-Nunnink BD, Cuypers HT. The duration of fixation influences the yield of HCV cDNA-PCR products from formalin-fixed, paraffin-embedded liver tissue. J Virol Methods 1994 Jul;48(2-3):267-72.

(95) Finke J, Fritzen R, Ternes P, Lange W, Dolken G. An improved strategy and a useful housekeeping gene for RNA analysis from formalin-fixed, paraffin-embedded tissues by PCR. Biotechniques 1993 Mar;14(3):448-53.

(96) Park YN, Abe K, Li H, Hsuih T, Thung SN, Zhang DY. Detection of hepatitis C virus RNA using ligation-dependent polymerase chain reaction in formalin-fixed, paraffin-embedded liver tissues. Am J Pathol 1996 Nov;149(5):1485-91.

(97) Feldman MY. Reactions of nucleic acids and nucleoproteins with formaldehyde. Prog Nucleic Acid Res Mol Biol 1973;13:1-49.

(98) Auerbach C, Moutschen-Dahmen M, Moutschen J. Genetic and cytogenetical effects of formaldehyde and related compounds. Mutat Res 1977;39(3-4):317-61.

(99) Masuda N, Ohnishi T, Kawamoto S, Monden M, Okubo K. Analysis of chemical modification of RNA from formalin-fixed samples and optimization of molecular biology applications for such samples. Nucleic Acids Res 1999 Nov 15;27(22):4436-43.

(100) McGhee JD, von Hippel PH. Formaldehyde as a probe of DNA structure. 3. Equilibrium denaturation of DNA and synthetic polynucleotides. Biochemistry 1977 Jul 26;16(15):3267-76.

(101) Srinivasan M, Sedmak D, Jewell S. Effect of fixatives and tissue processing on the content and integrity of nucleic acids. Am J Pathol 2002 Dec;161(6):1961-71.

(102) Lewis F, Maughan NJ, Smith V, Hillan K, Quirke P. Unlocking the archive--gene expression in paraffin-embedded tissue. J Pathol 2001 Sep;195(1):66-71.

(103) Cronin M, Pho M, Dutta D, Stephans JC, Shak S, Kiefer MC, et al. Measurement of gene expression in archival paraffin-embedded tissues: development and performance of a 92-gene reverse transcriptase-polymerase chain reaction assay. Am J Pathol 2004 Jan;164(1):35-42.

(104) Ribeiro-Silva A, Zhang H, Jeffrey SS. RNA extraction from ten year old formalin-fixed paraffin-embedded breast cancer samples: a comparison of column purification and magnetic bead-based technologies. BMC Mol Biol 2007;8:118.

(105) Gruber AD, Moennig V, Hewicker-Trautwein M, Trautwein G. Effect of formalin fixation and long-term storage on the detectability of bovine viral-diarrhoea-virus (BVDV) RNA in archival brain tissue using polymerase chain reaction. Zentralbl Veterinarmed B 1994 Dec;41(10):654-61.

(106) Abrahamsen HN, Steiniche T, Nexo E, Hamilton-Dutoit SJ, Sorensen BS. Towards quantitative mRNA analysis in paraffin-embedded tissues using real-time reverse transcriptase-polymerase chain reaction: a methodological study on lymph nodes from melanoma patients. J Mol Diagn 2003 Feb;5(1):34-41.

(107) Godfrey TE, Kim SH, Chavira M, Ruff DW, Warren RS, Gray JW, et al. Quantitative mRNA expression analysis from formalin-fixed, paraffin-embedded tissues using 5' nuclease quantitative reverse transcription-polymerase chain reaction. J Mol Diagn 2000 May;2(2):84-91.

(108) Li J, Smyth P, Cahill S, Denning K, Flavin R, Aherne S, et al. Improved RNA quality and TaqMan Pre-amplification method (PreAmp) to enhance expression analysis from formalin fixed paraffin embedded (FFPE) materials. BMC Biotechnol 2008;8:10.

(109) Elkahloun AG, Gaudet J, Robinson GS, Sgroi DC. In situ gene expression analysis of cancer using laser capture microdissection, microarrays and real time quantitative PCR. Cancer Biol Ther 2002 Jul;1(4):354-8.

(110) van't Veer LJ, Bernards R. Enabling personalized cancer medicine through analysis of gene-expression patterns. Nature 2008 Apr 3;452(7187):564-70.

(111) Xiang CC, Chen M, Ma L, Phan QN, Inman JM, Kozhich OA, et al. A new strategy to amplify degraded RNA from small tissue samples for microarray studies. Nucleic Acids Res 2003 May 1;31(9):e53.

(112) Scicchitano MS, Dalmas DA, Bertiaux MA, Anderson SM, Turner LR, Thomas RA, et al. Preliminary comparison of quantity, quality, and microarray performance of RNA extracted from formalin-fixed, paraffin-embedded, and unfixed frozen tissue samples. J Histochem Cytochem 2006 Nov;54(11):1229-37.

(113) Bibikova M, Talantov D, Chudin E, Yeakley JM, Chen J, Doucet D, et al. Quantitative gene expression profiling in formalin-fixed, paraffin-embedded tissues using universal bead arrays. Am J Pathol 2004 Nov;165(5):1799-807.

(114) Tordai A, Liedtke C, Pusztai L. Metastatic gene signatures and emerging novel prognostic tests in the management of early stage breast cancer. Clin Exp Metastasis 2009;26(7):625-32.

(115) Du P, Kibbe WA, Lin SM. lumi: a pipeline for processing Illumina microarray. Bioinformatics 2008 Jul 1;24(13):1547-8.

(116) Bianchini G, Iwamoto T, Qi Y, Coutant C, Shiang CY, Wang B, et al. Prognostic and therapeutic implications of distinct kinase expression patterns in different subtypes of breast cancer. Cancer Res 2010 Nov 1;70(21):8852-62.

(117) Gautier L, Cope L, Bolstad BM, Irizarry RA. affy--analysis of Affymetrix GeneChip data at the probe level. Bioinformatics 2004 Feb 12;20(3):307-15.

(118) McCall MN, Bolstad BM, Irizarry RA. Frozen robust multiarray analysis (fRMA). Biostatistics 2010 Apr;11(2):242-53.

(119) Barrett T, Troup DB, Wilhite SE, Ledoux P, Evangelista C, Kim IF, et al. NCBI GEO: archive for functional genomics data sets--10 years on. Nucleic Acids Res 2011 Jan;39(Database issue):D1005-D1010.

(120) McCall MN, Irizarry RA. Thawing Frozen Robust Multi-array Analysis (fRMA). BMC Bioinformatics 2011;12:369.

(121) van d, V, He YD, van't Veer LJ, Dai H, Hart AA, Voskuil DW, et al. A gene-expression signature as a predictor of survival in breast cancer. N Engl J Med 2002 Dec 19;347(25):1999-2009.

(122) Foekens JA, Atkins D, Zhang Y, Sweep FC, Harbeck N, Paradiso A, et al. Multicenter validation of a gene expression-based prognostic signature in lymph node-negative primary breast cancer. J Clin Oncol 2006 Apr 10;24(11):1665-71.

(123) Bernards R, Weinberg RA. A progression puzzle. Nature 2002 Aug 22;418(6900):823.

(124) Bianchini G, Iwamoto T, Qi Y, Coutant C, Shiang CY, Wang B, et al. Prognostic and therapeutic implications of distinct kinase expression patterns in different subtypes of breast cancer. Cancer Res 2010 Nov 1;70(21):8852-62.

(125) Pichlmair A, Lassnig C, Eberle CA, Gorna MW, Baumann CL, Burkard TR, et al. IFIT1 is an antiviral protein that recognizes 5'-triphosphate RNA. Nat Immunol 2011;12(7):624-30.

(126) Sadler AJ, Williams BR. Interferon-inducible antiviral effectors. Nat Rev Immunol 2008 Jul;8(7):559-68.

(127) Perou CM, Jeffrey SS, van de RM, Rees CA, Eisen MB, Ross DT, et al. Distinctive gene expression patterns in human mammary epithelial cells and breast cancers. Proc Natl Acad Sci U S A 1999 Aug 3;96(16):9212-7.

(128) Perou CM, Sorlie T, Eisen MB, van de RM, Jeffrey SS, Rees CA, et al. Molecular portraits of human breast tumours. Nature 2000 Aug 17;406(6797):747-52.

(129) Einav U, Tabach Y, Getz G, Yitzhaky A, Ozbek U, Amariglio N, et al. Gene expression analysis reveals a strong signature of an interferon-induced pathway in childhood lymphoblastic leukemia as well as in breast and ovarian cancer. Oncogene 2005 Sep 22;24(42):6367-75.

(130) Weichselbaum RR, Ishwaran H, Yoon T, Nuyten DS, Baker SW, Khodarev N, et al. An interferon-related gene signature for DNA damage resistance is a predictive marker for chemotherapy and radiation for breast cancer. Proc Natl Acad Sci U S A 2008 Nov 25;105(47):18490-5.

(131) de Visser KE, Eichten A, Coussens LM. Paradoxical roles of the immune system during cancer development. Nat Rev Cancer 2006 Jan;6(1):24-37.

(132) Denardo DG, Johansson M, Coussens LM. Immune cells as mediators of solid tumor metastasis. Cancer Metastasis Rev 2008 Mar;27(1):11-8.

(133) Yu JX, Sieuwerts AM, Zhang Y, Martens JW, Smid M, Klijn JG, et al. Pathway analysis of gene signatures predicting metastasis of node-negative primary breast cancer. BMC Cancer 2007;7:182.

(134) Rody A, Holtrich U, Pusztai L, Liedtke C, Gaetje R, Ruckhaeberle E, et al. T-cell metagene predicts a favorable prognosis in estrogen receptor-negative and HER2-positive breast cancers. Breast Cancer Res 2009;11(2):R15.

(135) Schmidt M, Bohm D, von TC, Steiner E, Puhl A, Pilch H, et al. The humoral immune system has a key prognostic impact in node-negative breast cancer. Cancer Res 2008 Jul 1;68(13):5405-13.

(136) Teschendorff AE, Miremadi A, Pinder SE, Ellis IO, Caldas C. An immune response gene expression module identifies a good prognosis subtype in estrogen receptor negative breast cancer. Genome Biol 2007;8(8):R157.

(137) Abraham G, Kowalczyk A, Loi S, Haviv I, Zobel J. Prediction of breast cancer prognosis using gene set statistics provides signature stability and biological context. BMC Bioinformatics 2010;11:277.

(138) Alexe G, Dalgin GS, Scanfeld D, Tamayo P, Mesirov JP, Delisi C, et al. High expression of lymphocyte-associated genes in node-negative HER2+ breast cancers correlates with lower recurrence rates. Cancer Res 2007 Nov 15;67(22):10669-76.

(139) Staaf J, Ringner M, Vallon-Christersson J, Jonsson G, Bendahl PO, Holm K, et al. Identification of subtypes in human epidermal growth factor receptor 2--positive breast cancer reveals a gene signature prognostic of outcome. J Clin Oncol 2010 Apr 10;28(11):1813-20.

(140) Egeblad M, Nakasone ES, Werb Z. Tumors as organs: complex tissues that interface with the entire organism. Dev Cell 2010 Jun 15;18(6):884-901.

(141) Tyan SW, Kuo WH, Huang CK, Pan CC, Shew JY, Chang KJ, et al. Breast cancer cells induce cancer-associated fibroblasts to secrete hepatocyte growth factor to enhance breast tumorigenesis. PLoS One 2011;6(1):e15313.

(142) Giannoni E, Bianchini F, Masieri L, Serni S, Torre E, Calorini L, et al. Reciprocal activation of prostate cancer cells and cancer-associated fibroblasts stimulates epithelial-mesenchymal transition and cancer stemness. Cancer Res 2010 Sep 1;70(17):6945-56.

(143) Mantovani A, Schioppa T, Porta C, Allavena P, Sica A. Role of tumor-associated macrophages in tumor progression and invasion. Cancer Metastasis Rev 2006 Sep;25(3):315-22.

(144) Chen P, Mo Q, Wang B, Weng D, Wu P, Chen G. Breast cancer associated fibroblasts promote MCF-7 invasion in vitro by secretion of HGF. J Huazhong Univ Sci Technolog Med Sci 2012 Feb;32(1):92-6.

(145) Buess M, Nuyten DS, Hastie T, Nielsen T, Pesich R, Brown PO. Characterization of heterotypic interaction effects in vitro to deconvolute global gene expression profiles in cancer. Genome Biol 2007;8(9):R191.

(146) Lee GY, Kenny PA, Lee EH, Bissell MJ. Three-dimensional culture models of normal and malignant breast epithelial cells. Nat Methods 2007 Apr;4(4):359-65.

(147) Bissell MJ, Radisky DC, Rizki A, Weaver VM, Petersen OW. The organizing principle: microenvironmental influences in the normal and malignant breast. Differentiation 2002 Dec;70(9-10):537-46.

(148) Pusztai L, Gianni L. Technology insight: Emerging techniques to predict response to preoperative chemotherapy in breast cancer. Nat Clin Pract Oncol 2004 Nov;1(1):44-50.

(149) Hess KR, Anderson K, Symmans WF, Valero V, Ibrahim N, Mejia JA, et al. Pharmacogenomic predictor of sensitivity to preoperative chemotherapy with paclitaxel and fluorouracil, doxorubicin, and cyclophosphamide in breast cancer. J Clin Oncol 2006 Sep 10;24(26):4236-44.

(150) Liedtke C, Hatzis C, Symmans WF, Desmedt C, Haibe-Kains B, Valero V, et al. Genomic grade index is associated with response to chemotherapy in patients with breast cancer. J Clin Oncol 2009 Jul 1;27(19):3185-91.

(151) Bonadonna G, Brusamolino E, Valagussa P, Rossi A, Brugnatelli L, Brambilla C, et al. Combination chemotherapy as an adjuvant treatment in operable breast cancer. N Engl J Med 1976 Feb 19;294(8):405-10.

(152) Bonadonna G, Moliterni A, Zambetti M, Daidone MG, Pilotti S, Gianni L, et al. 30 years' follow up of randomised studies of adjuvant CMF in operable breast cancer: cohort study. BMJ 2005 Jan 29;330(7485):217.

(153) Zambetti M, Bonadonna G, Valagussa P, Daidone MG, Coradini D, Bignami P, et al. Adjuvant CMF for node-negative and estrogen receptor-negative breast cancer patients. J Natl Cancer Inst Monogr 1992;(11):77-83.

(154) Moliterni A, Bonadonna G, Valagussa P, Ferrari L, Zambetti M. Cyclophosphamide, methotrexate, and fluorouracil with and without doxorubicin in the adjuvant treatment of resectable breast cancer with one to three positive axillary nodes. J Clin Oncol 1991 Jul;9(7):1124-30.

(155) Menard S, Valagussa P, Pilotti S, Gianni L, Biganzoli E, Boracchi P, et al. Response to cyclophosphamide, methotrexate, and fluorouracil in lymph node-positive breast cancer according to HER2 overexpression and other tumor biologic variables. J Clin Oncol 2001 Jan 15;19(2):329-35.

(156) Moliterni A, Menard S, Valagussa P, Biganzoli E, Boracchi P, Balsari A, et al. HER2 overexpression and doxorubicin in adjuvant chemotherapy for resectable breast cancer. J Clin Oncol 2003 Feb 1;21(3):458-62.

(157) Bonadonna G, Zambetti M, Moliterni A, Gianni L, Valagussa P. Clinical relevance of different sequencing of doxorubicin and cyclophosphamide, methotrexate, and Fluorouracil in operable breast cancer. J Clin Oncol 2004 May 1;22(9):1614-20.

(158) Gianni L, Baselga J, Eiermann W, Porta VG, Semiglazov V, Lluch A, et al. Phase III trial evaluating the addition of paclitaxel to doxorubicin followed by cyclophosphamide, methotrexate, and fluorouracil, as adjuvant or primary systemic therapy: European Cooperative Trial in Operable Breast Cancer. J Clin Oncol 2009 May 20;27(15):2474-81.

(159) Symmans WF, Hatzis C, Sotiriou C, Andre F, Peintinger F, Regitnig P, et al. Genomic index of sensitivity to endocrine therapy for breast cancer. J Clin Oncol 2010 Sep 20;28(27):4111-9.

(160) Lu M, Shi B, Wang J, Cao Q, Cui Q. TAM: a method for enrichment and depletion analysis of a microRNA category in a list of microRNAs. BMC Bioinformatics 2010;11:419.

(161) Williams PM, Li R, Johnson NA, Wright G, Heath JD, Gascoyne RD. A novel method of amplification of FFPET-derived RNA enables accurate disease classification with microarrays. J Mol Diagn 2010 Sep;12(5):680-6.

(162) Gautier L, Moller M, Friis-Hansen L, Knudsen S. Alternative mapping of probes to genes for Affymetrix chips. BMC Bioinformatics 2004 Aug 14;5:111.

(163) Lu M, Zhang Q, Deng M, Miao J, Guo Y, Gao W, et al. An analysis of human microRNA and disease associations. PLoS One 2008;3(10):e3420.

(164) Sotiriou C, Wirapati P, Loi S, Harris A, Fox S, Smeds J, et al. Gene expression profiling in breast cancer: understanding the molecular basis of histologic grade to improve prognosis. J Natl Cancer Inst 2006 Feb 15;98(4):262-72.

(165) Hatzis C, Pusztai L, Valero V, Booser DJ, Esserman L, Lluch A, et al. A genomic predictor of response and survival following taxane-anthracycline chemotherapy for invasive breast cancer. JAMA 2011 May 11;305(18):1873-81.